Supplementary Information

Catalytic Acceptorless Complete Dehydrogenation of Cycloalkanes

Rahul A. Jagtap,[1] Yuki Nishioka,[1] Stephen M. Geddis,[1] Yu Irie,[1] Tsukasa Takanashi,[2] Rintaro Adachi,[2] Akira Yamakata,[2] Masaaki Fuki, [3,4,5] Yasuhiro Kobori, [3,4,5] Harunobu Mitsunuma,[1,6,*] and Motomu Kanai[1,*]

[1]Graduate School of Pharmaceutical Sciences, The University of Tokyo, Tokyo 113-0033, Japan

[2]Graduate School of Natural Science & Technology, Okayama University, Okayama 700-8530, Japan

[3]Molecular Photoscience Research Center, Kobe University, Kobe 657-8501, Japan

[4]Department of Chemistry, Graduate School of Science, Kobe University, Kobe 657-8501, Japan

[5]JST, CREST, 4-1-8 Honcho, Kawaguchi, Saitama 332-0012, Japan

[6]JST, PRESTO, 4-1-8 Honcho, Kawaguchi, Saitama 332-0012, Japan

Contents

		Page #
1.	General Experimental	S3
2.	Optimization of Reaction Conditions	S4
3.	Synthesis of Cobaloxime Catalysts	S10
4.	Procedures for Synthesis of TPA-TBA Salt and Starting Materials	S12
5.	Representative Procedures for Dehydrogenation	S14
6.	Characterization Data of Dehydrogenated Compounds	S15
7.	Procedure for Gram Scale Synthesis	S24
8.	Confirmation of Hydrogen Gas Evolution	S24
9.	Procedure for Continuous Flow Reactions	S26
10.	Procedure for Control Experiments	S27
11.	Effect of *p*-Xylene Additive (Product Inhibition)	S29
12.	Time Resolved EPR Spectroscopy	S30
13.	Transient Absorption Spectroscopy	S37
14.	NMR Experiments	S44
15.	Absorption Spectra	S48
16.	Redox Profiles	S49
17.	^{1}H and ^{13}C NMR Spectra	S50
18.	References	S66

1. General Experimental

All manipulations were conducted under an argon atmosphere either in a glove box or using standard Schlenk techniques in pre-dried glass wares. The catalytic reactions were performed in oven-dried reaction vessels with Teflon screw caps. Liquid reagents were flushed with argon prior to use. The cobaloxime catalysts were synthesized according to the reported procedure.[1] Catalyst **Co-2** was synthesized following the literature procedure.[2] Substrate **1i** was synthesized by reported literature.[3] All other chemicals were purchased from Aldrich, Tokyo Chemical Industry Co., Ltd. (TCI), Kanto Chemical Co., Inc., and Wako Pure Chemical Industries, Ltd. and were used without further purification. NMR (^{1}H and ^{13}C) spectra were recorded at a JEOL ECX500 (500 MHz for ^{1}H NMR and 125.65 MHz for ^{13}C NMR) or a JEOL ECS400 (400 MHz for ^{1}H NMR and 100 MHz for ^{13}C NMR) spectrometer, respectively in $CDCl_3$ solutions, if not otherwise specified. Chemical shifts (δ) are given in ppm, referenced to residual solvent signals ($CDCl_3$: δ H = 7.26 ppm, δ C = 77.2 ppm). GC-MS spectra were recorded on Shimadzu GCMS-QP2020NX and Shimadzu GC-8A. A Kessil Tuna Blue 40W LED lamp was used as the 430 nm light source.

GC Method. Gas Chromatography analyses were performed using a Shimadzu GC-2010 gas chromatograph equipped with a Shimadzu AOC-20s auto sampler and a Shimadzu SH-RTx-624 column (30 m x 250 μm). The instrument was set to an injection volume of 1 μL, an inlet split ratio of 30, and inlet and detector temperature of 240 °C. UHP-grade nitrogen was used as the carrier gas with a total flow rate of 59.8 mL/min. The temperature program used for all the analyses is as follows: 40 °C, 0 min; 30 °C/min to 200 °C, 5 min. Response factors for all the necessary compounds with respect to standard *n*-decane were calculated from the average of three independent GC runs.

2. Optimization of Reaction Conditions

2.1 Screening of Chloride Salts

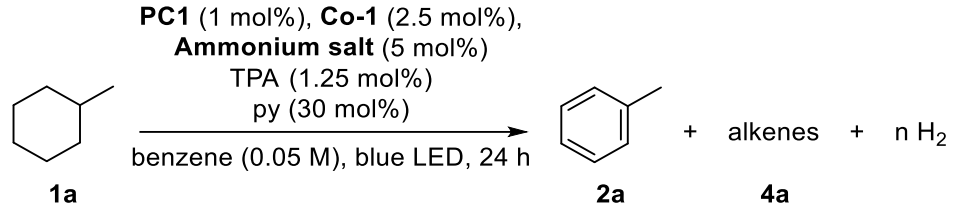

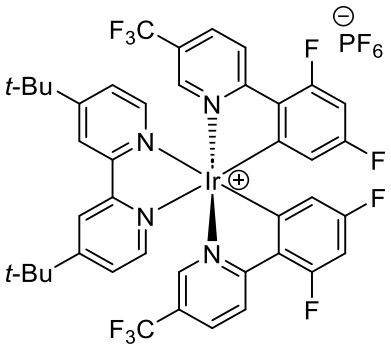

PC1

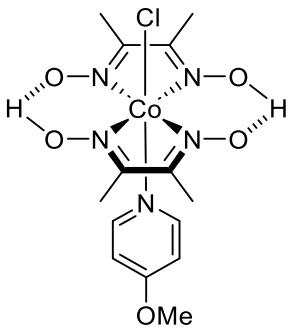

Co-1

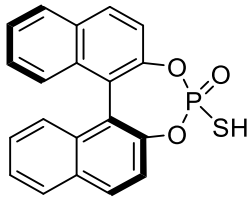

TPA

Entry	Ammonium salt	Alkenes	Toluene
1	Bu_4NCl	trace	36
2	Me_4NCl	trace	15
3	Et_4NCl	trace	13
4	$Me_3(C_{14}H_{29})NCl$	--	13
5	Bu_3BnNCl	--	14
6	NCS	--	5
7	TBAB	--	Trace
8	TBAI	--	Trace
9	TBAF	--	NR

Table S1. Evaluation of various salt additives.

2.2 Screening of Solvents

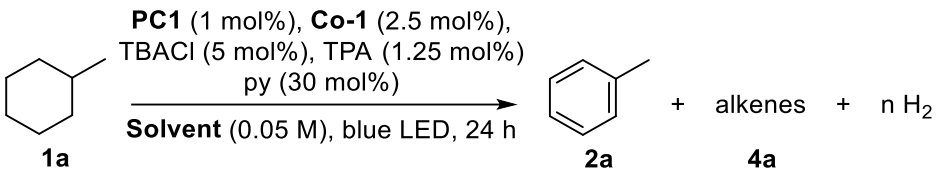

Entry	Solvent	Alkenes	Toluene
1	Benzene	trace	36
2	^{t}Bu-benzene	ND	2
3	*p*-Xylene	ND	ND
4	PhCl	--	23

The observed dramatic difference in yield of product toluene (**2a**) between using benzene and *p*-xylene solvents was likely due to the presence of two benzylic methyl groups in *p*-xylene. The benzylic C–H bonds existing in a high concentration as a solvent, would compete with the substrate in the hydrogen atom transfer step.

Table S2. Solvent screening.

2.3 Screening of Second HAT Catalysts:

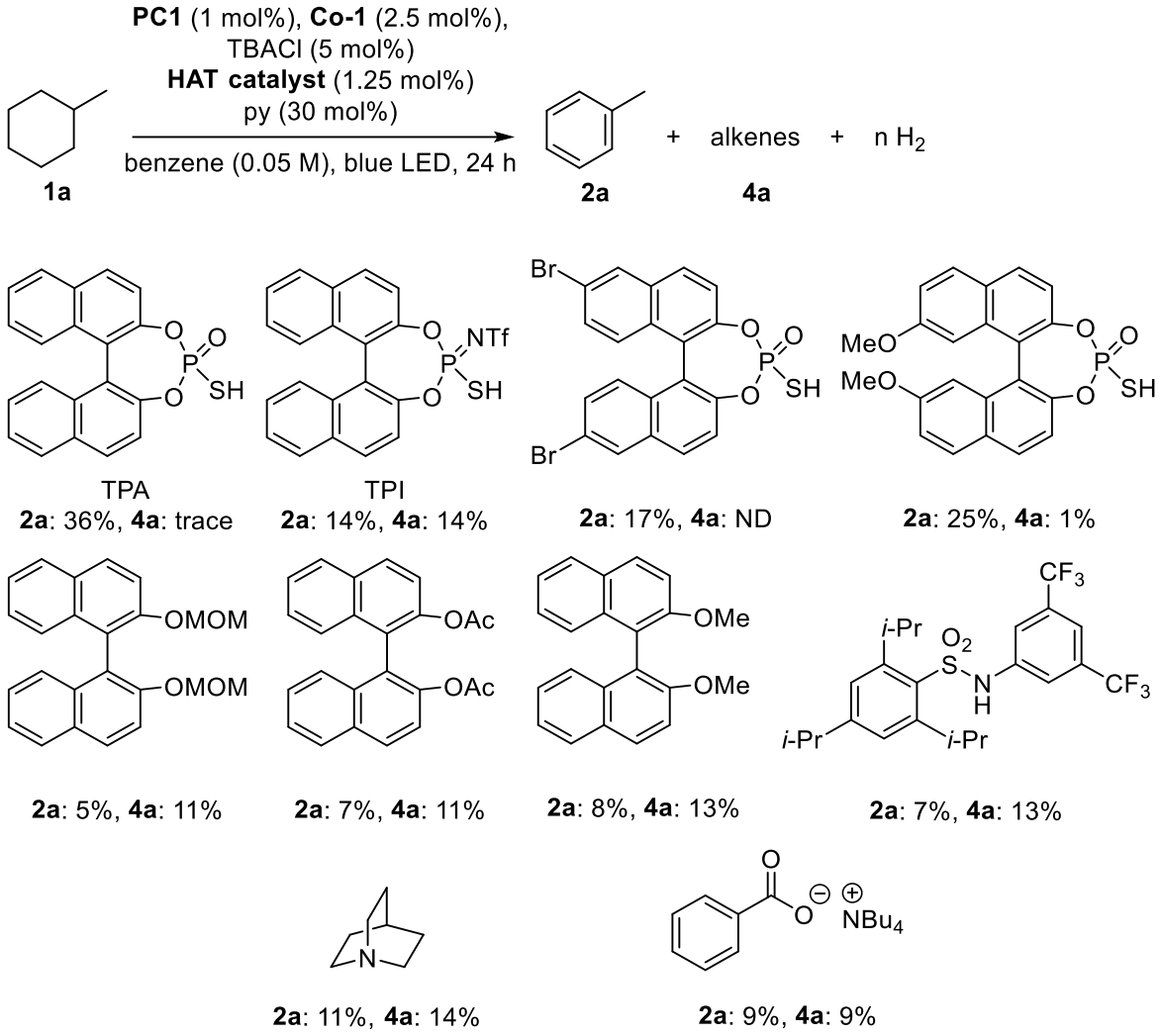

Figure S1. Evaluation of various second HAT catalysts.

2.4 Screening the Amount of Pyridines

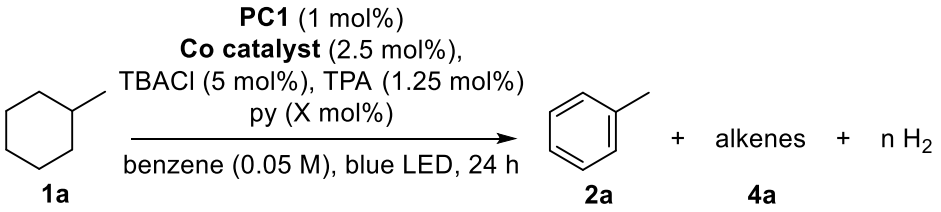

Entry	Pyridine (mol %)	2a	Alkenes
1	--	14	3
2	10	20	--
3	30	36	traces
4	50	20	3

Table S3. Effect of the amount of pyridine.

2.5 Screening of Pyridine Derivatives:

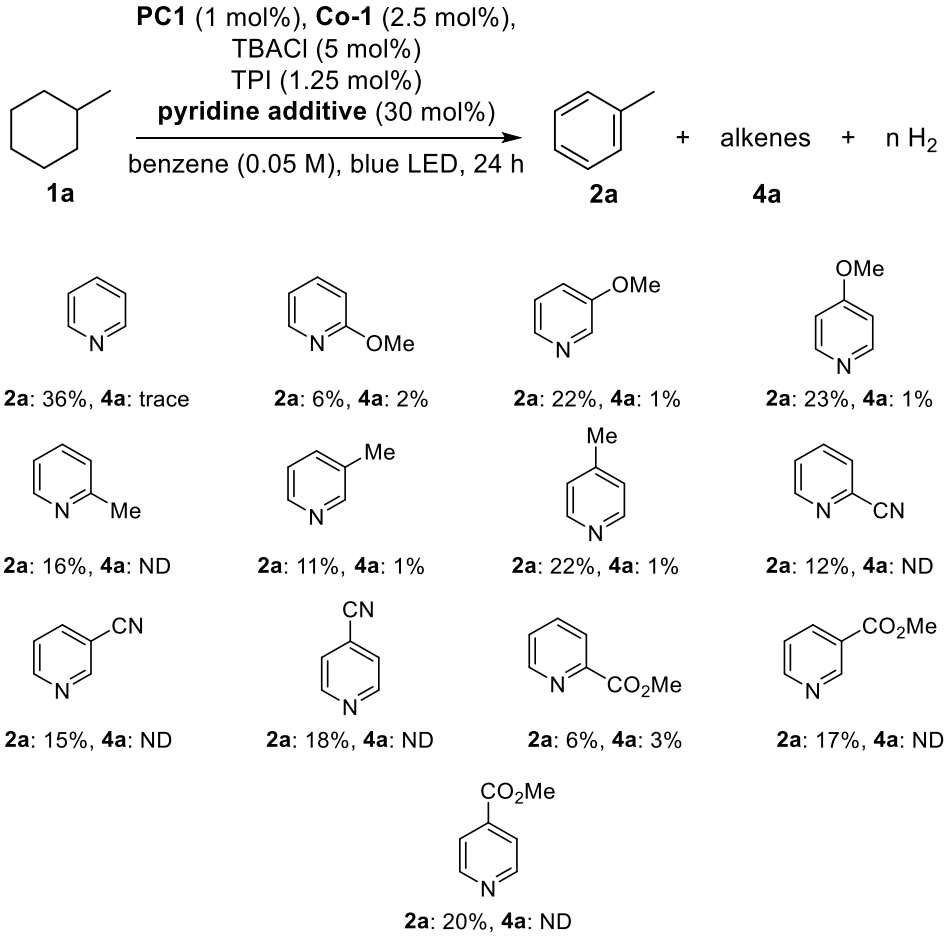

Figure S2. Evaluation of various pyridine derivatives as additives.

2.6 Screening of Cobaloxime Catalysts

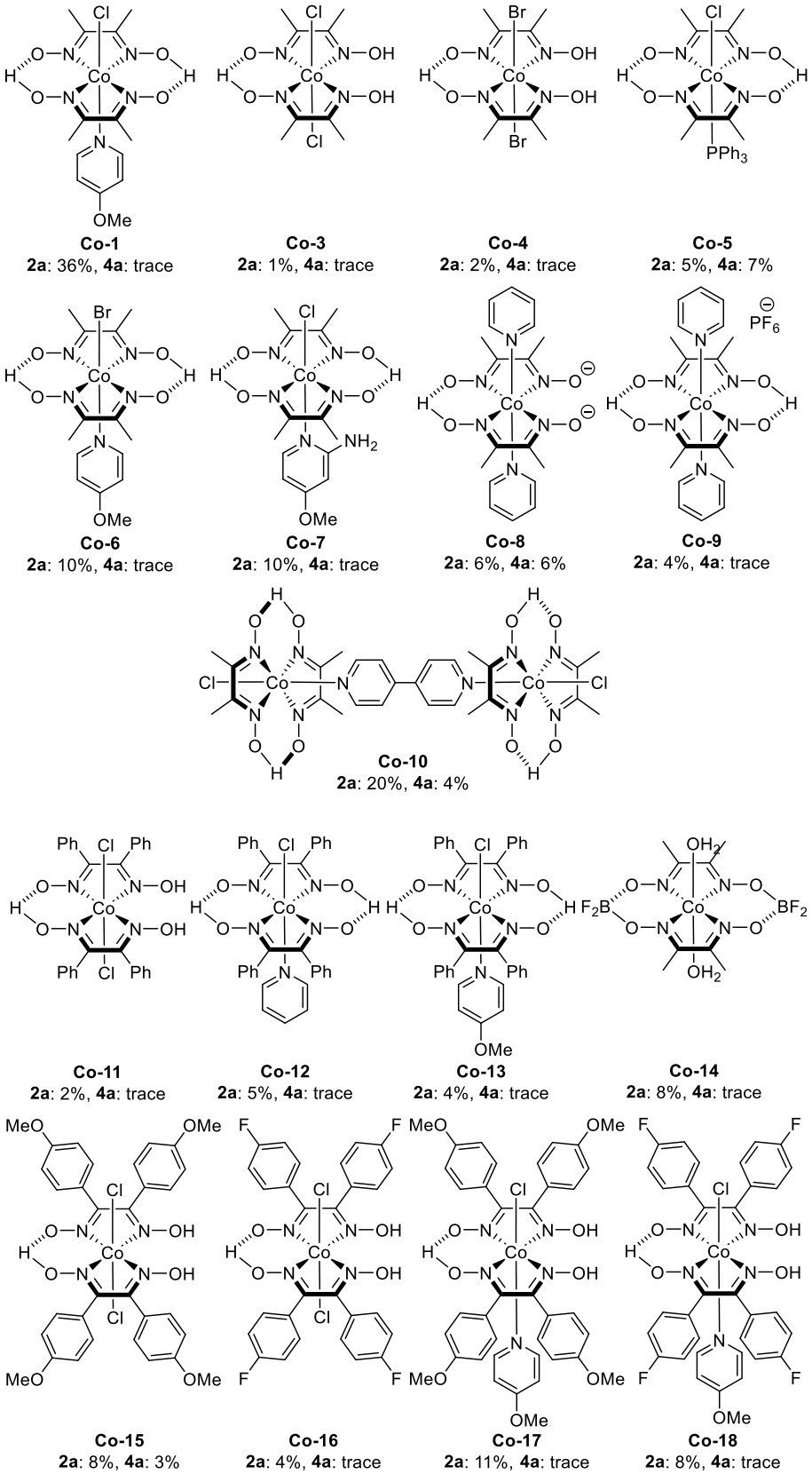

Figure S3. Evaluation of various electronically and sterically distinct cobaloxime catalysts.

2.7 Optimization Using Cyclohexane as a Substrate:

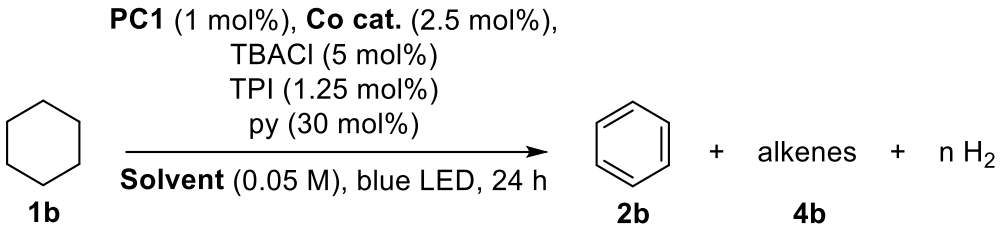

Entry	Solvent	Catalyst	Benzene (%)
1	Acetonitrile	**Co-1**	ND
2	DCE	**Co-1**	ND
3	PhCN	**Co-1**	ND
4	$PhCF_3$	**Co-1**	6
5	PhOMe	**Co-1**	trace
6	PhOPh	**Co-1**	4
7	PhCl	**Co-1**	9
8	**PhCl**	**Co-2**	**21**

Table S4. Evaluation of solvent.

2.8 Screening of Pyridine Derivatives:

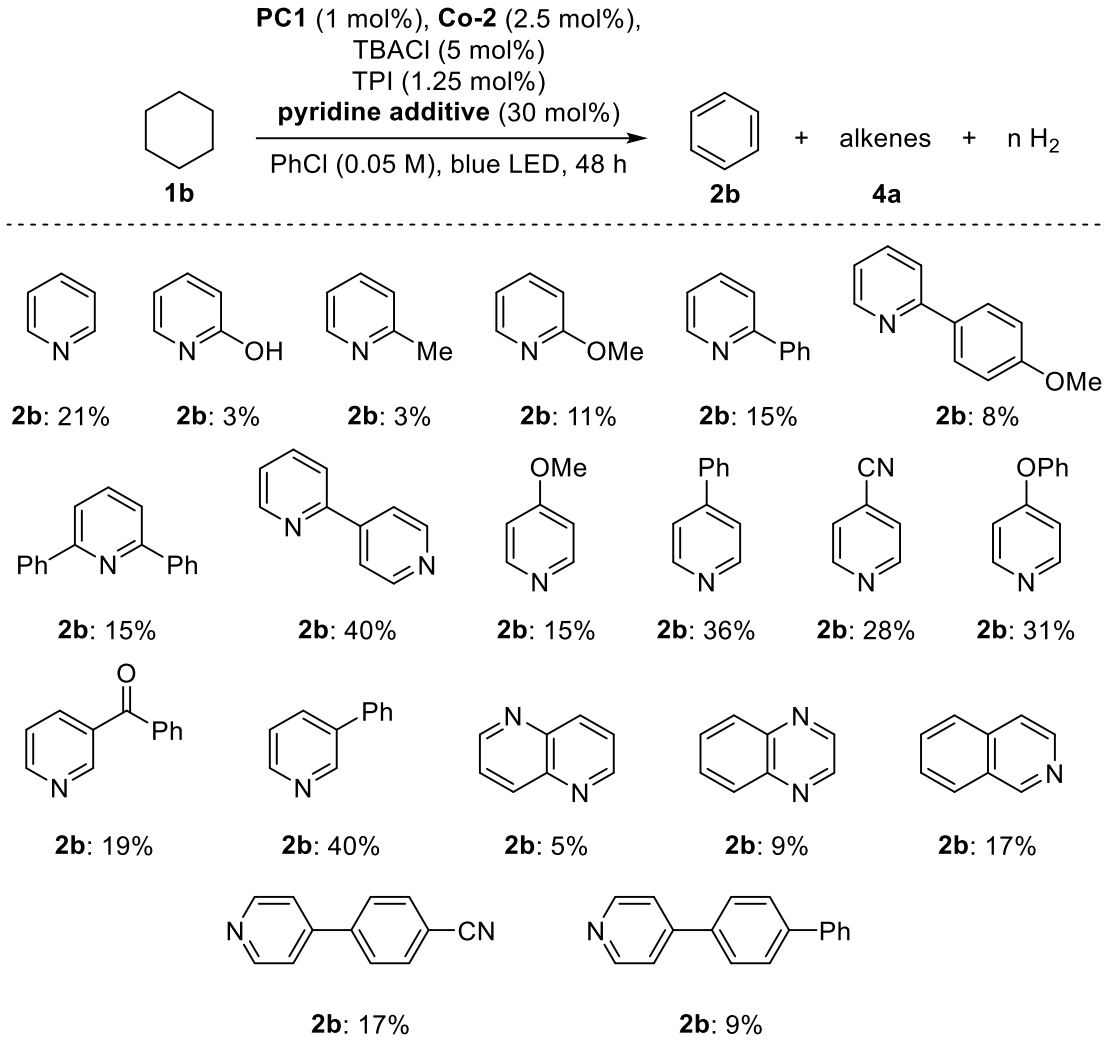

Figure S4. Evaluation of various pyridine derivatives as additives for cyclohexane dehydrogenation.

3. Synthesis of Cobaloxime Catalysts

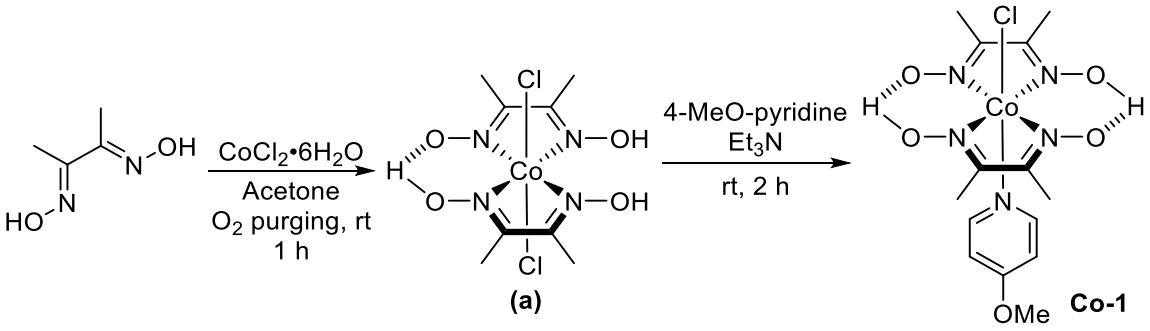

Synthesis of dichloro(dimethylglyoxime)(dimethylglyoximato) cobalt(III) (a):

To a 50 mL round-bottomed flask, dimethylglyoxime (1.00 g, 8.61 mmol) and $CoCl_2 \cdot 6H_2O$ (1.06 g, 4.48 mmol) were dissolved in 20 mL of acetone and the mixture was allowed to stir for 1 h with oxygen purging. After 1 h, the reaction was cooled at -10 ^oC. The resulting precipitate was filtered and washed with cold acetone (2 X 5 mL) and dried in vacuum to give green colored solid in quantitative yield. This solid was used for the next reaction without further purification.

Synthesis of chloro-bis(dimethylglyoximato) (4-OMe pyridine)cobalt(III) (Co-1):

To a suspension of dichloro(dimethylglyoxime)(dimethyl-glyoximato)cobalt(III) (0.60 g, 1.67 mmol) in 20 mL of MeOH, triethylamine (0.17 g, 1.67 mmol) was added at room temperature. The resulting reaction mixture was allowed to stir for 30 min till the mixture turned from a green to a clear dark brown solution. Then, 4-methoxy pyridine (0.18 g, 1.67 mmol) was added and was allowed to stir for the next 1 h. During which golden-coloured precipitate was observed, the reaction mixture was kept at −10 °C for 2 h and the precipitate was filtered and washed with 5 mL water followed by cold methanol (2 × 5 mL). The obtained brown solid was dried under vacuum for a short time. ^{1}H-NMR (400 MHz, $CDCl_3$) δ 8.0 (d, *J* = 7.4 Hz, 2H), 6.70 (d, *J* = 7.4 Hz, 2H), 3.81 (s, 3H), 2.39 (s, 12H). ^{13}C-NMR (100 MHz, $CDCl_3$) δ 167.7, 152.9, 151.8, 112.3, 56.2, 13.3.

Synthesis of [Co(dmgH)$_2$ 4-OMepy SnPh$_3$] (Co-2):

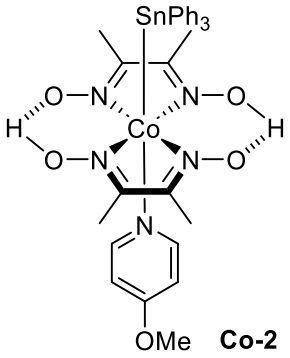

Co-2

The procedure was adopted from the reported precedent. [S2] In a 100 mL round-bottomed flask containing $CoCl_2$ (0.55 g, 4.3 mmol) dissolved in dry MeOH (30 mL), dimethylglyoxime (1.0 g, 8.6 mmol) was added, and the resulting mixture was stirred for 10 min at room temperature. 4-Methoxy pyridine (0.49 g, 4.5 mmol) and NaOH (1.07 M in degassed H_2O, 8.1 mL, 8.65 mmol) were added, which resulted in a dark solution. The resulting mixture was stirred for 10 min at room temperature and cooled at 0 °C. A suspension of Ph_3SnCl (1.61 g, 4.3 mmol) in degassed MeOH (10 mL) and NaOH (1.07 M in degassed H_2O, 4.0 mL, 4.3 mmol) was then added at 0 °C. This mixture was allowed to stir for 10 min and $NaBH_4$ (0.33 g, 8.5 mmol) was added portionwise at 0 °C. The mixture was allowed to stir at room temperature for 90 min. Then, H_2O (40 mL) was added carefully and the mixture was stirred for another 60 min open to air. The orange precipitate was filtered and rinsed successively with H_2O (5 mL), MeOH (10 mL), diethyl ether (10 mL), and hexanes (10 mL). The filtered precipitate was dissolved in DCM (30 mL), dried over Na_2SO_4, filtrated, and concentrated under reduced pressure. The dark red solution was kept for crystallization (18 h) by layering with hexanes (20 mL). The resulting crystals were collected, washed with hexanes (5 ml), and dried in a high vacuum to afford **[Co(dmgH)$_2$ 4-OMepy SnPh$_3$]** (2.18 g, 68%) as a dark red crystal. ^{1}H-NMR (400 MHz, $CDCl_3$) δ 8.35-8.33 (m, 2H), 7.48-7.46 (m, 5H), 7.26-7.22 (m, 10H), 6.78-6.76 (m, 2H), 3.78 (s, 3H), 1.70 (s, 12H). ^{13}C-NMR (100 MHz, $CDCl_3$) δ 150.6, 150.4, 141.2, 137.2, 129.3, 128.2, 128.2, 111.7, 55.67, 12.1.

Synthesis of TPA-TBA salt:

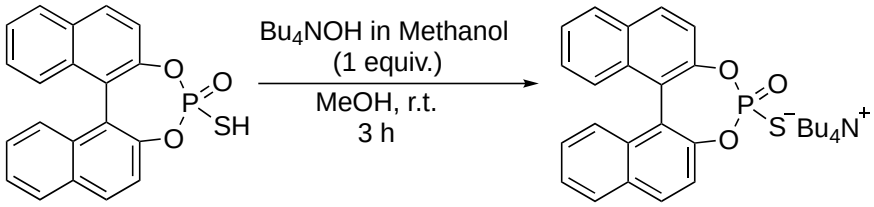

To a 50 mL round bottom flask, TPA (0.137 mmol, 50 mg) was dissolved in methanol (10 mL) and tetrabutylammonium hydroxide (1 M in methanol, 0.137 mmol) was added dropwise. The solution was stirred for 2 h at rt. The resulting reaction mixture was evaporated till dryness followed by repetitive addition and evaporation cycles using MeOH (5 mL X 2). The concentrate was dried in vacuo to afford $[Bu_4N]^+$ TPA$^-$ (TPA-TBA; 79 mg, 95%) as a white solid. ^{1}H NMR (400 MHz, CD_2Cl_2): δ 7.94- 7.88 (m, 4H), 7.51-7.44 (m, 2H), 7.40-7.33 (m, 4H), 7.24-7.19 (m, 2H), 2.99-2.91 (m, 8H), 1.45-1.37 (m, 8H), 1.30-1.20 (m, 8H), 0.89 (t, J = 7.3 Hz, 12H); ^{13}C NMR (100 MHz, CD_2Cl_2): δ 150.3, 132.7, 131.1, 129.6, 128.4, 127.0, 125.8, 124.6, 123.4, 123.1, 58.5, 23.9, 19.7, 13.5; ^{31}P NMR (159 MHz, CD_2Cl_2): δ 66.3 (s).

4. Procedures for Synthesis of Starting Materials

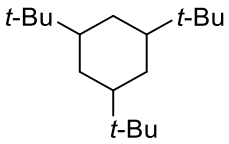

1d

Compound **1d** was synthesized by following the literature procedure.[4] A mixture of 1,3,5-tri-*tert*-butylbenzene (1.0 g, 4.06 mmol) and Rh/C (10 wt %) in ^{i}PrOH (10 mL) was stirred at 60 ^{o}C under 5 bar hydrogen pressure in a high-pressure reactor for 6 h. After cooling to room temperature, the reaction mixture was diluted with CH_3OH (20 mL) and the catalyst was removed by filtration through a celite pad. The filtrate was concentrated in vacuo to give **1d** (1.02 g, 4.06 mmol, 100%) as a white solid.

^{1}H-NMR (400 MHz, $CDCl_3$) δ1.79-1.76 (m, 3H), 0.99-0.92 (m, 3H), 0.85 (s, 27H), 0.60-0.51 (m, 3H), −0.07 (s, 9H). ^{13}C-NMR (125 MHz, $CDCl_3$) δ 48.4, 33.0, 28.3, 27.9.

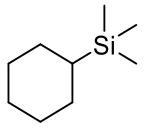

1e

In a round bottom flask, cyclohexyldimethylsilyl chloride (3.0 g, 17.0 mmol) was dissolved in 25 mL of THF and methylmagnesium chloride (22.0 mmol, 3M in THF) was slowly added at 0 °C. The reaction was refluxed for 3 h. After cooling to room temperature, the reaction was quenched with aqueous ammonium chloride. The resulting mixture was extracted with Et_2O (3 x 30 mL) and the combined organic layers were dried over Na_2SO_4. After filtration and evaporation of the solvent, the crude product was distilled under reduced pressure to afford **1e** (2.28 g, 14.6 mmol, 88%) as a colorless oil.

^{1}H-NMR (500 MHz, $CDCl_3$) δ 1.73-1.65 (m, 5H), 1.23-1.19 (m, 3H), 1.10-1.02 (m, 2H), 0.53 (tt, J = 12.6, 2.8 Hz, 1H), −0.07 (s, 9H).^{13}C-NMR (125 MHz, $CDCl_3$) δ 28.3, 27.5, 27.2, 26.3, −3.3. The NMR data is in accordance with the reported compound.[5]

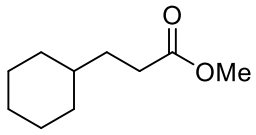

1g

Compound **1g** was synthesized by following the literature procedure.[6] 3-Cyclohexylpropanoic acid (9.0 g, 57.6 mmol) was dissolved in 150 mL of methanol. Subsequently 15 drops of sulfuric acid were added. The resulting reaction was stirred for 78 h at 60 °C. After the completion of the reaction, methanol was removed under reduced pressure. 150 mL of water

was added and products were extracted with Et_2O (3 x 100 mL) to afford pure product **1g** as a colorless liquid (9.4 g, 55.3 mmol, 96%).

^{1}H-NMR (400 MHz, $CDCl_3$) δ 3.66 (s, 3H), 2.31 (t, *J* = 8.1 Hz, 2H), 1.70-1.62 (m, 5H), 1.54-1.48 (m, 2H), 1.25-1.11 (m, 4H), 0.92-0.88 (m, 2H). ^{13}C-NMR (100 MHz, $CDCl_3$) δ 174.8, 51.6, 37.3, 33.1, 32.5, 31.8, 26.6, 26.3.

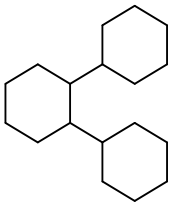

1n

Compound **1n** was synthesized by following the literature procedure.[5] A mixture of *o*-terphenyl (1.0 g, 4.34 mmol) and Rh/C (10 wt %) in ^{i}PrOH (10 mL) was stirred at 80 ^{o}C under 10 bar hydrogen pressure in high-pressure reactor for 16 h. After cooling to room temperature, the reaction mixture was diluted with CH_3OH (20 mL) and the catalyst was removed by filtration through a celite pad. The filtrate was concentrated in vacuo to give mixtures of isomers of tercyclohexane **1n** (0.33 g, 1.34 mmol, 31%) as a white solid.

^{1}H-NMR (400 MHz, $CDCl_3$) δ 2.16−0.87 (m, 32H).^{13}C-NMR (100 MHz, $CDCl_3$) δ 38.6, 33.1, 32.4, 27.3, 27.2, 26.9, 25.3.

5. Representative Procedures for Dehydrogenation

Procedure A: To an oven-dried screw-cap tube equipped with a magnetic stir bar were introduced methylcyclohexane (**1a**; 25.5 µL, 0.20 mmol), cobaloxime (**Co-1**; 2.1 mg, 0.005 mmol, 2.5 mol %), iridium photocatalyst (**PC1**; 2.2 mg, 0.002 mmol, 1.0 mol %), TPA (0.91 mg, 0.0025 mmol, 1.25 mol %), Bu_4NCl (2.8 mg, 0.01 mmol, 5.0 mol %) and pyridine (4.7 mg, 0.06 mmol, 30 mol %) inside the glove box. Then, benzene (4.0 mL) was added to the above

mixture in the tube. After taking out from the glove box, the resultant reaction mixture was subjected to blue LED irradiation and stirred for 18 h. Subsequently, the reaction tube was moved into the glove box, where the reaction mixture was passed through a short silica pad. Following this, all the catalyst components were reintroduced, and the reaction proceeded for an additional 18 h. The reaction was monitored by the GC analysis using *n*-decane as an internal standard.

Procedure B: To an oven-dried screw-cap tube equipped with a magnetic stir bar were introduced cyclohexane (**1b**; 21.7 µL, 0.20 mmol), cobaloxime (**Co-2**; 3.7 mg, 0.005 mmol, 2.5 mol %), iridium photocatalyst (**PC1**; 2.2 mg, 0.002 mmol, 1.0 mol %), TPA (0.91 mg, 0.0025 mmol, 1.25 mol %), Bu_4NCl (2.8 mg, 0.01 mmol, 5.0 mol %), and 3-phenyl pyridine (9.3 mg, 0.06 mmol, 30 mol %) inside the glove box. Then, chlorobenzene (4.0 mL) was added to the above mixture in the tube. After taking out from the glove box, the resultant reaction mixture was subjected to blue LED irradiation and stirred for 18 h. Subsequently, the reaction tube was moved into the glove box, where the reaction mixture passed through a short silica pad. Following this, all catalyst components were reintroduced, and the reaction proceeded for an additional 18 h. The reaction was monitored by the GC analysis using *n*-decane as an internal standard.

6. Characterization Data of Dehydrogenated Compounds

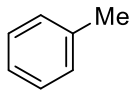

2a

The representative procedure **A** was followed, using (**1a**; 25.5 µL, 0.2 mmol). Yield was determined by GC analysis.

<クロマトグラム>

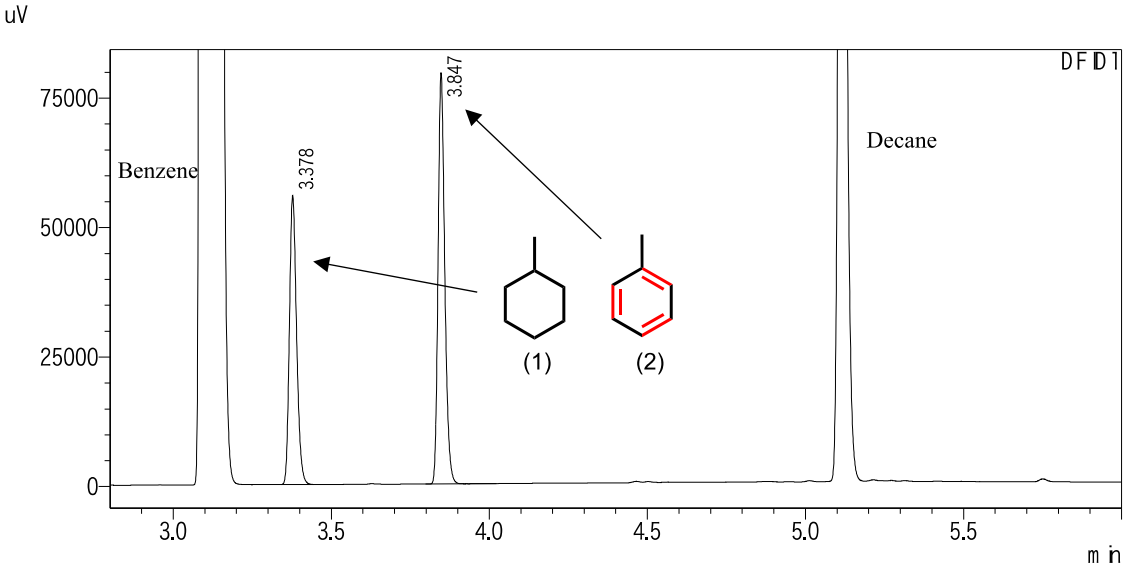

<ピークレポート>

DFID1

ピーク#	保持時間	面積	Area%	Height%
1	3.378	87933	42.943	41.253
2	3.847	116835	57.057	58.747
Total		204768	100.000	100.000

2b

The representative procedure **B** was followed, using (**1b**; 21.7 μL, 0.2 mmol). Yield was determined by GC analysis.

<クロマトグラム>

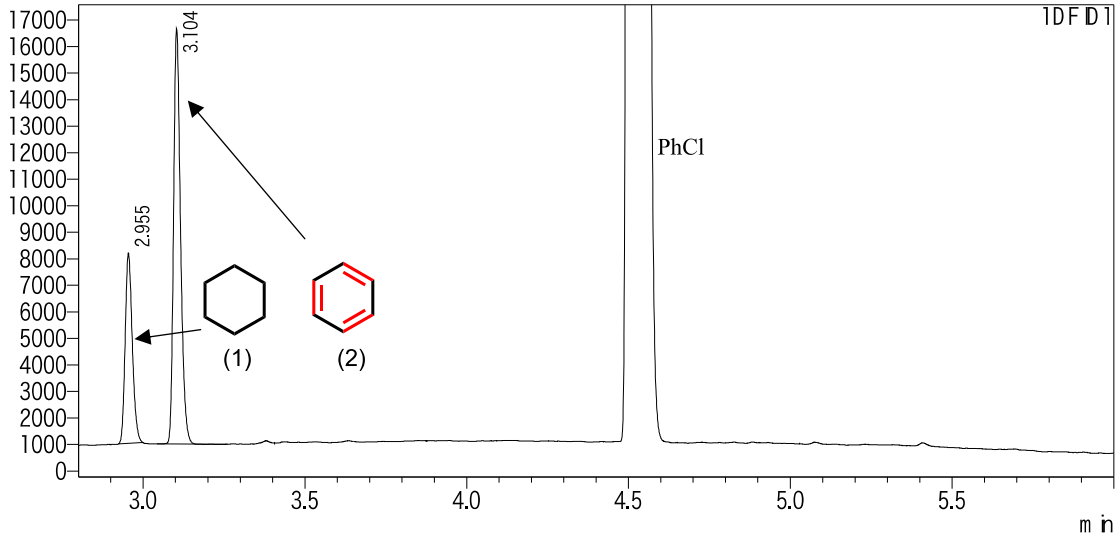

<ピークレポート>

DFID1

保持時間	面積	化合物名	Area%	Height%
2.955	10950		31.939	31.343
3.104	23335		68.061	68.657
	34285		100.000	100.000

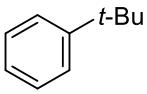

2c

The representative procedure **A** was followed, using (**1c**; 34.6 µL, 0.2 mmol). Yield was determined by GC analysis.

<クロマトグラム>

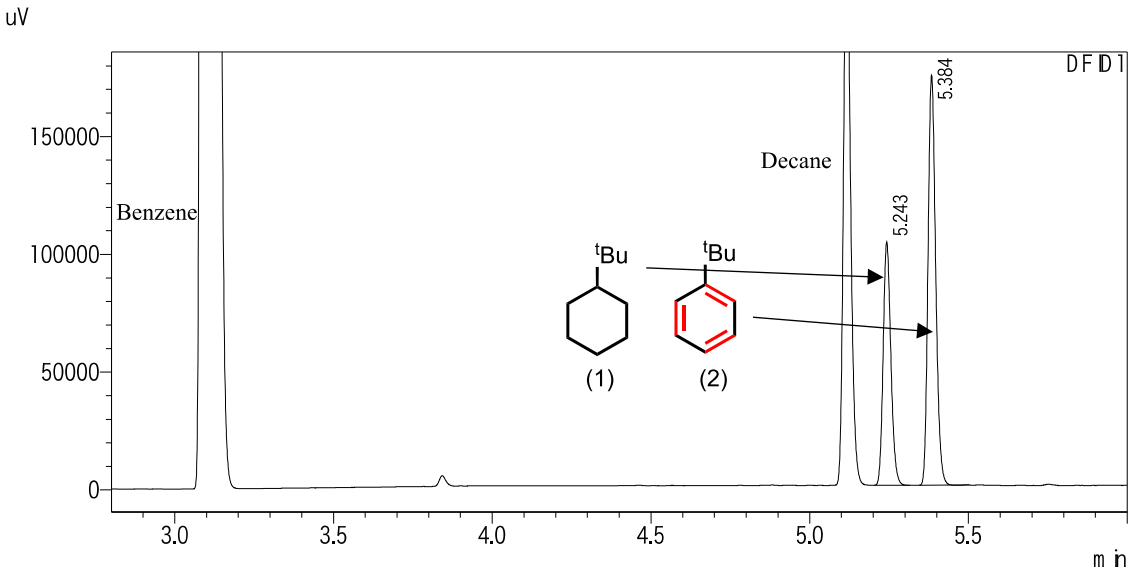

<ピークレポート>

DFID1

ピーク#	保持時間	面積	Area%	Height%
1	5.243	173981	37.515	37.177
2	5.384	289784	62.485	62.823
Total		463765	100.000	100.000

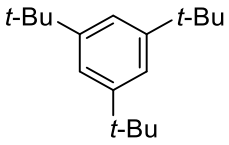

2d

The representative procedure **A** was followed, using (**1d**; 50 mg, 0.20 mmol). Purification by column chromatography on silica gel (petroleum ether 100%) yielded **2d** (45 mg, 73%) as a pale yellow solid. ^{1}H-NMR (500 MHz, $CDCl_3$): δ = 7.25 (s, 3H), 1.33 (s, 27H), ^{13}C-NMR (125 MHz, $CDCl_3$) δ = 150.1, 119.7, 35.2, 31.8.

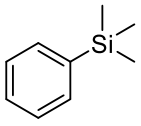

2e

The representative procedure **A** was followed, using (**1e**; 31 mg, 0.20 mmol). Yield was determined by GC analysis using *n*-decane as an internal standard and crude NMR (76%). ^{1}H-NMR (400 MHz, $CDCl_3$): δ = 7.55-7.54 (m, 2H), 7.38-7.36 (m, 3H), 0.29 (s, 9H). ^{13}C-NMR (100 MHz, $CDCl_3$) δ = 140.7, 133.5, 128.9, 128.5, 127.9, -0.9.

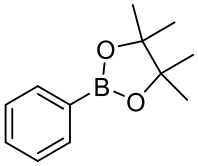

2f

The representative procedure **A** was followed, using (**1f**; 42 mg, 0.20 mmol). Purification by column chromatography on silica gel (petroleum ether 100%) yielded **2n** (21 mg, 51%) as a light brown liquid. ^{1}H-NMR (400 MHz, $CDCl_3$): δ = 7.83-7.81 (m, 2H), 7.47 (tt, J = 6.3, 2.2 Hz, 1H), 7.40-7.36 (m, 2H), 1.36 (s, 12H). ^{13}C-NMR (100 MHz, $CDCl_3$) δ = 134.9, 134.9, 131.4, 127.9, 83.9, 25.1.

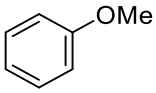

2g

The representative procedure **A** was followed, using (**1g**; 26.1 µL, 0.2 mmol). Yield was determined by GC-MS analysis.

<クロマトグラム>

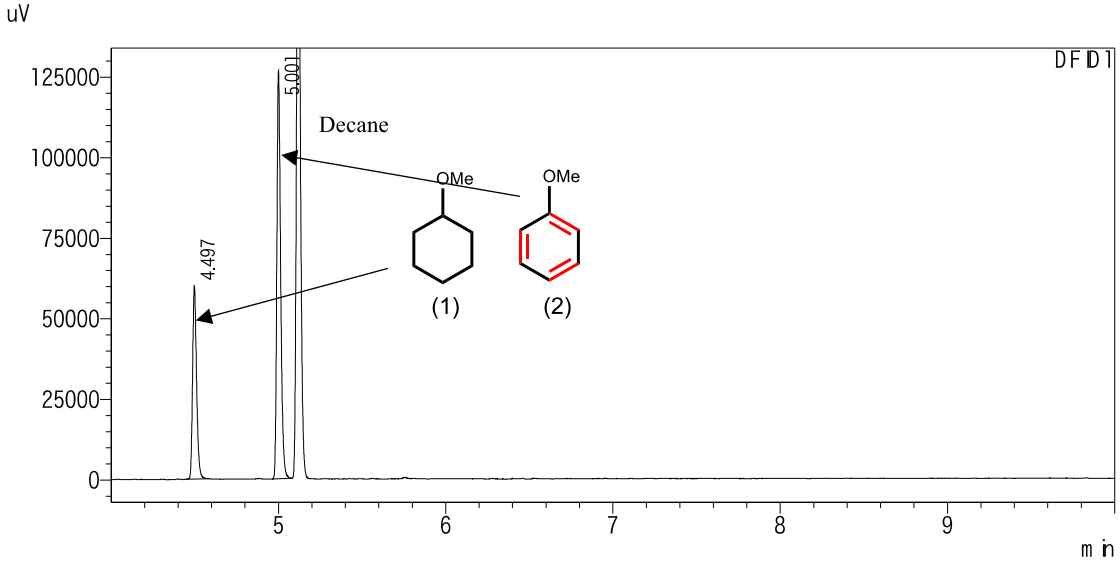

<ピークレポート>

DFID1

ピーク#	保持時間	面積	Area%	Height%
1	4.497	98361	32.906	32.319
2	5.001	200556	67.094	67.681
Total		298917	100.000	100.000

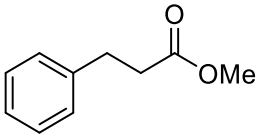

2h

The representative procedure **A** was followed, using (**1h**; 34 mg, 0.20 mmol). Purification by column chromatography on silica gel (petroleum ether/ethyl acetate = 100/2) yielded **2h** (21 mg, 64%) as a light brown liquid. ^{1}H-NMR (400 MHz, $CDCl_3$): δ = 7.31-7.27 (m, 2H), 7.22-7.19 (m, 3H), 3.67 (s, 3H), 2.95 (t, J = 8.0 Hz, 2H), 2.64 (t, J = 8.0 Hz, 2H). ^{13}C-NMR (125 MHz, $CDCl_3$) δ = 173.5, 140.7, 128.7, 128.4, 126.4, 51.8, 35.9, 31.1.

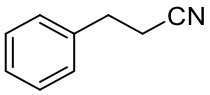

2i

The representative procedure **A** was followed, using (**1i**; 27 mg, 0.20 mmol). Purification by column chromatography on silica gel (petroleum ether/ethyl acetate = 100/10) yielded **2i** (10 mg, 40%) as a light brown liquid. ^{1}H-NMR (400 MHz, $CDCl_3$): δ = 7.35-7.21 (m, 5H), 2.95 (t, J = 7.4 Hz, 2H), 2.61 (t, J = 7.4 Hz, 2H). ^{13}C-NMR (125 MHz, $CDCl_3$) δ = 138.2, 129.1, 128.4, 127.4, 119.3, 31.8, 19.6.

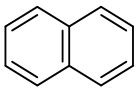

2j

The representative procedure **B** was followed, using (**1j**; 31.8 µL, 0.2 mmol). Yield was determined by GC analysis.

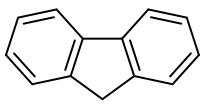

2k

The representative procedure **A** was followed, using (**1k**; 37.8 µL, 0.2 mmol). Yield was determined by GC-MS analysis.

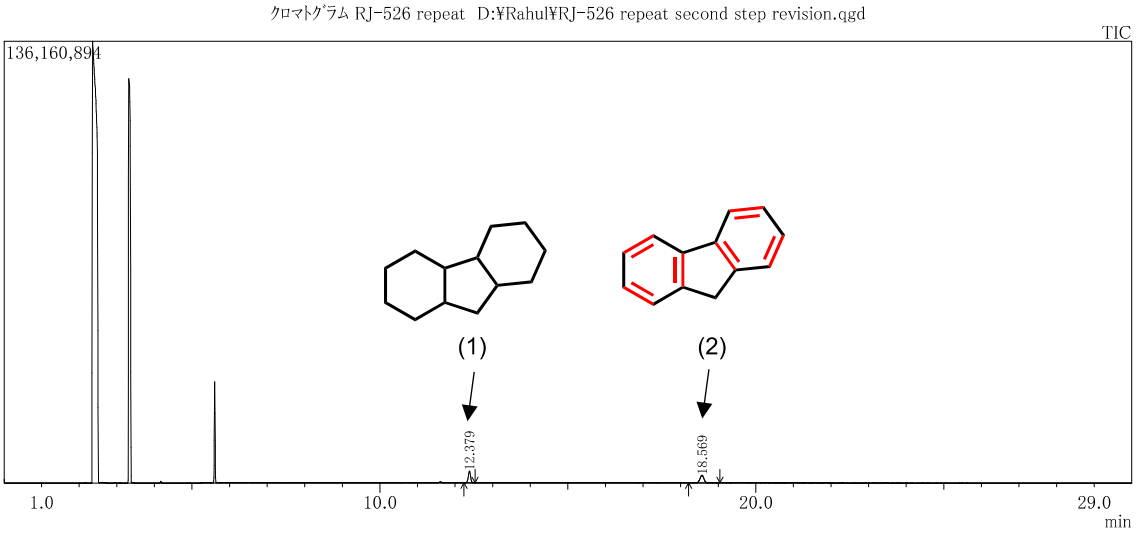

ピークテーブル TIC

ピーク#	保持時間	ピーク開始	ピーク終了	面積	面積%	高さ	高さ%	A/H	マーク	化合物
1	12.379	12.235	12.530	15771867	47.66	3626624	60.74	4.35	MI	
2	18.569	18.210	19.040	17317813	52.34	2344312	39.26	7.39	MI	
				33089680	100.00	5970936	100.00			

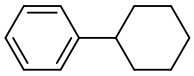

2l

The representative procedure **B** was followed, using (**1l**; 38.5 µL, 0.2 mmol). Yield was determined by GC analysis.

<クロマトグラム>

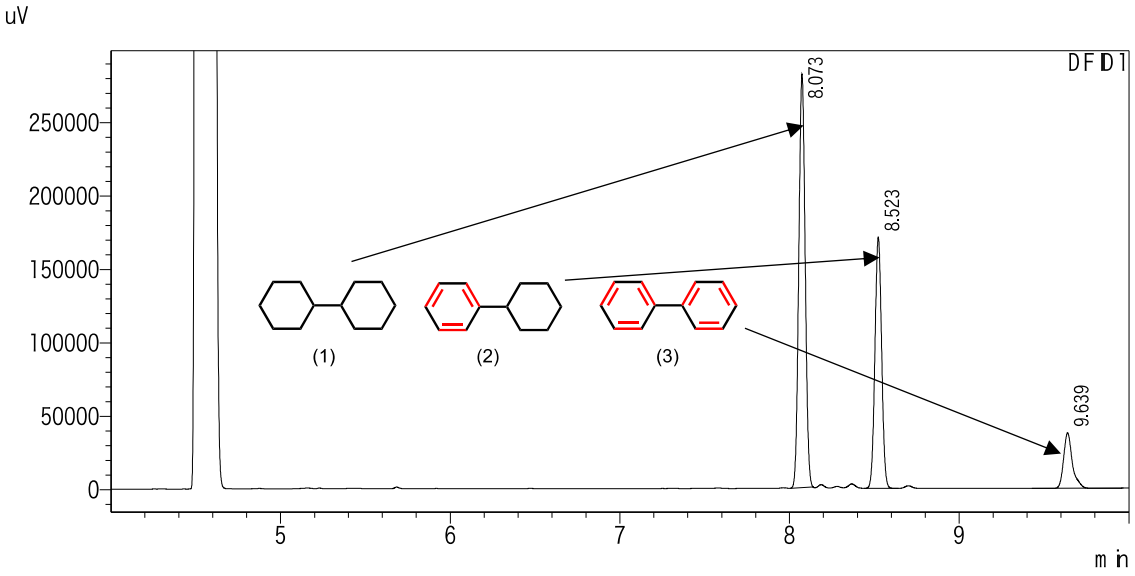

<ピークレポート>

DFID1

ピーク#	保持時間	面積	Area%	Height%
1	8.073	732633	54.902	57.575
2	8.523	468326	35.095	34.713
3	9.639	133487	10.003	7.712
Total		1334446	100.000	100.000

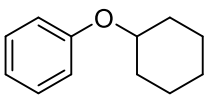

2m

The representative procedure **A** was followed, using (**1m**; 0.036 g, 0.20 mmol). Purification by column chromatography on silica gel (petroleum ether/ethyl acetate 100/5) yielded **2m** (0.025 g, 71%) as a light brown liquid, and diphenyl ether (**2m'**) was determined by GC analysis and crud NMR (11%) as a light brown liquid. ^{1}H-NMR (500 MHz, $CDCl_3$): δ = 7.28-7.24 (m, 2H), 6.92-6.88 (m, 3H), 4.25-4.21 (m, 1H), 2.01-1.97 (m, 2H), 1.81-1.78 (m, 2H), 1.59-1.46 (m, 3H), 1.40-1.31 (m, 3H). ^{13}C-NMR (100 MHz, $CDCl_3$) δ = 157.9, 129.6, 120.6, 116.2, 75.5, 32.0, 25.8, 24.0.

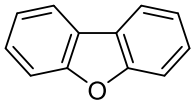

2n

The representative procedure **A** was followed, using (**1n**; 0.036 g, 0.20 mmol). Purification by column chromatography on silica gel (petroleum ether 100%) yielded **2n** (0.015 g, 42%) as a white solid. ^{1}H-NMR (400 MHz, $CDCl_3$): δ = 7.97 (d, J = 7.4 Hz, 2H), 7.59 (d, J = 7.8 Hz, 2H), 7.48 (dd, J = 7.4, 7.2 Hz, 2H), 7.36 (dd, J = 7.8, 7.2 Hz, 2H). ^{13}C-NMR (100 MHz, $CDCl_3$) δ = 156.3, 127.3, 124.4, 122.8, 120.8, 111.8.

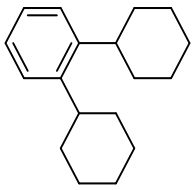

2o

The representative procedure **A** was followed, using (**1o**; 0.05 g, 0.20 mmol). Purification by column chromatography on silica gel (petroleum ether/ethyl acetate 100/1) yielded **2o** (0.020 g, 42%) as as a light brown liquid, and biphenyl cyclohexane (**2o'**) was determined by GC-MS analysis (11%) as a light brown liquid. ^{1}H-NMR (400 MHz, $CDCl_3$): δ = 7.25-7.21 (m, 2H), 7.17-7.13 (m, 2H), 2.81-2.75 (m, 2H), 1.87-1.84 (m, 4H), 1.79-1.76 (m, 6H), 1.51-1.25 (m, 10H), ^{13}C-NMR (100 MHz, $CDCl_3$) δ = 144.9, 126.0, 125.8, 39.4, 34.8, 27.4, 26.5.

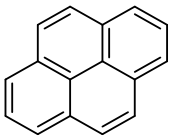

2p

The representative procedure **A** was followed, using (**1p**; 0.043 g, 0.20 mmol). Purification by column chromatography on silica gel (petroleum ether/ethyl acetate 100/2) yielded **2p** (0.009 g, 22%) as a white solid. ^{1}H-NMR (400 MHz, $CDCl_3$): δ = 8.19 (d, J = 7.6 Hz, 4H), 8.09 (s, 4H), 8.03-7.99 (m, 2H). ^{13}C-NMR (125 MHz, $CDCl_3$) δ = 131.3, 127.6, 126.0, 125.1, 124.8.

7. Procedure for Gram Scale Synthesis

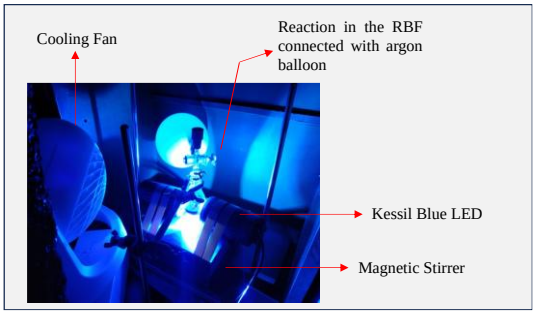

The representative procedure **A** was followed. To a 50 mL round bottom flask (**1e**, 0.156 g, 1.0 mmol), cobaloxime (**Co-1**; 11 mg, 0.025 mmol, 2.5 mol %), iridium photocatalyst (**PC1**; 11 mg, 0.01 mmol, 1.0 mol %), TPA (4.5 mg, 0.0125 mmol, 1.25 mol %), Bu_4NCl (14 mg, 0.05 mmol, 5.0 mol %), and pyridine (23 mg, 0.3 mmol, 30 mol %) were added inside the glove box. After the completion of the reaction, the GC conversion was found to be 70%. Yield was determined by NMR analysis of crude mixture (55%).

8. Confirmation of Hydrogen Gas Evolution

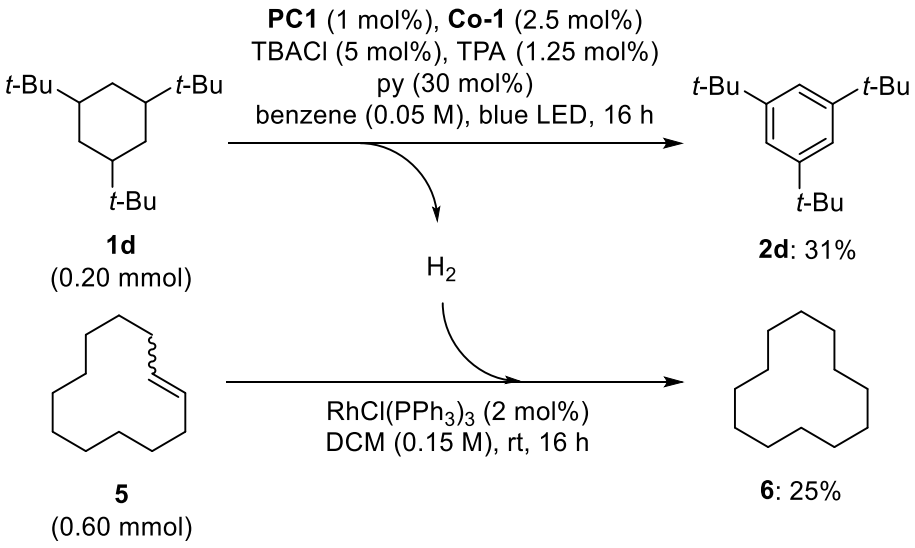

In one side of a screw-capped two-chamber glass system (COware: https://www.sigmaaldrich.com/JP/en/product/aldrich/stw5, accessed on December 12th, 2023), 1,3,5-tri-*tert*-butylcyclohexane (**1d**: 50 mg, 0.20 mmol), cobaloxime (**Co-1**; 2.1 mg, 0.005 mmol, 2.5 mol %), Iridium photocatalyst (**PC1**; 2.2 mg, 0.002 mmol, 1.0 mol %), TPA (0.91

mg, 0.0025 mmol, 1.25 mol %), Bu_4NCl (2.8 mg, 0.01 mmol, 5.0 mol %) and pyridine (4.7 mg, 0.06 mmol, 30 mol %) were dissolved in degassed benzene (4.0 mL). In the other side of the apparatus, cyclododecene (**5**: 114 μL, 0.60 mmol) and $RhCl(PPh_3)_3$ (1.1 mg, 0.012 mmol) were dissolved in degassed CH_2Cl_2 (4.0 mL). One side of the apparatus containing **5** was wrapped with aluminum foil, and the apparatus was subjected to irradiation by blue LED for 16 h under temperature control (ca. 27–29 ºC). Then, the reaction mixture of **1d** was passed through a short silica pad with CH_2Cl_2, and the solvent was removed under reduced pressure. 1,1,2,2-Tetrachloroethane was added as an internal standard, and the yield of **2d** was determined to be 31% by ^1H NMR analysis. The reaction mixture from the hydrogenation chamber was passed through a pad of silica gel with CH_2Cl_2, and the solvent was removed under reduced pressure. 1,1,2,2-Tetrachloroethane was added as an internal standard, and the yield of cyclododecane **6** was determined to be 25% by ^1H NMR analysis.

Hydrogen Gas Evaluation by GC:

To an oven-dried septum-cap tube equipped with a magnetic stir bar were introduced methylcyclohexane (**1a**; 25.5 μL, 0.20 mmol), cobaloxime (**Co-1**; 2.1 mg, 0.005 mmol, 2.5 mol %), iridium photocatalyst (**PC1**; 2.2 mg, 0.002 mmol, 1.0 mol %), TPA (0.91 mg, 0.0025 mmol, 1.25 mol %), Bu_4NCl (2.8 mg, 0.01 mmol, 5.0 mol %) and pyridine (4.7 mg, 0.06 mmol, 30 mol %) inside the glove box. To the above mixture in the tube was added benzene (4.0 mL). The resultant reaction mixture was subjected to blue LED irradiation and stirred for 18 h. The 0.5 mL gas was withdrawn by using the gas-tight syringe and subjected to GC analysis. The analysis data was compared with calibrated 4% hydrogen gas. This experiment has directly showed the generation of hydrogen gas and overall supports the catalytic acceptorless dehydrogenation process.

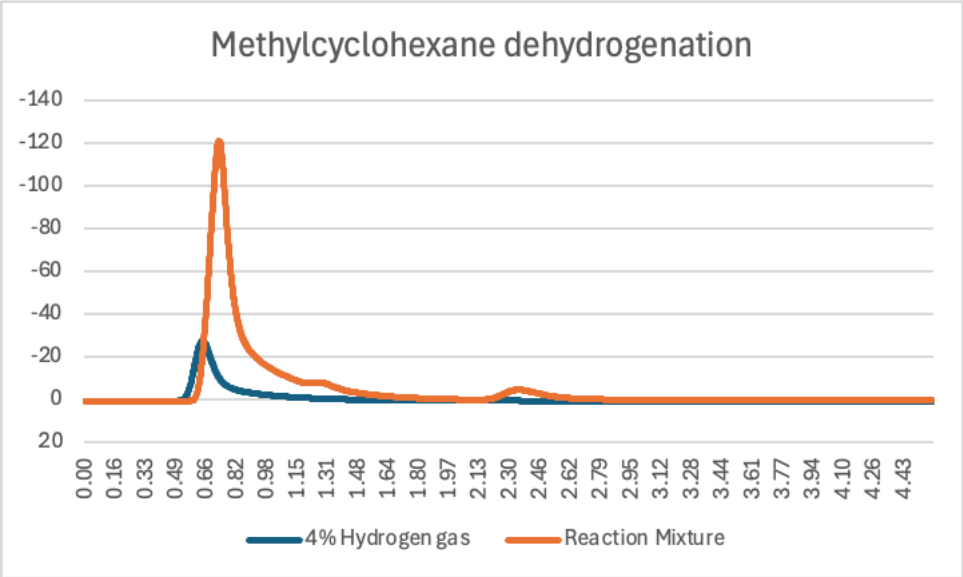

Figure S5. GC analysis chart for confirmation of hydrogen gas.

9. Procedure for Continuous Flow Reactions

A syringe pump [YSP-202 (Double syringe type)] equipped with a 10 mL syringe and needle was used to infuse the liquid reagents into a reactor coil fabricated from a high-purity perfluoroalkoxyalkane (PFA) and allowed to flow by 0.1 mL/min flow rate. The microreactor assembly was constructed of high-purity PFA tubing (JASCO cooperation, 1.0ID X 1/16'' OD 10 m, L = 10 meters, ID = 1.0 mm, V = 7.85 ml) in combination with Kessil Tuna Blue LEDs (40 W). The outlet of the microreactor led to the collection vial. The reactor was cooled with the help of a fan to maintain at room temperature. For substrates **2a** and **2c** (0.2 mmol), general procedure A was followed, and for substrate **2b** (0.2 mmol), general procedure B was followed. The reaction mixture was transferred to a 10 mL syringe inside the glove box and allowed to flow through the reactor. After pumping the reaction mixture to the reactor additional solvent was pumped using another syringe to take out the reaction mixture with the same flow rate. The detail of assembling the reactor is based on the literature and as shown in the pictures below.[7]

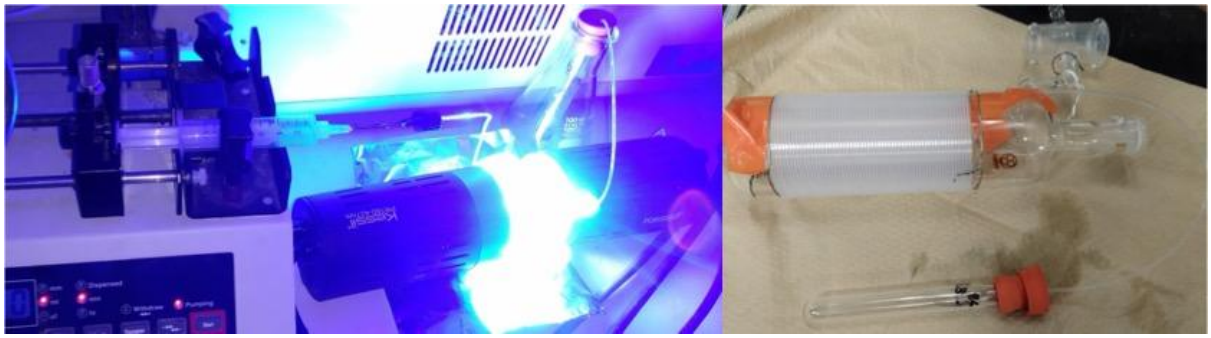

Figure S6. Representation of photo-flow reactor.

10. Procedure for Control Experiments

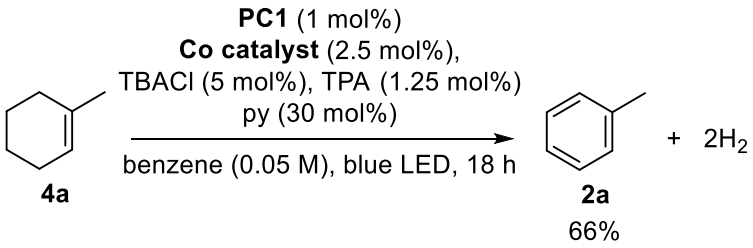

To an oven-dried screw-cap tube equipped with a magnetic stir bar were introduced 1-methyl-1-cyclohexene (**4a**: 0.019 g, 0.20 mmol), cobaloxime (**Co-1**: 0.0021 g, 0.005 mmol, 2.5 mol %), Iridium photocatalyst (**PC1**: 0.0022 g, 0.002 mmol, 1.0 mol %), TPA (0.0009 g, 0.0025 mmol, 1.25 mol %), Bu_4NCl (0.0028 g, 0.01 mmol, 5.0 mol %), pyridine (0.0047 g, 0.06 mmol, 30 mol %) and benzene (4.0 mL) was added inside the glove box. After taking out from the glove box, the resultant reaction mixture was subjected to blue LED irradiation and stirred for 18 h. The reaction was monitored by the GC analysis using *n*-decane as an internal standard. The GC yield was found to be 66%.

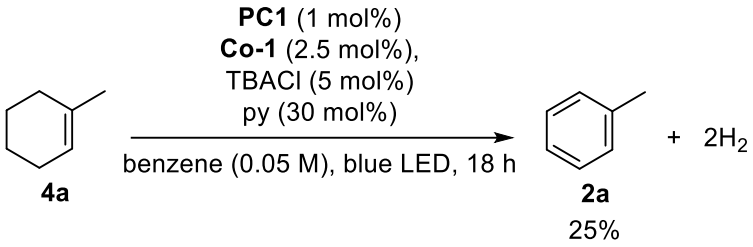

To an oven-dried screw-cap tube equipped with a magnetic stir bar were introduced 1-methyl-1-cyclohexene (**4a**: 0.019 g, 0.20 mmol), cobaloxime (**Co-1**: 0.0021g, 0.005 mmol, 2.5 mol %), Iridium photocatalyst (**PC1**: 0.0022 g, 0.002 mmol, 1.0 mol %), Bu_4NCl (0.0028 g, 0.01 mmol, 5.0 mol %) and pyridine (0.0047 g, 0.06 mmol, 30 mol %) inside the glove box. To the above mixture in the tube was added benzene (4.0 mL). The resultant reaction mixture was subjected to blue LED irradiation and stirred for 18 h. The reaction was monitored by the GC analysis using *n*-decane as an internal standard. The GC yield was found to be 25%, highlighting the crucial role of the TPA catalyst to promote the second HAT.

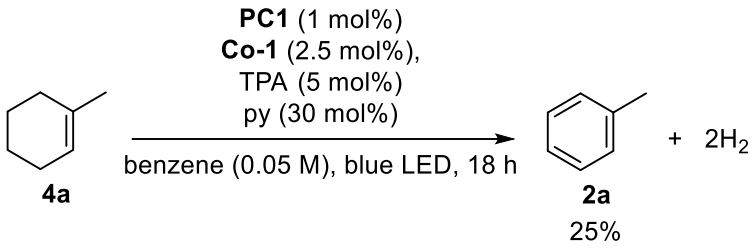

To an oven-dried screw-cap tube equipped with a magnetic stir bar were introduced 1-methyl-1-cyclohexene (**4a**: 0.019 g, 0.20 mmol), cobaloxime (**Co-1**: 0.0021g, 0.005 mmol, 2.5 mol %), iridium photocatalyst (**PC1**: 0.0022 g, 0.002 mmol, 1.0 mol %), TPA (3.64 mg, 0.01 mmol, 5 mol %), pyridine (0.0047 g, 0.06 mmol, 30 mol %) and the benzene (4.0 mL) was added inside the glove box. After taking out from the glove box, the resultant reaction mixture was subjected to blue LED irradiation and stirred for 18 h. The reaction was monitored by the GC analysis using *n*-decane as an internal standard. The GC yield was found to be 25%.

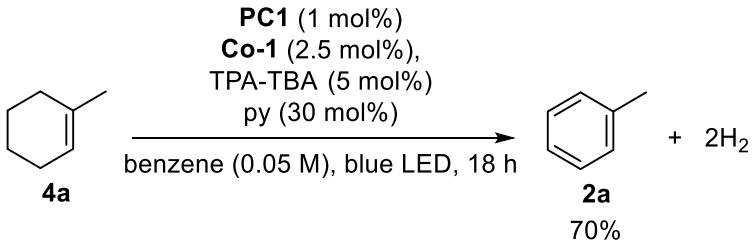

To an oven-dried screw-cap tube equipped with a magnetic stir bar were introduced 1-methyl-1-cyclohexene (**4a**: 0.019 g, 0.20 mmol), cobaloxime (**Co-1**: 0.0021g, 0.005 mmol, 2.5 mol %), iridium photocatalyst (**PC1**: 0.0022 g, 0.002 mmol, 1.0 mol %), TPA-TBA (6.0 mg, 0.01 mmol, 5 mol %), pyridine (0.0047 g, 0.06 mmol, 30 mol %) and benzene (4.0 mL) was added inside the glove box. After taking out from the glove box, the resultant reaction mixture was subjected to blue LED irradiation and stirred for 18 h. The reaction was monitored by the GC analysis using *n*-decane as an internal standard. The GC yield was found to be 70%.

11. Effect of *p*-Xylene Additive (Product Inhibition)

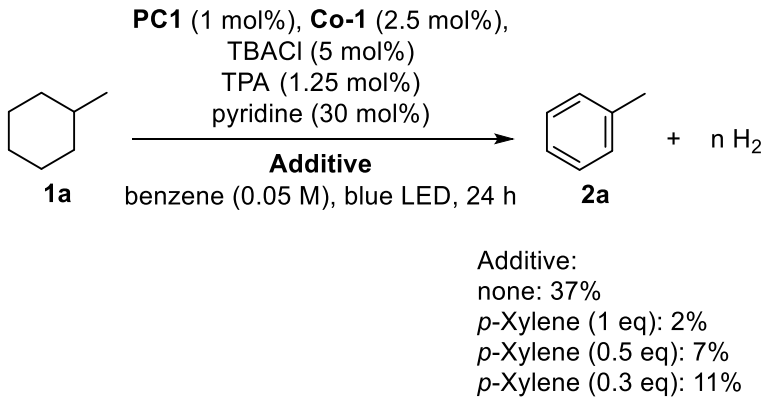

To an oven-dried screw-cap tube equipped with a magnetic stir bar, methylcyclohexene (**1a**: 25.5 μL, 0.20 mmol), cobaloxime (**Co-1**: 0.0021 g, 0.005 mmol, 2.5 mol %), Iridium photocatalyst (**PC1**: 0.0022 g, 0.002 mmol, 1.0 mol %), TPA (0.0009 g, 0.0025 mmol, 1.25 mol %), Bu_4NCl (0.0028 g, 0.01 mmol, 5.0 mol %), pyridine (0.0047 g, 0.06 mmol, 30 mol %), and benzene (4.0 mL) with *p*-xylene (0.3 eq, 0.5 eq, or 1 eq) were added inside the glove box. After removing from the glove box, the resultant reaction mixture was subjected to blue LED irradiation and stirred for 18 h. The reaction was monitored by the GC analysis using *n*-decane as an internal standard.

12. Time Resolved EPR Spectroscopy

X-band time-resolved electron paramagnetic resonance (TREPR) spectroscopy was performed using Bruker EMXPlus spectrometer in which the preamplifier has been replaced by a wide-band amplifier to enhance the time resolution at room temperature. Microwave frequency and power were 9.833 GHz and 5 mW, respectively. Photoexcitations were performed by the third harmonics (355 nm) of a Nd:YAG laser (Continuum, Minilite II; full width at half maximum of ~ 5 ns). A light depolarizer (Sigmakoki, DEQ-1N) was placed between the laser output and the optical window of the EPR cavity. Repetition rate and pulse energy were 10 Hz and 1 mJ/pulse, respectively. The mixture solutions of the samples were deoxygenated by the bubbling with argon gas and flowed by using a pump (Shimadzu, LC-20AD). The sample solutions were flowed through a quartz tube (o.d. = 5 mm) installed in the EPR cavity. The EPR signals were transferred to a digital oscilloscope (Tektronix, DPO3054) and then stored in a **PC**. The obtained TREPR data were background corrected and smoothed with the simple moving average at the window of 900 ns toward the time direction for denoising. Furthermore, the spectrum at 0 ns after laser excitations was subtracted from the TREPR spectra at each time.

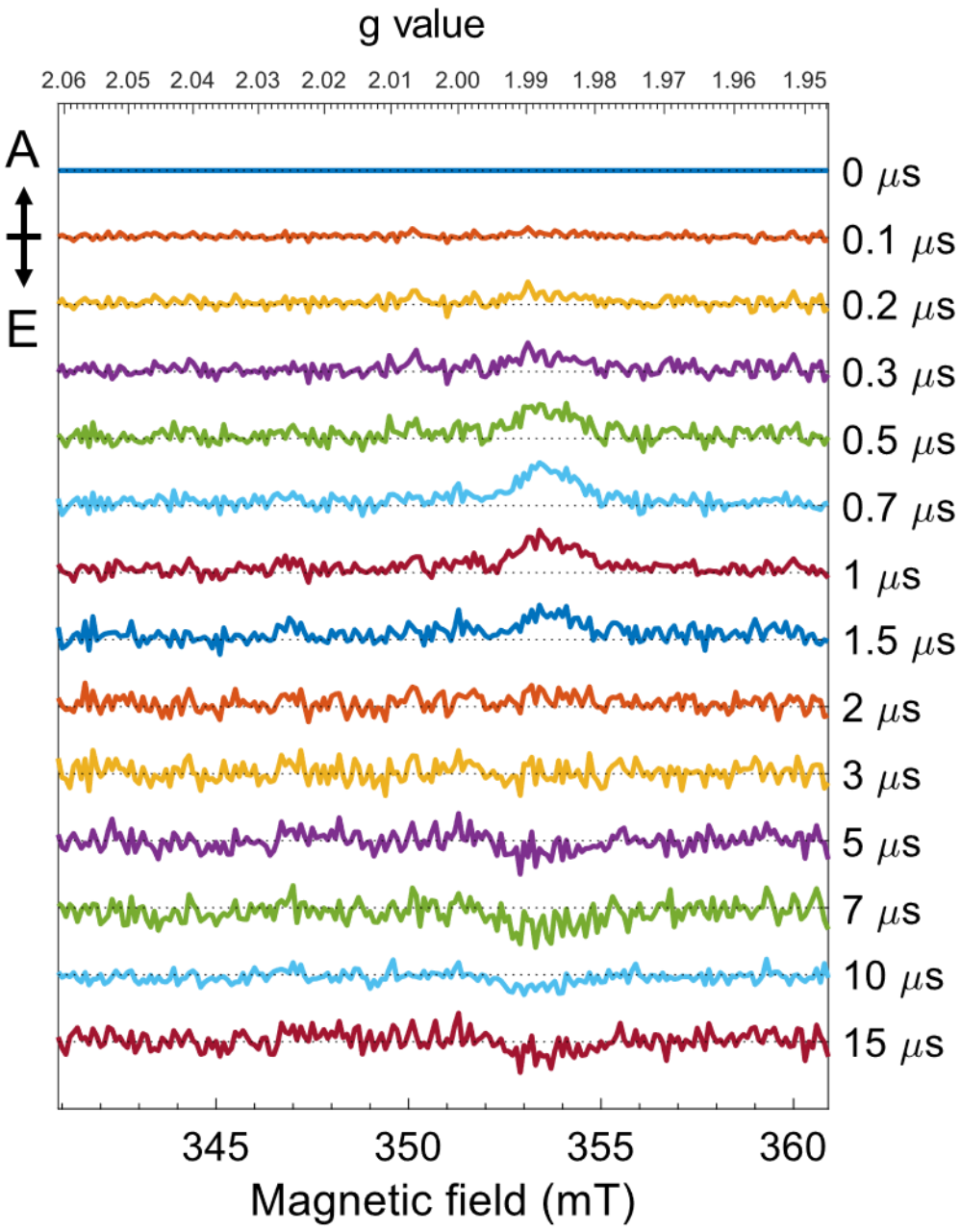

Figure S7. TREPR spectra of a mixture of **PC1** (0.0003 M) and TBACl (0.005 M) excited by 355 nm laser irradiations in benzene. Microwave absorption (A) is initially observed with respect to the baseline until 2 μs after laser irradiations. This absorptive signal appeared at around g = 1.988. This g value is in good agreement with a EPR signal (g = 1.9840) of reduced $Ir(ppy)_2(bpy)$ radical obtained under light irradiation.[8] Therefore, the initial absorptive signal is assigned to the reduced species of **PC1**, indicating that the photoinduced quick charge-separation takes place from the excited singlet state of ^{1}**PC1***

to Cl^{-}. The oxidized species (Cl radical-benzene complex) was not observed. This is probably because the dynamic tautomerization between chlorine radical-benzene π-complex and its adduct to benzene (6-chlorocyclohexadienyl radical) is causing a broadening of the EPR spectrum.[9]

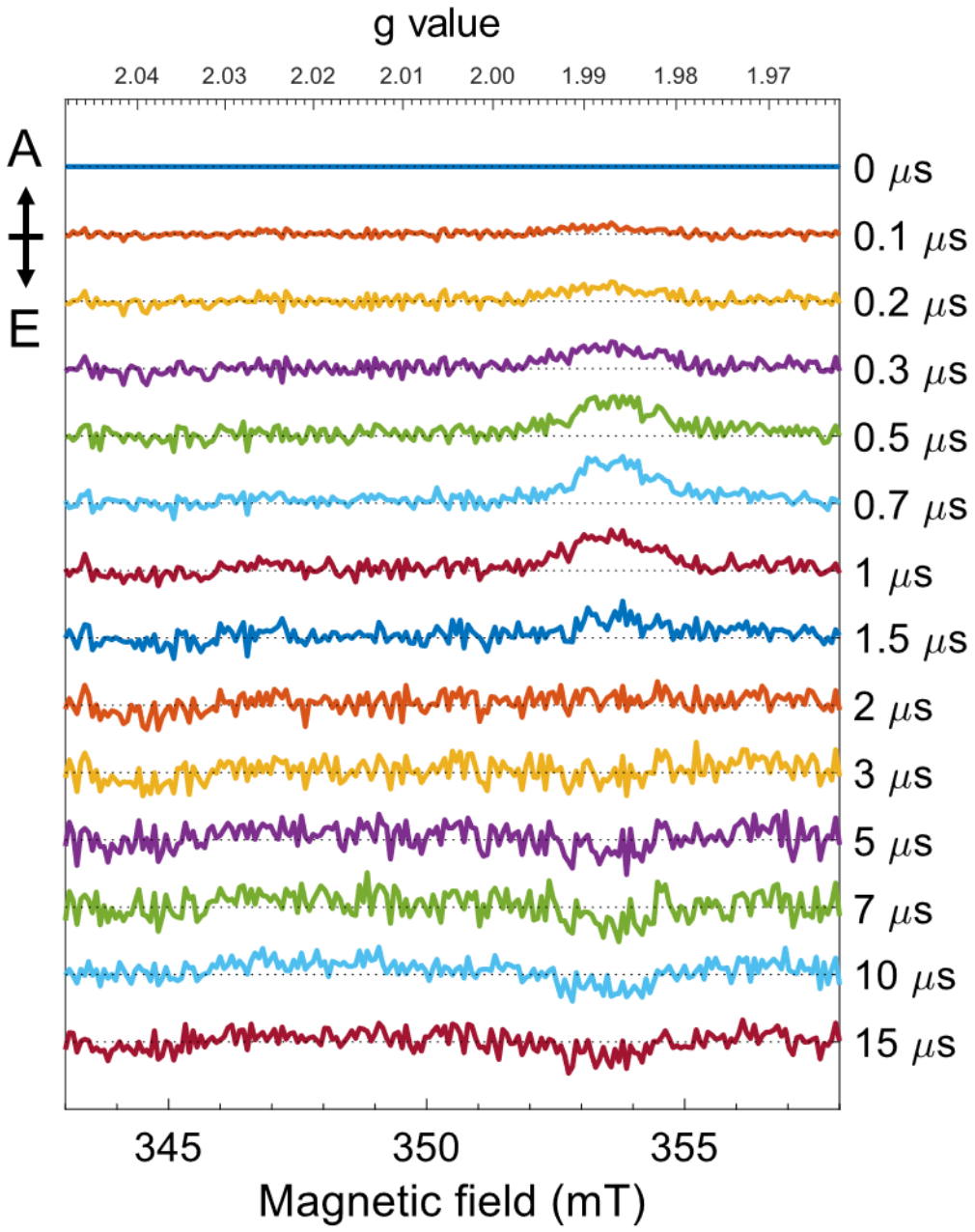

Figure S8. TREPR spectra of a mixture of **PC1** (0.0003 M), TBACl (0.005 M), and pyridine (0.03 M) excited by 355 nm laser irradiations in benzene. The absorptive signal was also

observed at around g = 1.988 immediately after laser irradiations and is assigned to the reduced species of **PC1**. The lack of the oxidized radical is also explained by the dynamic tautomerization effect.

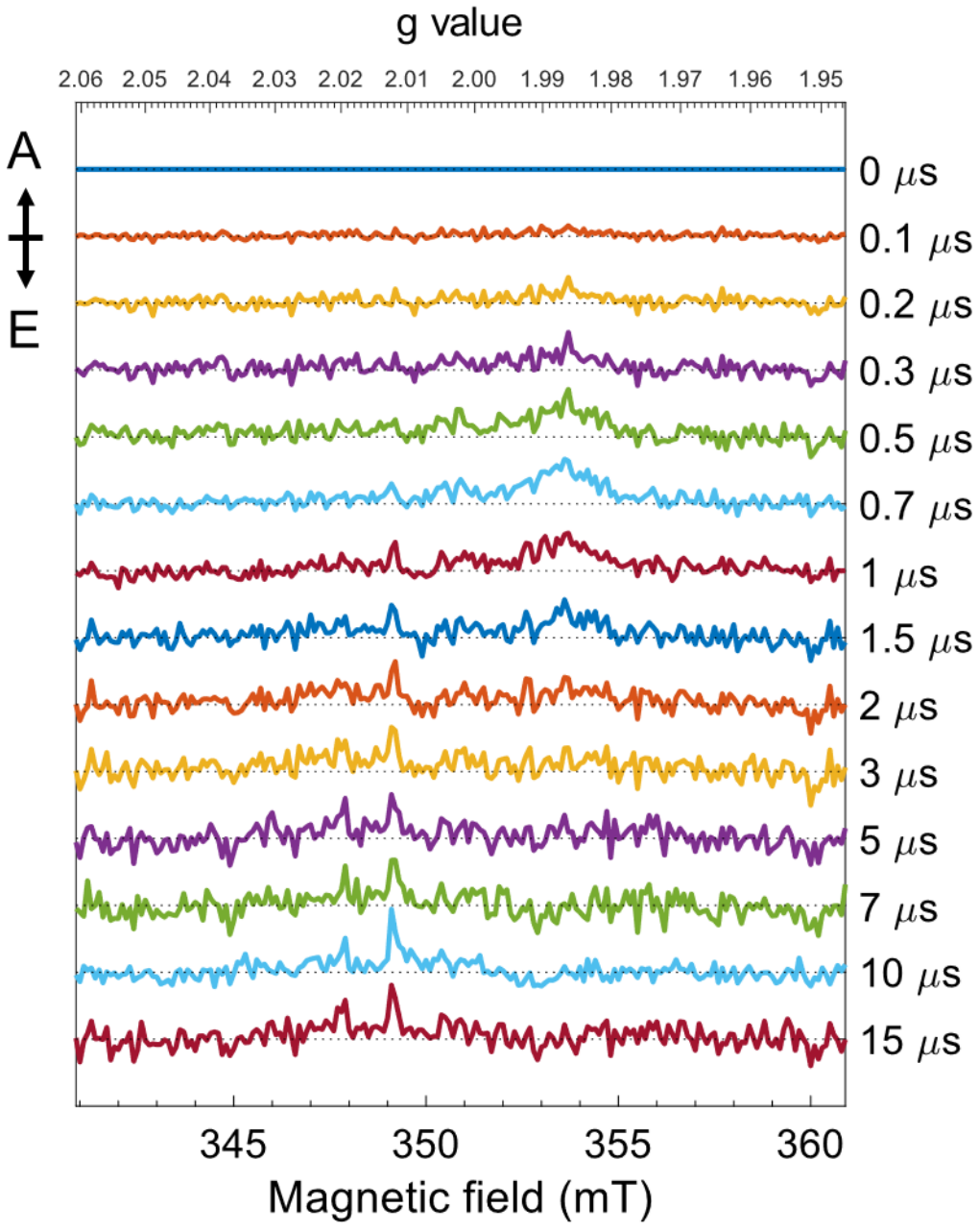

Figure S9. TREPR spectra of a mixture of **PC1** (0.0003 M), TBACl (0.005 M), pyridine (0.03 M), and TPA (0.0025 M) excited by 355 nm laser irradiations in benzene. In addition to the signal at around g = 1.988, the absorptive two peak signals emerged in a lower magnetic field

of g = 2.016 with hyperfine splitting by a_{hf} = 1.2 mT after 1 us. This g value and the hyperfine coupling constant well coincides with a thiyl radical of 7,7'-OMe-TPA, as reported previously.[10] This indicates that the two different charge-separation processes coexist: 1) between ^{3}**PC1*** and TBACl and 2) between ^{3}**PC1*** and TPA.

Ultrafast electron-transfer kinetics was observed (Figure S15), while the rise of the TPA radical was microseconds in the TREPR. This discrepancy is due to the fast radical dissociation from radical pairs in the complexes of TPA-**PC1** and Cl-**PC1** in picoseconds. If ultrafast electron-transfer is followed by fast dissociation, electron spin polarization after the singlet electron-transfer is hardly possible. When the singlet radical pair dissociates without spin polarization, there is no difference between the α and β spin populations. Thus, no TREPR signal is initially produced. The weak microwave absorption observed after microseconds can be interpreted as a thermal equilibrium state due to spin-lattice relaxation after the quick dissociation. The quicker rise of the PC radical than that of the TPA radical in the TREPR measurement is also interpreted by the shorter spin-relaxation in the PC radical because of larger g-anisotropy in the Ir complex.

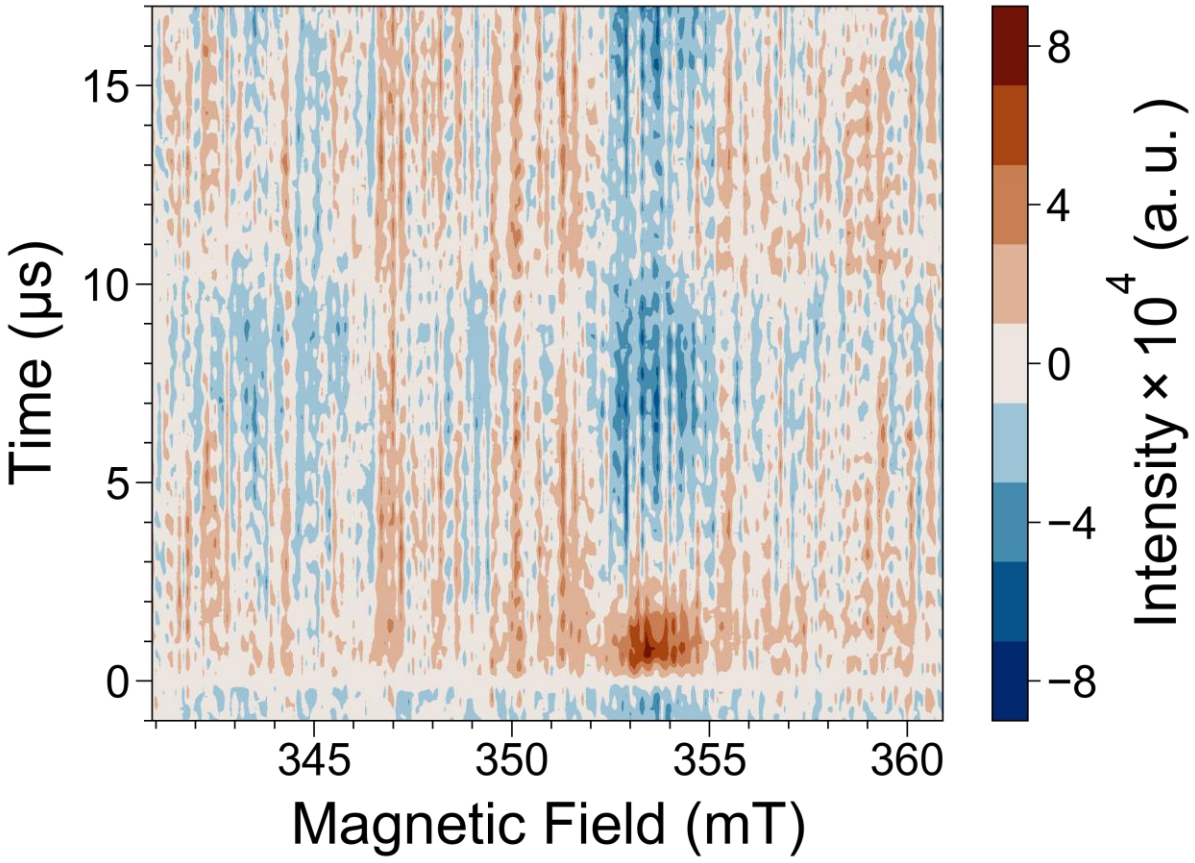

Figure S10. Two-dimensional data of the TREPR in Figure S7. The microwave absorption is indicated by the positive intensity (red map), while the emission is indicated by the negative intensity in the counter plot. The inversion of the spin polarization to the emission could be originating from the spin nutation effect introduced by the microwave.

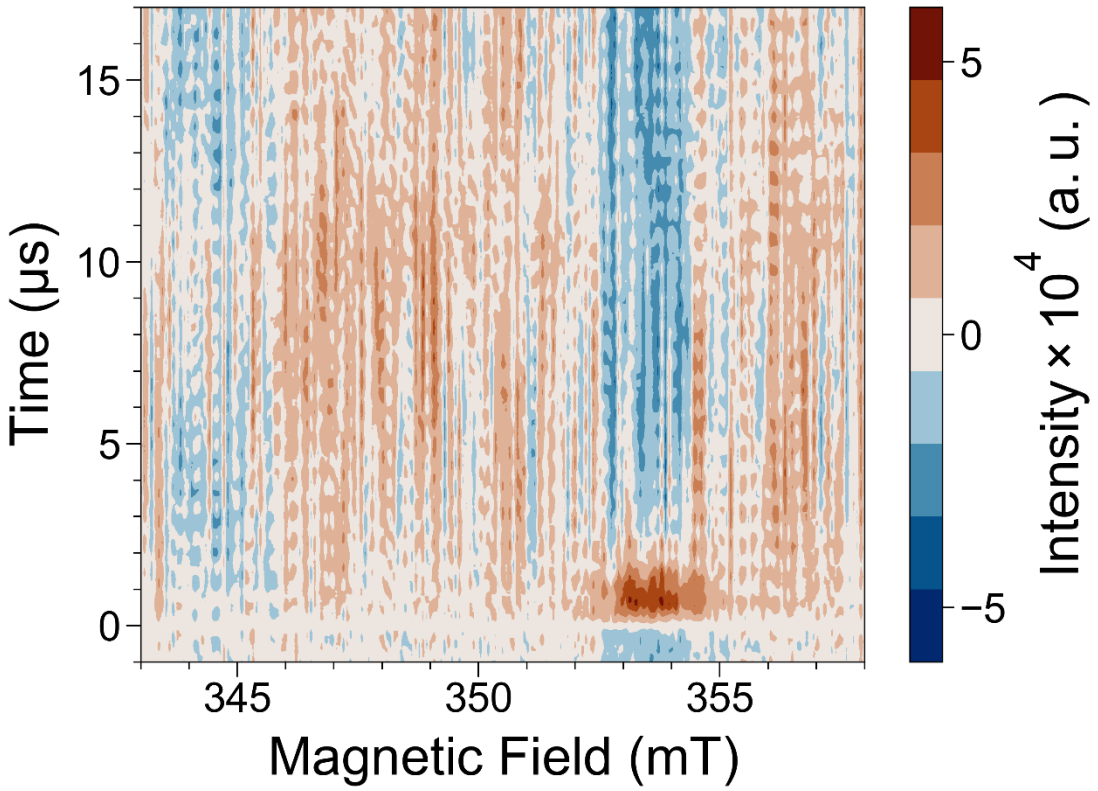

Figure S11. Two-dimensional data of the TREPR in Figure S8.

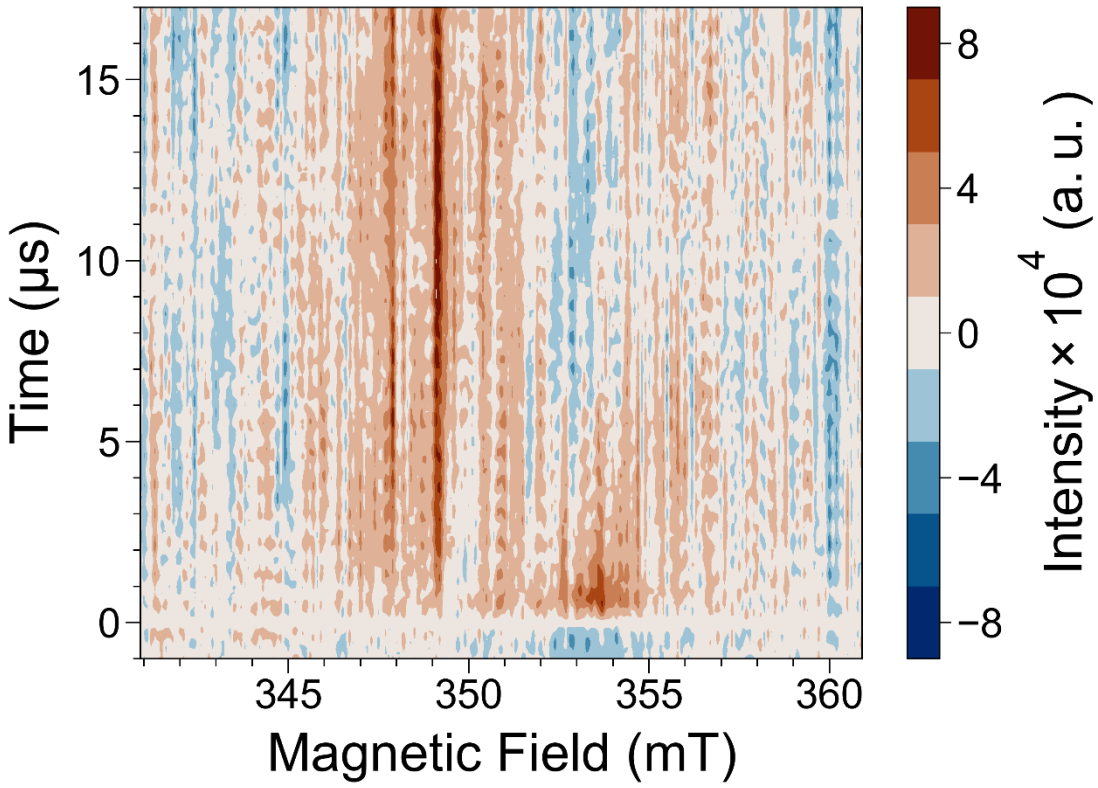

Figure S12. Two-dimensional data of the TREPR in Figure S9.

13. Transient Absorption Spectroscopy

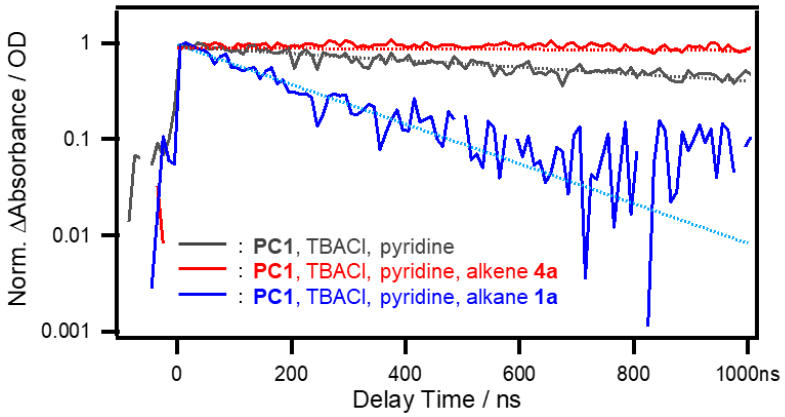

Condition	Time constant / ns	Standard Dev. / ns
a	1.22×10^3	58
b	1.3×10^4	3860
c	211	8.74

Figure S13. Time profiles of transient absorption of a mixture of **PC1** (0.0005 M), TBACl (0.000625 M), and pyridine (0.015 M) in benzene with and without MCH (**1a**, 0.05 M) or methylcyclohexene (**4a**, 0.05 M) at 400 nm with fitting curves (dotted lines) using single exponential decay as a model function. The sample was excited by a 2 μJ, 355 nm laser pulse with 800 ps duration at 500 Hz. Temporal changes in TA intensity indicate a decrease in chlorine radical-benzene π-complex concentration in the presence of **1a**. This observation suggests that the chlorine radical promotes hydrogen atom abstraction from a C–H bond of MCH after a specific delay time (100-600 ns). On the other hand, temporal changes of TA intensity in the presence of alkene **4a** showed a slower decay of the chlorine radical than in the absence of **1a** or **4a**. This result was likely due to the formation of an alkene π-complex between **4a** and the chlorine radical, stabilizing the chlorine radical and retarding the HAT process. [12]

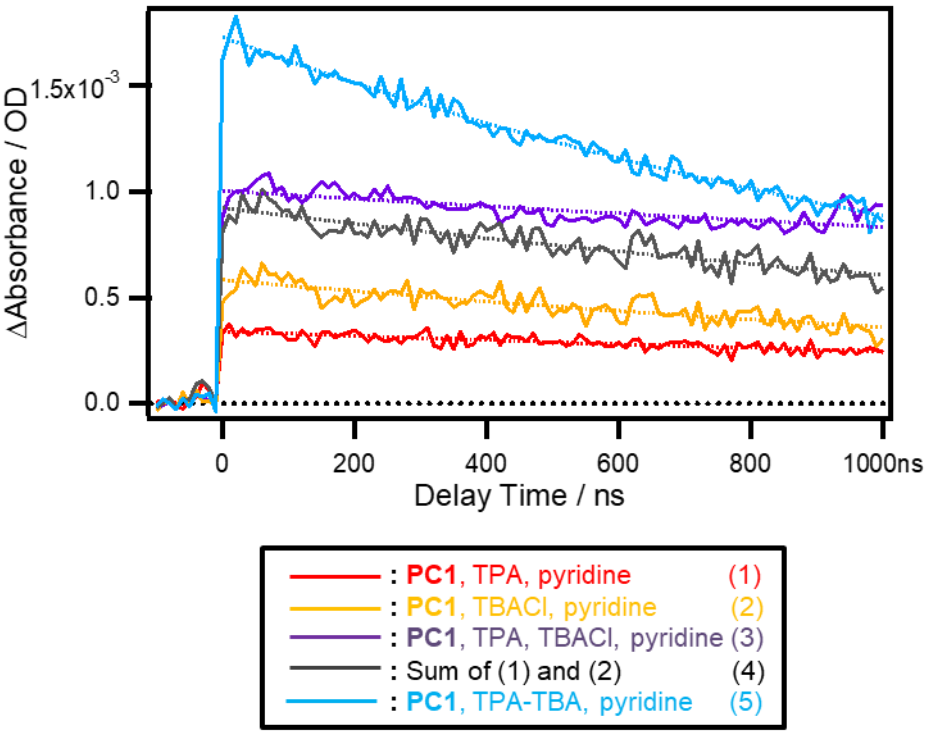

Condition	Time constant / ns	Standard Dev. / ns
(1)	3.1 x 10^3	260
(3)	5.4 x 10^3	487
(2)	2.1 x 10^3	144
(5)	1.50 x 10^3	25.6
((1) + (2))	2.4 x 10^3	132

Figure S14. Time profiles of transient absorption of a mixture of **PC1** (0.0005 M), TPA (0.000156 M), and pyridine (0.015 M) in benzene (red line, 1); a mixture of **PC1** (0.0005 M), TBACl (0.000625 M), and pyridine (0.015 M) in benzene (orange line, 2); a mixture of **PC1** (0.0005 M), TPA (0.000156 M), TBACl (0.000625 M), and pyridine (0.015 M) in benzene (purple line, 3); and a mixture of **PC1** (0.0005 M), TPA-TBA (0.000156 M), and pyridine (0.015 M) in benzene (light blue line, 5) at 400 nm with fitting curves (dotted lines) using single exponential decay as a model function. The sample was excited by a 2 μJ, 355 nm laser pulse with 800 ps duration at 500 Hz, and the transient absorption intensities at 400 nm, which

correspond to the absorption of chlorine radical-benzene π-complex[11] and TPA-thiyl radical[10] are shown. The black line (4) is the sum of the transient absorption intensities of (1) and (2). The dotted lines correspond to the fitting curves assuming single exponential decay as a model function.

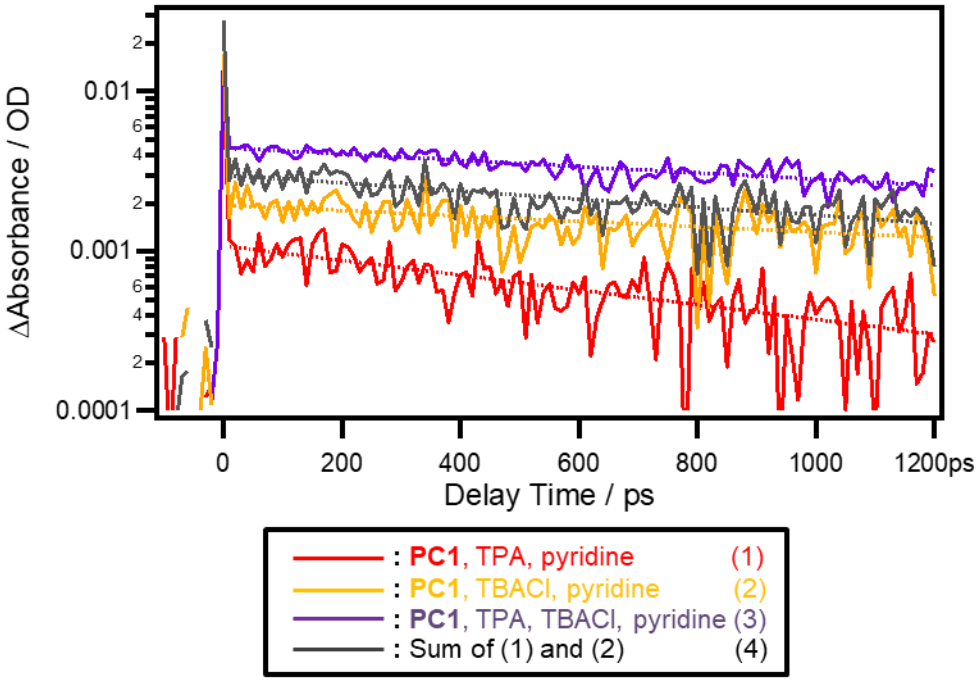

Condition	Time constant / ps	Standard Dev. / ps
(1)	9.4×10^2	80.5
(3)	2.2×10^3	146
(2)	2.6×10^3	470
((1) + (2))	1.7×10^3	173

Figure S15. Time profiles of transient absorption of a mixture of **PC1** (0.0005 M), TPA (0.000156 M), and pyridine (0.015 M) in benzene (red line, 1), a mixture of **PC1** (0.0005 M), TBACl (0.000625 M), and pyridine (0.015 M) in benzene (orange line, 2), and a mixture of **PC1** (0.0005 M), TPA (0.000156 M), TBACl (0.000625 M), and pyridine (0.015 M) in benzene (purple line, 3) at 400 nm with fitting curves (dotted lines) using single exponential decay as a

model function. The sample was excited by a 2 μJ, 355 nm laser pulse with 90 fs duration at 500 Hz, and the averaged intensity at 395-405 nm, which corresponds to the absorption of chlorine radical-benzene π-complex[11] and TPA-thiyl radical[10] are shown. The black line (4) is the sum of the transient absorption intensities of (1) and (2). Picoseconds ultrafast electron-transfer kinetics were observed. Similarly to the results of nanosecond TA experiments (Fig. S8), the transient absorption intensity under the coexistence of TPA and TBACl [condition (3) in Figs S16, 7d, and S14; purple lines] was greater than the sum of the absorption intensities [(4); black lines] of TPA only [(1); red lines] and TBACl only [(2); orange lines]. This result suggests synergistic effects between TPA and TBACl in enhancing the total radical concentration also at the picosecond scale.

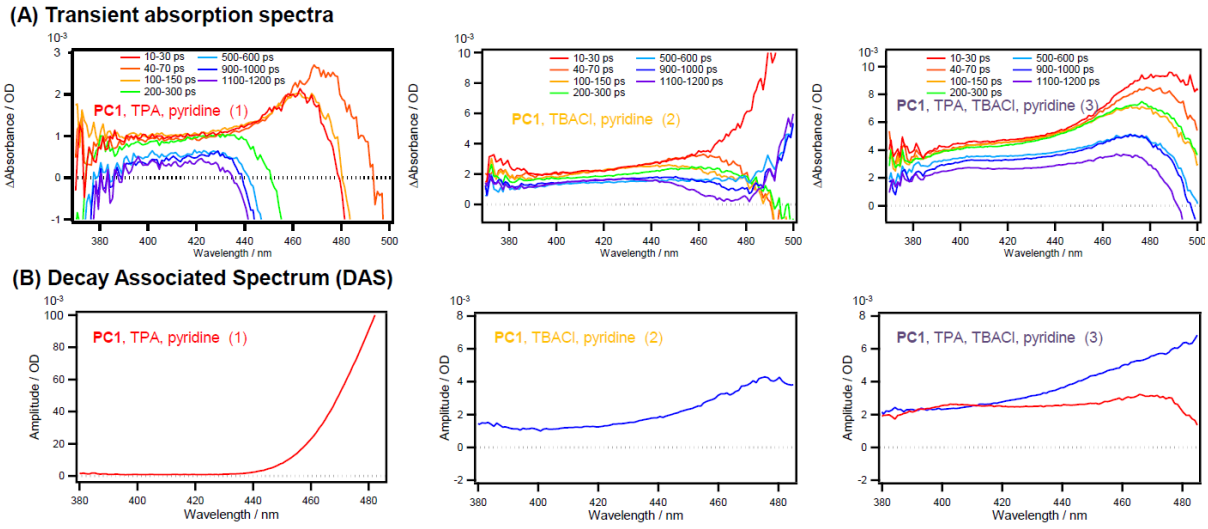

Figure S16. A global analysis of the TA results shown in Figure S15 was performed using the GLOTARAN software[13] with the sum of exponential decay components as a fitting function. The obtained decay associated spectra (DAS) of the TPA thiyl radical (red) and chlorine radical-benzene π-complex (blue) under conditions (1), (2), and (3) are shown in Figure S16B (same as Fig. 7e). (A) Transient absorption spectra. See Figure S15 for detailed conditions. (B) Decay associated spectra (DAS).

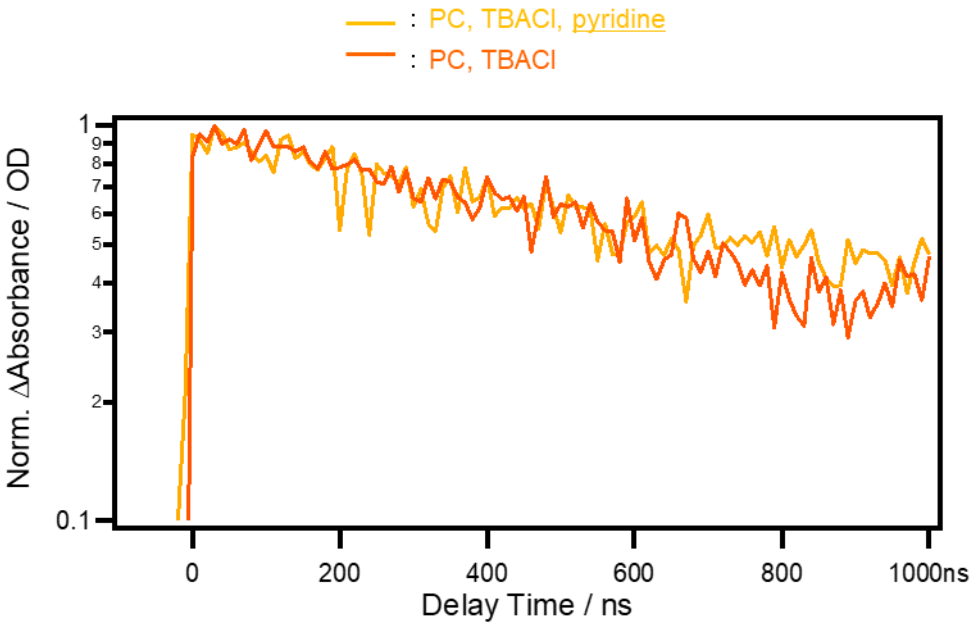

Figure S17. Effects of pyridine additive for chlorine radical generation. Time profiles of transient absorption of a mixture of **PC1** (0.0005 M) and TBACl (0.000625 M) in benzene with and without pyridine (0.015 M) at 400 nm. The sample was excited by a 2 μJ, 355 nm laser pulse with 800 ps duration at 500 Hz.

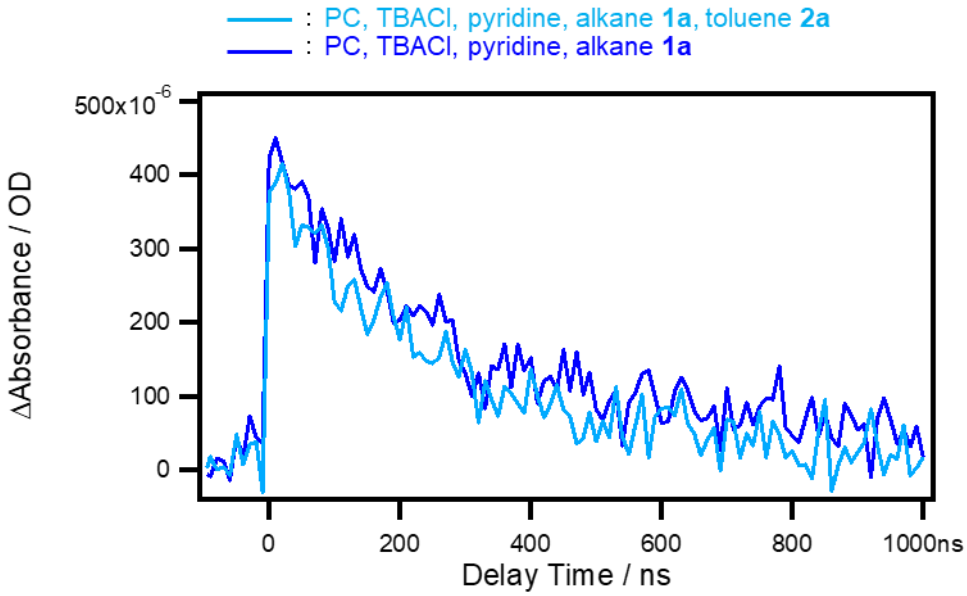

Figure S18. Time profiles of transient absorption of a mixture of **PC1** (0.0005 M), TBACl (0.000625 M), pyridine (0.015 M), and methylcyclohexane (**1a**, 0.05 M) in benzene with and without toluene (**2a**, 0.25 M) at 400 nm. The sample was excited by a 2 μJ, 355 nm laser pulse with 800 ps duration at 500 Hz. A slight decrease in chlorine radical concentration was observed by adding **2a**, suggesting that the C-H abstraction of **2a**, the product of complete dehydrogenation, competes in the HAT process.

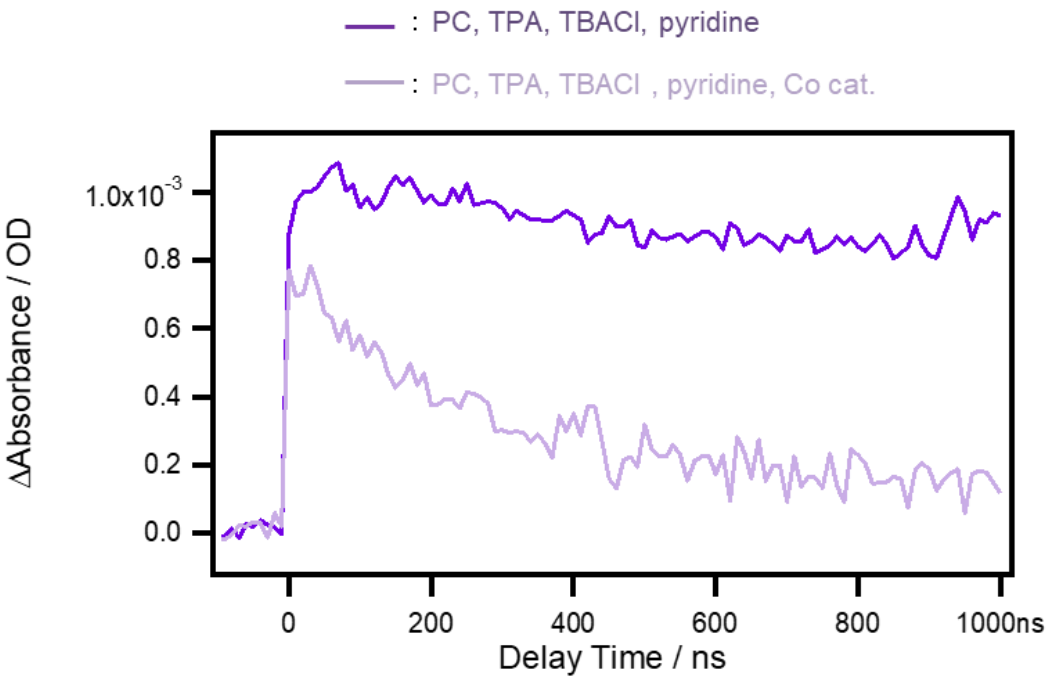

Figure S19. Effect of **Co-1** on the concentration of chlorine and TPA radicals. Time profiles of transient absorption of a mixture of **PC1** (0.0005 M), TBACl (0.000625 M), TPA (0.000156 M), and pyridine (0.015 M) in benzene with and without **Co-1** (0.0003125 M) at 400 nm. The sample was excited by a 2 mJ, 355 nm laser pulse with 800 ps duration at 500 Hz.

The transient absorption intensity, corresponding to the concentrations of chlorine and TPA radicals, decreased but was still significantly observed especially in the early delay times. Furthermore, the following results support that **Co-1** decreased the concentration of chlorine radical, but still a significant concentration of chlorine radical existed for HAT to proceed.

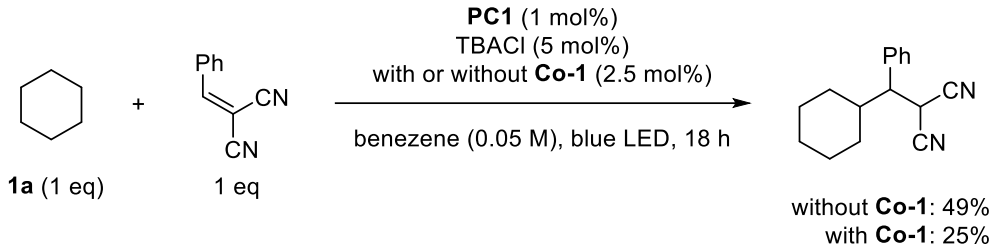

14. NMR experiments

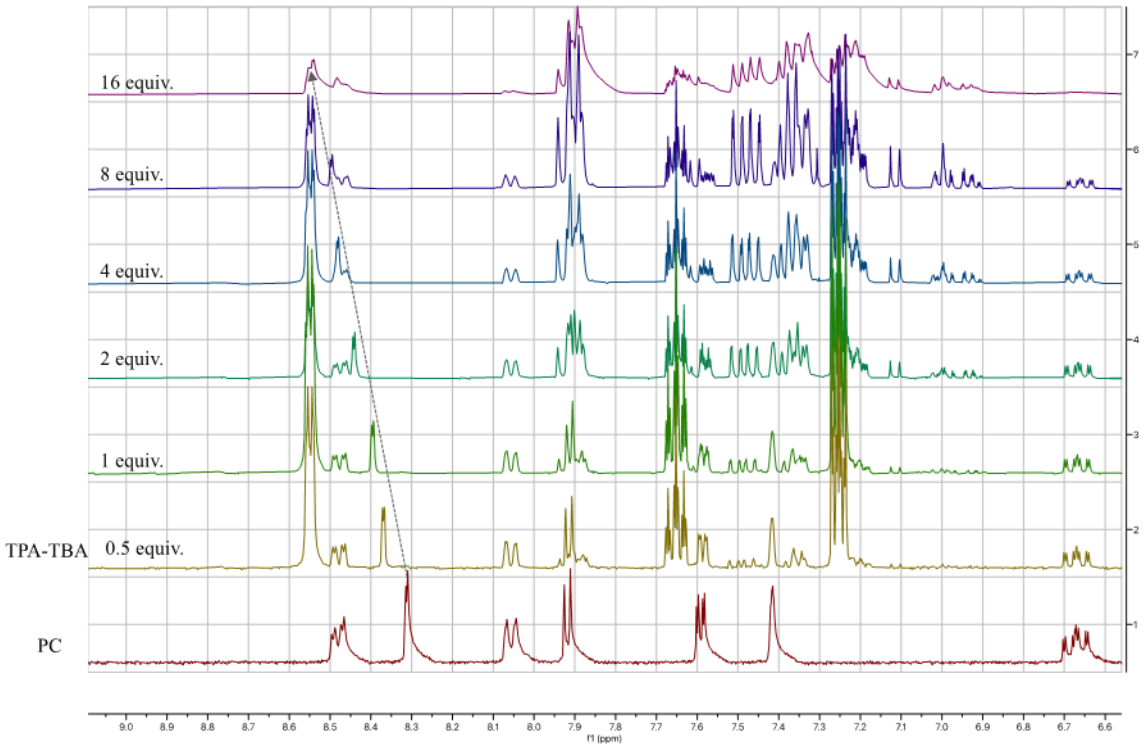

Figure S20. The ^{1}H NMR titration of increasing amounts of TPA-TBA (bottom to top) into a solution of **PC1**. In an oven-dried glass vial iridium photocatalyst (**PC1**: 0.0022 g, 0.002 mmol), pyridine (0.0047 g, 0.06 mmol), and varying concentrations of TPA-TBA salt were dissolved in CD_2Cl_2 (1 mL) inside the glove box. The samples were taken out from the glove box and subjected to NMR analysis. The gradual downfield chemical shift was observed upon increasing the concentration of TPA-TBA, indicating the interaction with the photocatalyst.

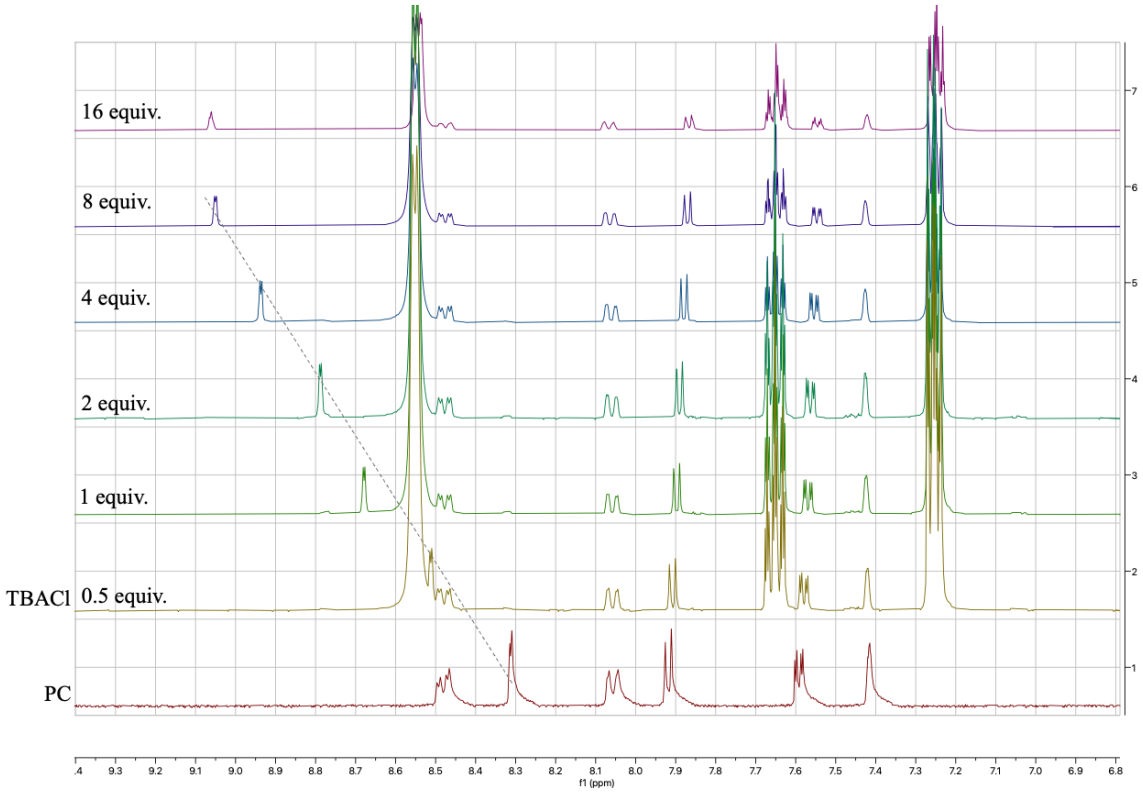

Figure S21. The ^{1}H NMR titration of increasing amounts of TBACl (bottom to top) into a solution of **PC1**. In an oven-dried glass vial iridium photocatalyst (**PC1**: 0.0022 g, 0.002 mmol), pyridine (0.0047 g, 0.06 mmol), and varying concentrations of TBACl were dissolved in CD_2Cl_2 (1 mL) inside the glove box. The samples were taken out from the glove box and subjected to NMR analysis. The gradual downfield chemical shift was observed upon increasing the concentration of TBACl, indicating the interaction with the photocatalyst.

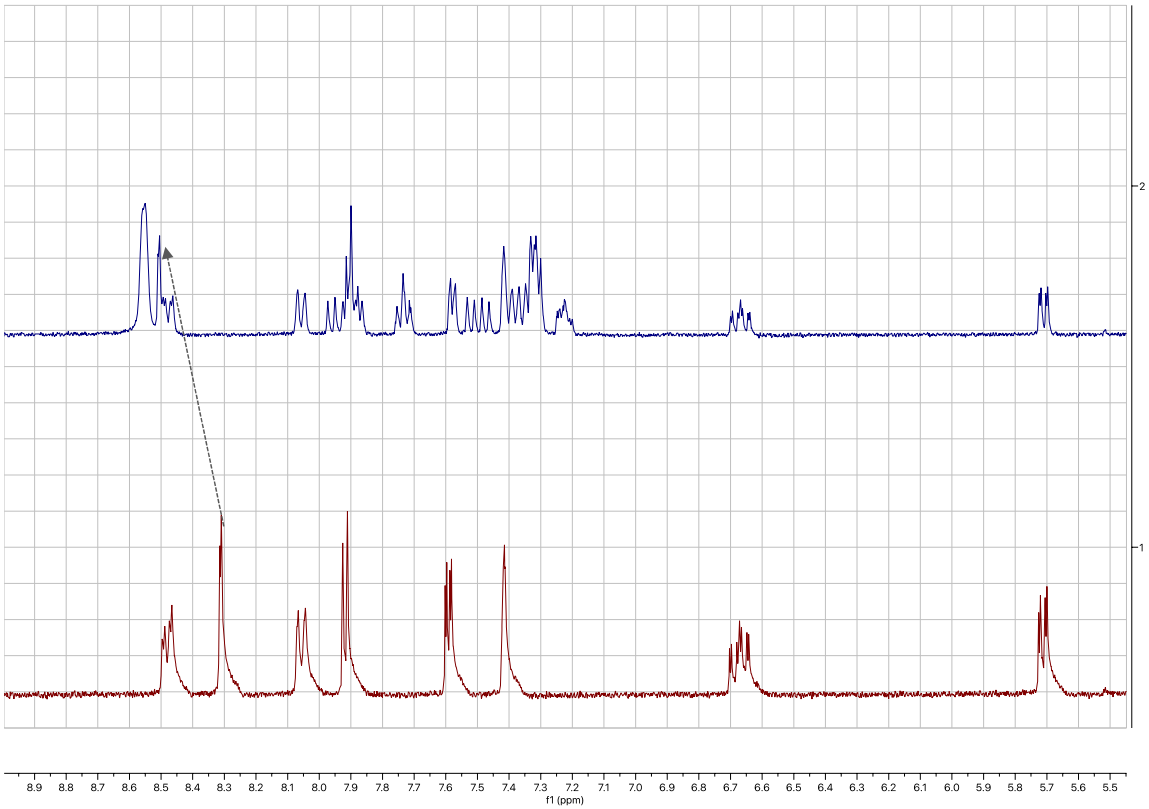

Figure S22. The ^{1}H NMR spectra of **PC1**, TBACl, TPA, and pyridine (upper chart) and **PC1** in pyridine (bottom chart). In an oven-dried glass vial iridium photocatalyst (**PC1**: 0.0022 g, 0.002 mmol), pyridine (0.0047 g, 0.06 mmol), TPA (0.72 mg, 0.002 mmol), and TBACl (0.55 mg, 0.002 mmol) were dissolved in CD_2Cl_2 (1 mL) inside the glove box. The samples were taken out from the glove box and subjected to NMR analysis. The observed downfield chemical shift (Δ = 0.189 ppm) was between the Δ values observed for a mixture of **PC1** + TPA-TBA (Δ = 0.131 ppm) and a mixture of **PC1** + TBACl (Δ = 0.475 ppm). This result suggests the coexistence of Cl-**PC1** and TPA-**PC1**. These complexes generate chlorine-benzene π-complex and TPA radical, respectively, by photoirradiation.

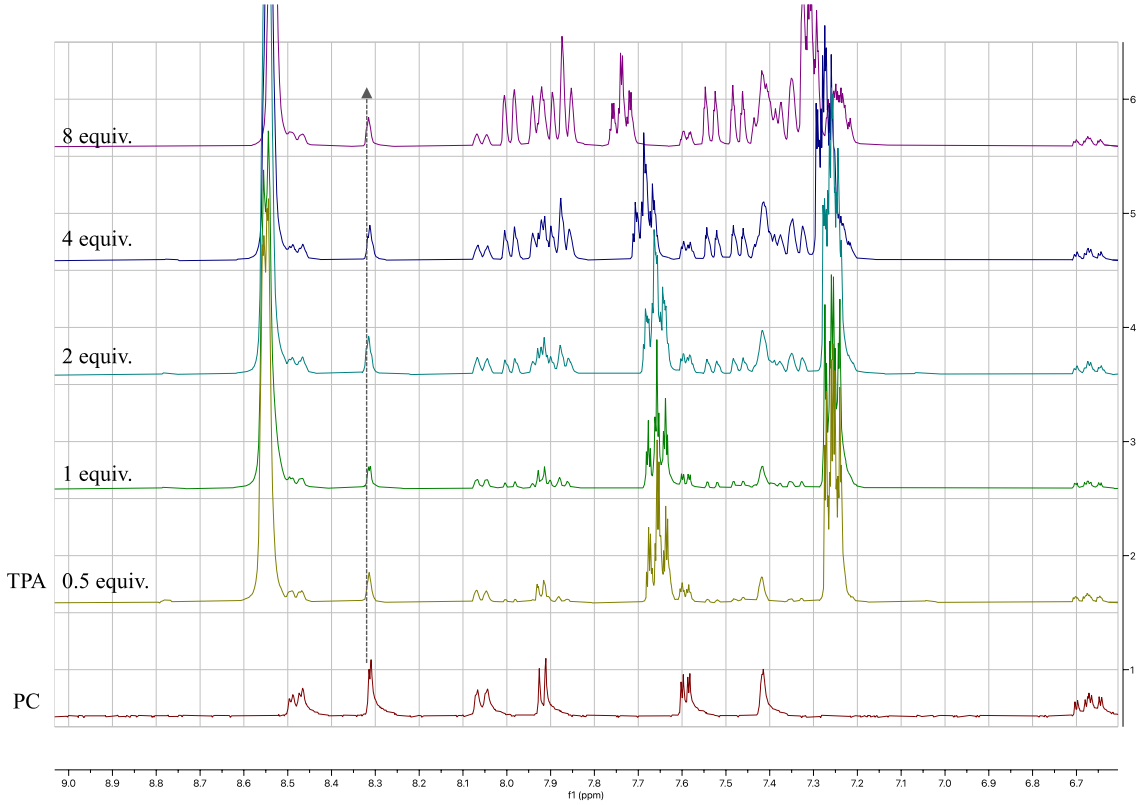

Figure S23. The ^{1}H NMR titration of increasing amounts of TPA (bottom to top) into a solution of **PC1**. In an oven-dried glass vial iridium photocatalyst (**PC1**: 0.0022 g, 0.002 mmol), pyridine (0.0047 g, 0.06 mmol), and varying concentrations of TPA were dissolved in CD_2Cl_2 (1 mL) inside the glove box. The samples were taken out from the glove box and subjected to NMR analysis. Increasing the concentration of TPA did not result in any spectral changes, suggesting undetectable interactions between **PC1** and TPA-py.

15. Absorption spectra

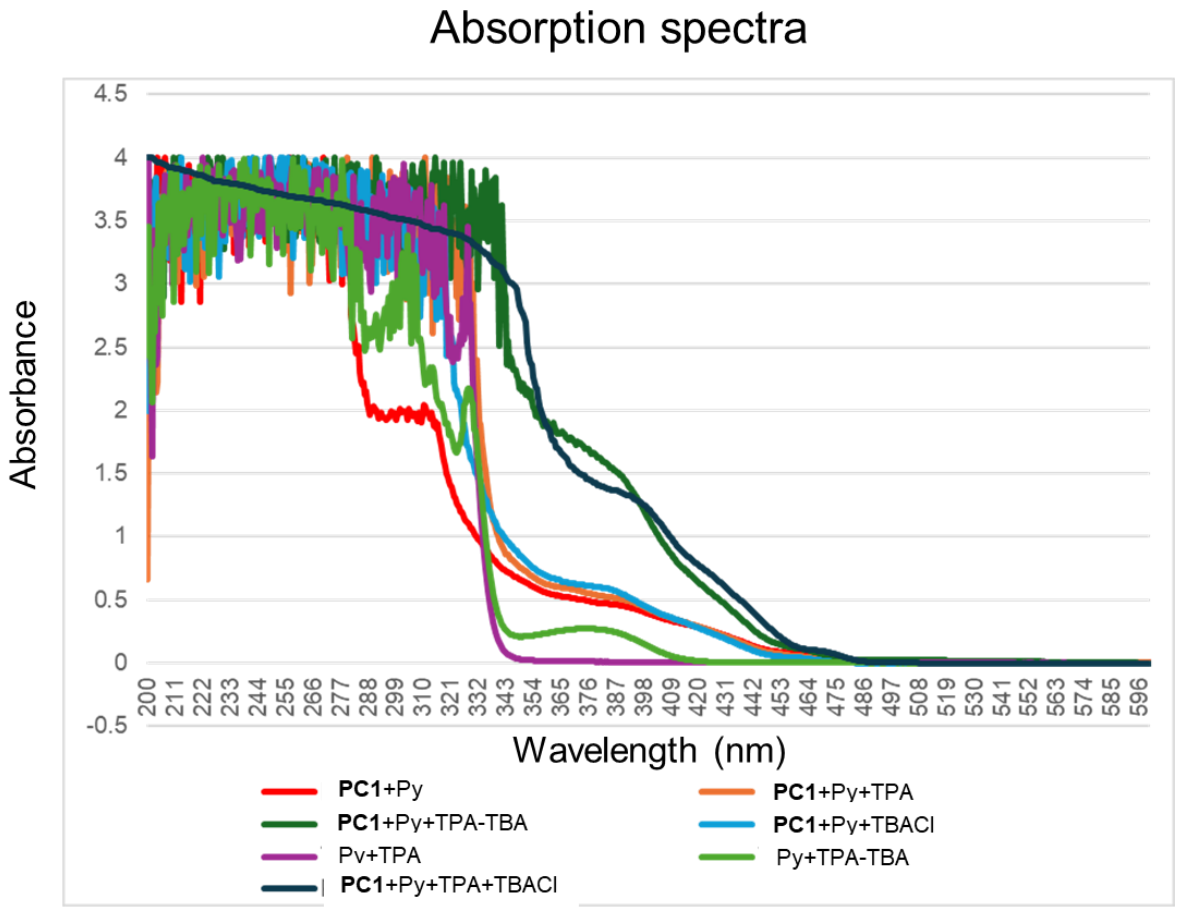

Figure S24. Absorption spectra of a mixture of **PC1** (0.0005 M) + pyridine (0.015 M) in benzene (red line), **PC1** (0.0005 M) + TPA (0.000156 M) + pyridine (0.015 M) in benzene (orange line), **PC1** (0.0005 M + TPA-TBA (0.000156 M) + pyridine (0.015 M) in benzene (green line), **PC1** (0.0005 M) + TBACl (0.000625 M) + pyridine (0.015 M) in benzene (light blue line), TPA (0.000156 M) + pyridine (0.015 M) in benzene (purple line), TPA-TBA (0.000156 M) + pyridine (0.015 M) in benzene (yellow green line), and **PC1** (0.0005 M) + TPA (0.000156 M) + TBACl (0.000625 M) + pyridine (0.015 M) in benzene (dark blue line). There is a large charge transfer (CT) band at around 380 nm in conditions of green line and dark blue line, when **PC1**, TPA, and TBA coexisted. This result suggests the facile formation of TPA-**PC1** in the presence of TBA. There is a small CT band at around 380 nm in conditions

of light blue line. This result suggests the formation of Cl-**PC1**. These data are consistent with NMR results.

16. Redox profiles

$[Ir(dF(CF_3)ppy)_2(dtbbpy)]^+$ (**PC1**)	$E_{1/2}^{M*/M-}$ = +1.21 V vs SCE
TBACl	$E_{1/2}^{ox}$ = +2.03 V vs SCE
TPA	$E_{1/2}^{ox}$ = +1.69 V vs SCE

The reduction potential of the triplet state of excited **PC1** is +1.21 V vs SCE.[14] Therefore, **PC1** can hardly oxidize TBACl (+2.03 V vs SCE)[15] or TPA (+1.69 V vs SCE)[16] from the excited triplet state. However, picosecond-scale transient absorption experiments (Figure S15) indicate rapid electron transfer. The rapid SET between **PC1** and chloride or **PC1** and TPA, is perhaps facilitated by the formation of Cl-**PC1** and TPA-**PC1** complexes, as was evidenced by NMR (Figure S20-23) and absorption experiments (Figure S24). These rapid SETs would proceed from the excited singlet state. This is because the CT state energy is estimated to be 3.2 eV from the 380 nm band in Figure S24, which is higher than the triplet exciton energy of 2.6 eV, [14] resulting in reduction potential of $E_{1/2}^{M*/M-}$ > 1.8 V to enable the oxidations of TPA and Cl^-. In addition, entropy gain is expected on the exergonic radical dissociation from the excited CT state for the efficient chlorine-benzene π-complex and TPA radical generations by photoirradiation.

17. ^{1}H and ^{13}C NMR Spectra

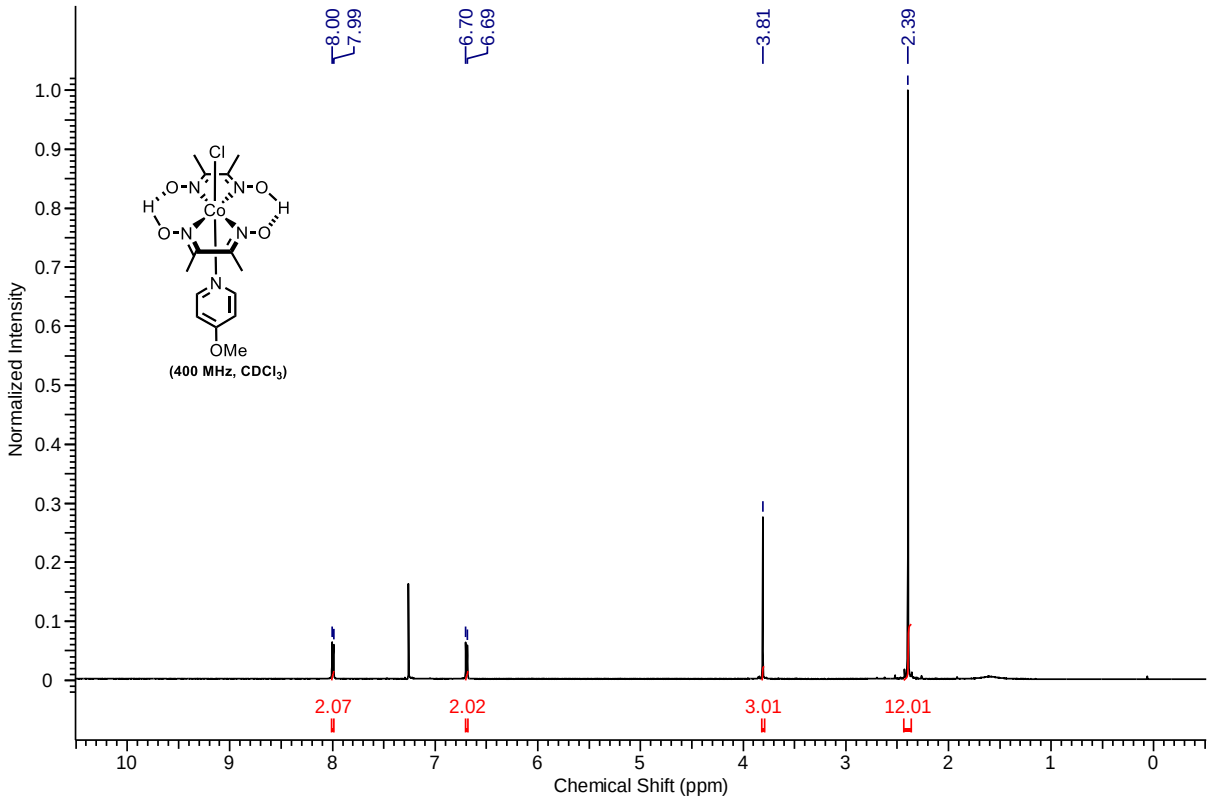

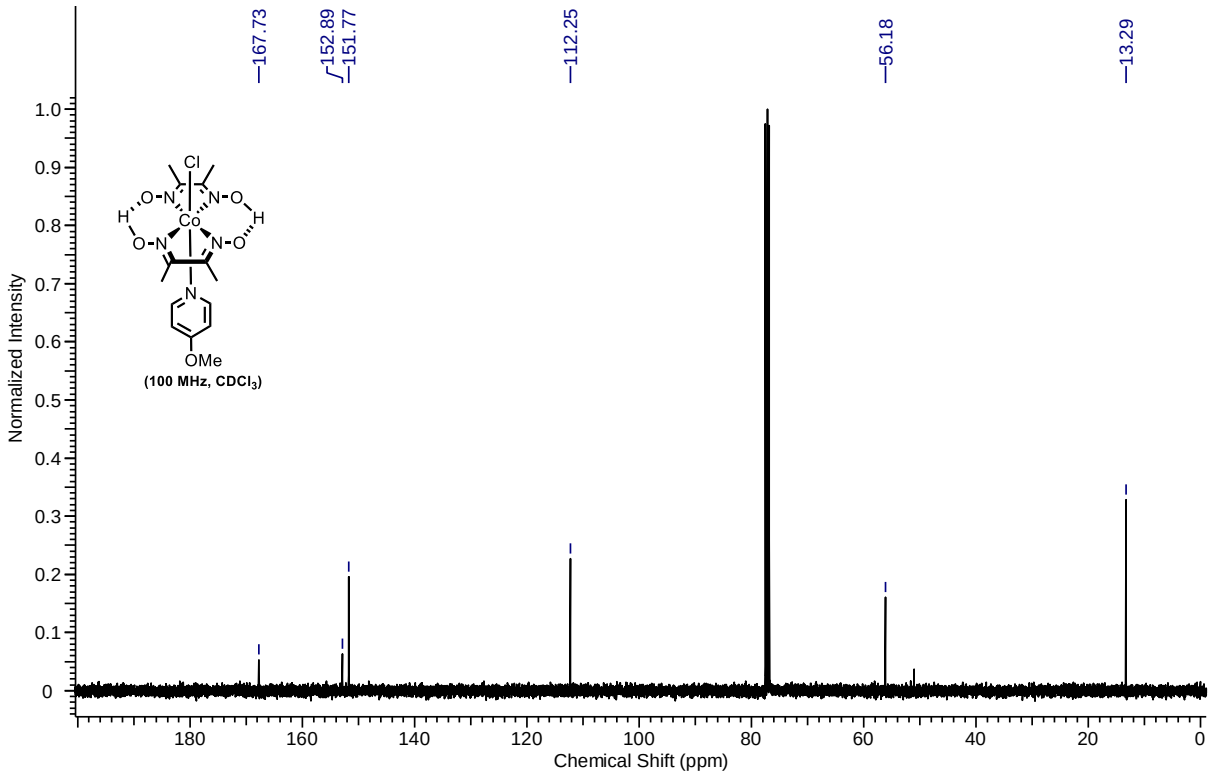

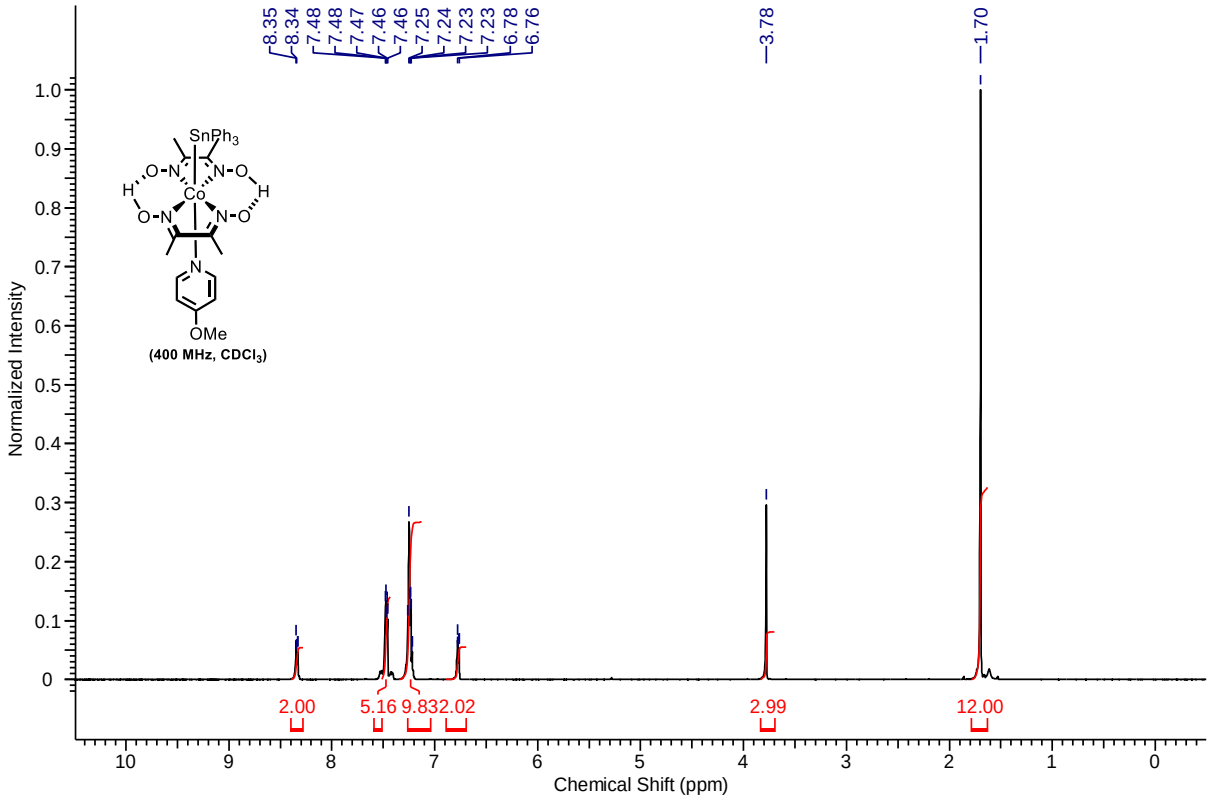
8.35
8.34
7.48
7.48
7.47
7.46
7.46
7.25
7.24
7.23
7.23
6.78
6.76
3.78
1.70
SnPh3
Co
OMe
(400 MHz, CDCl3)
Normalized Intensity
Chemical Shift (ppm)
2.00
5.16
9.83
2.02
2.99
12.00

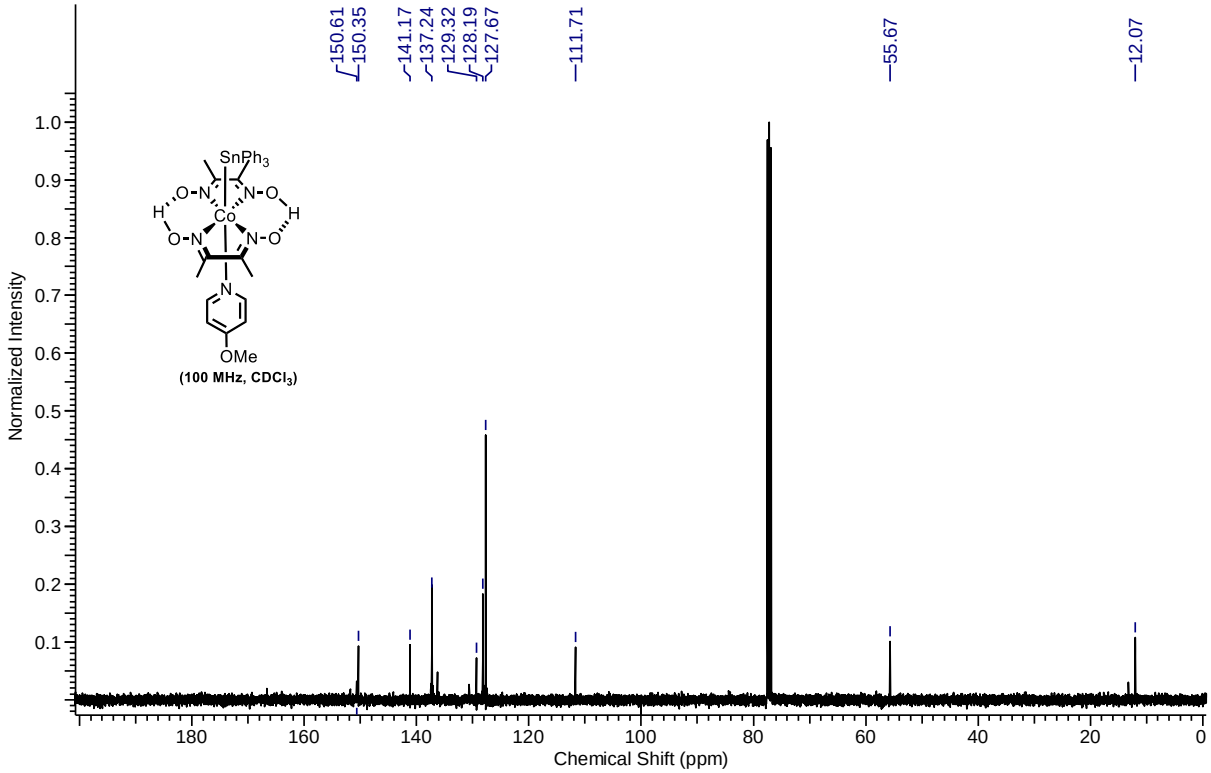
150.61
150.35
141.17
137.24
129.32
128.19
127.67
111.71
55.67
12.07
SnPh3
Co
OMe
(100 MHz, CDCl3)
Normalized Intensity
Chemical Shift (ppm)

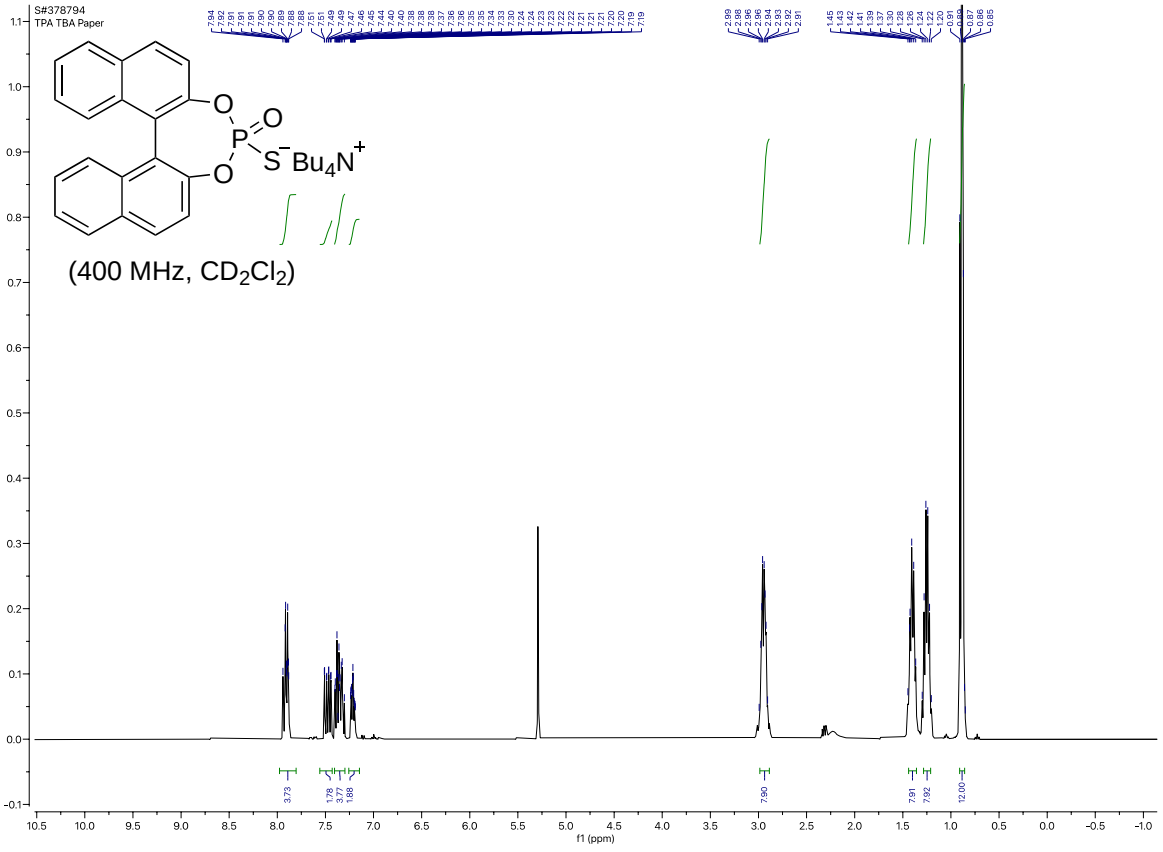
S#378794
TPA TBA Paper
(400 MHz, CD2Cl2)
f1 (ppm)

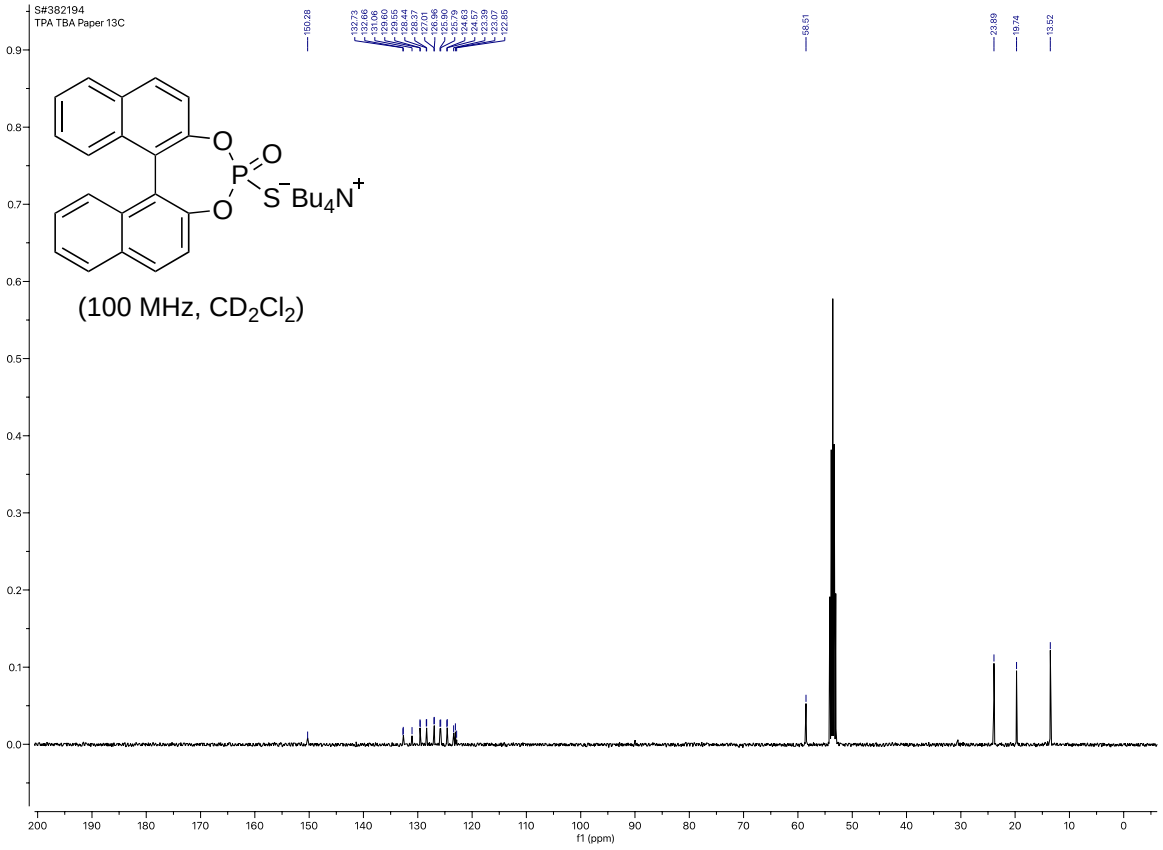
S#382194
TPA TBA Paper 13C
(100 MHz, CD2Cl2)
f1 (ppm)

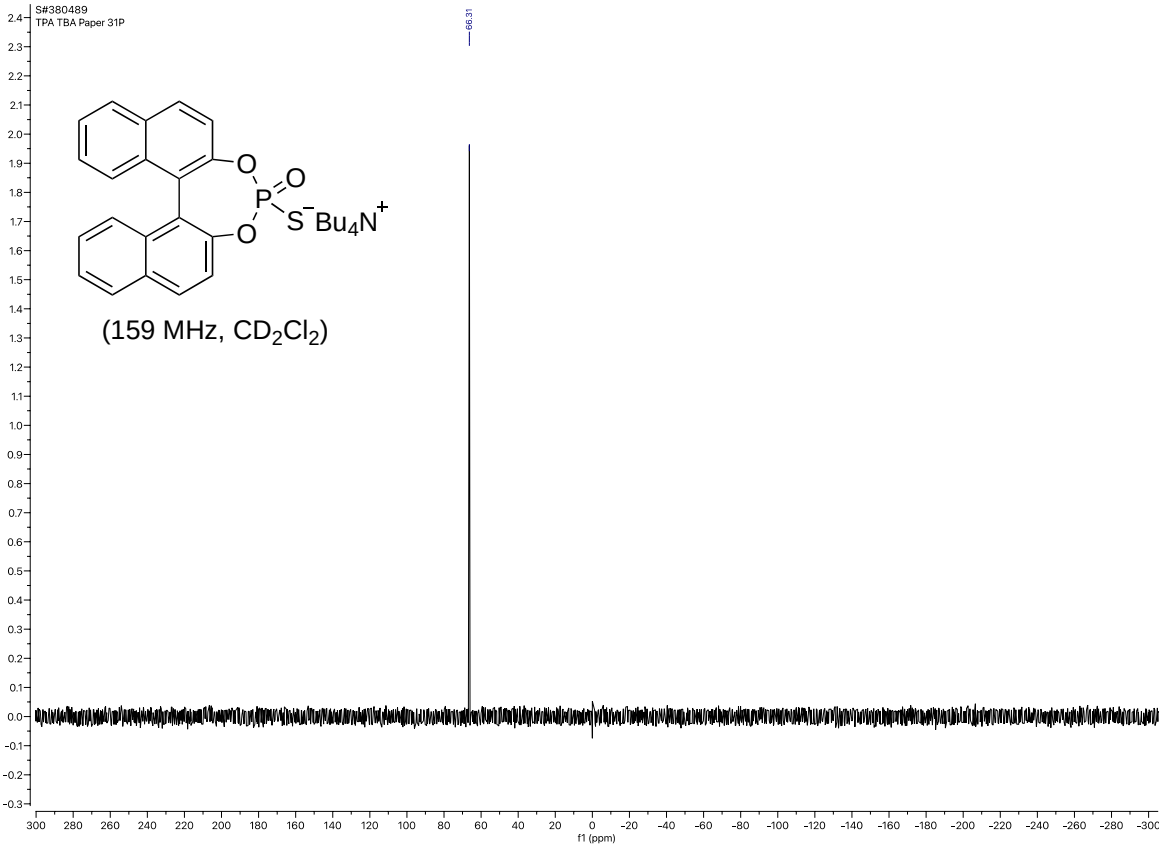
S#380489
TPA TBA Paper 31P
66.31
O
O
P
O
S⁻ Bu4N+
(159 MHz, CD2Cl2)
f1 (ppm)

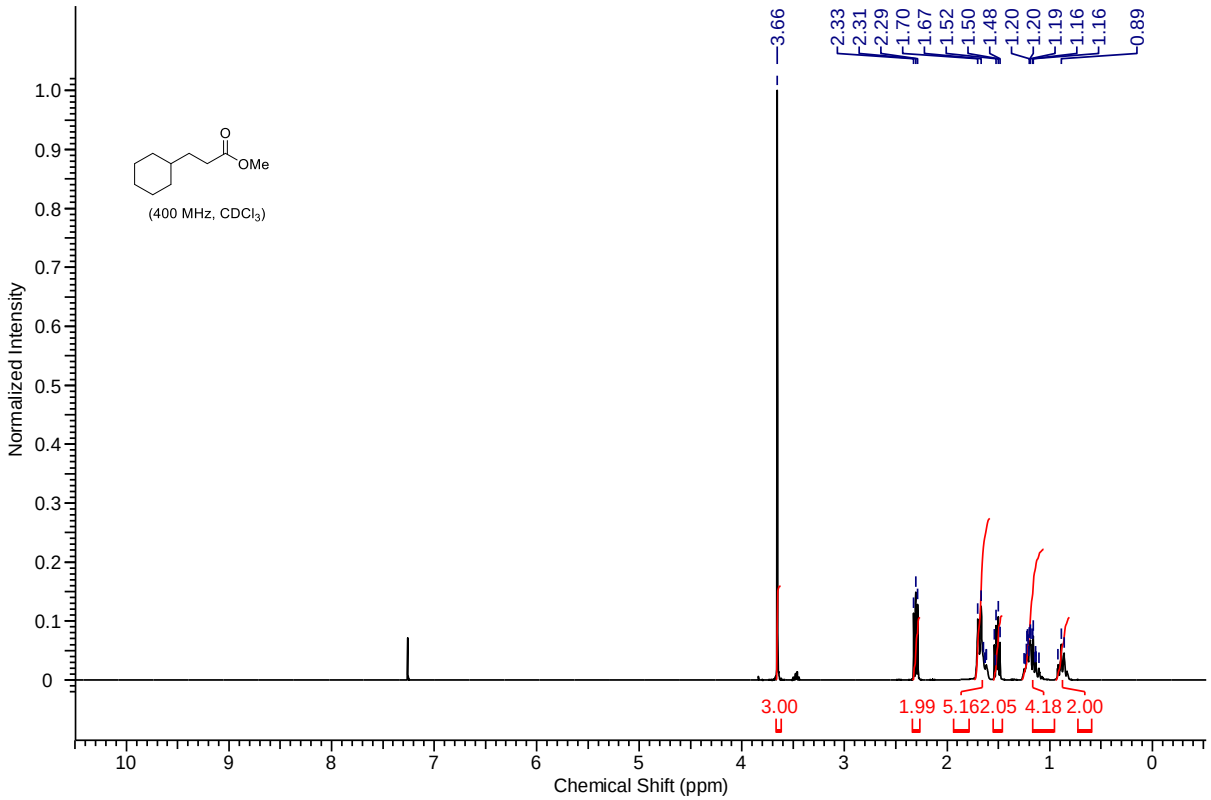
3.66
2.33
2.31
2.29
1.70
1.67
1.52
1.50
1.48
1.20
1.20
1.19
1.16
1.16
0.89
OMe
(400 MHz, CDCl3)
Normalized Intensity
Chemical Shift (ppm)
3.00
1.99
5.16
2.05
4.18
2.00

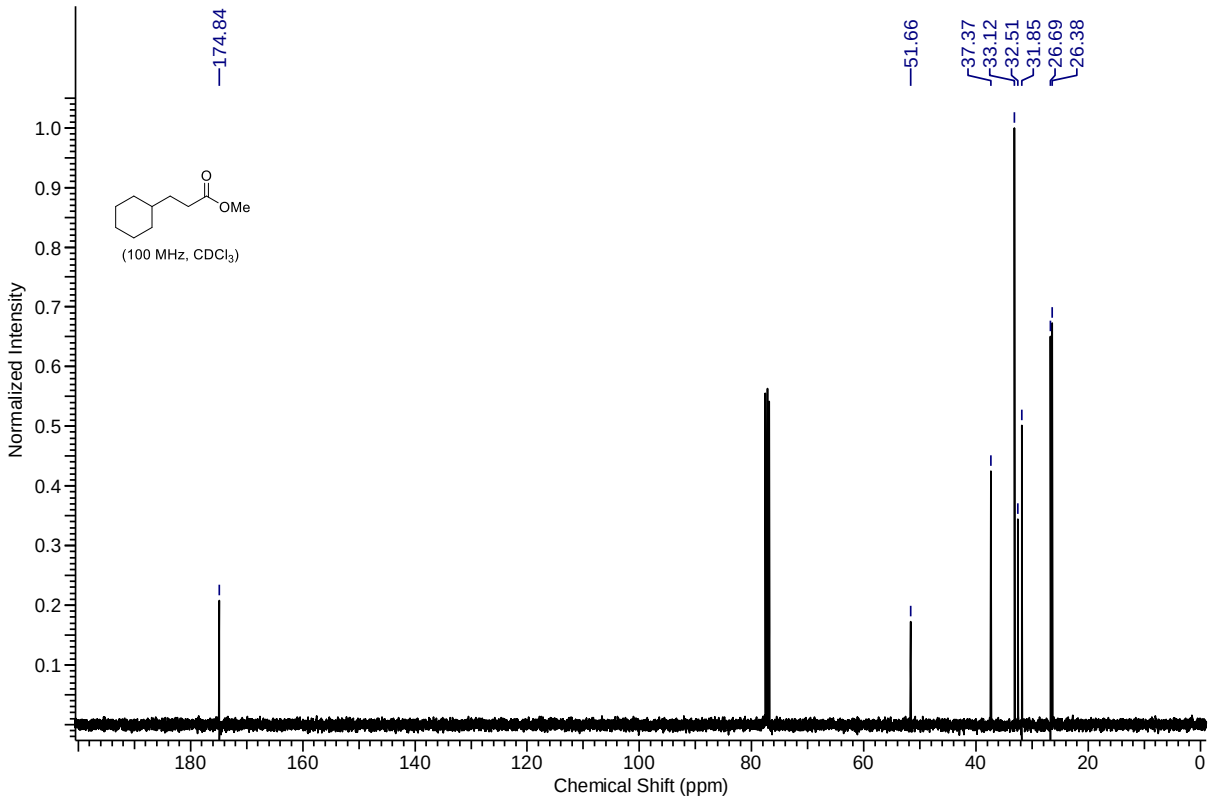
174.84
51.66
37.37
33.12
32.51
31.85
26.69
26.38
OMe
(100 MHz, CDCl3)
Normalized Intensity
Chemical Shift (ppm)

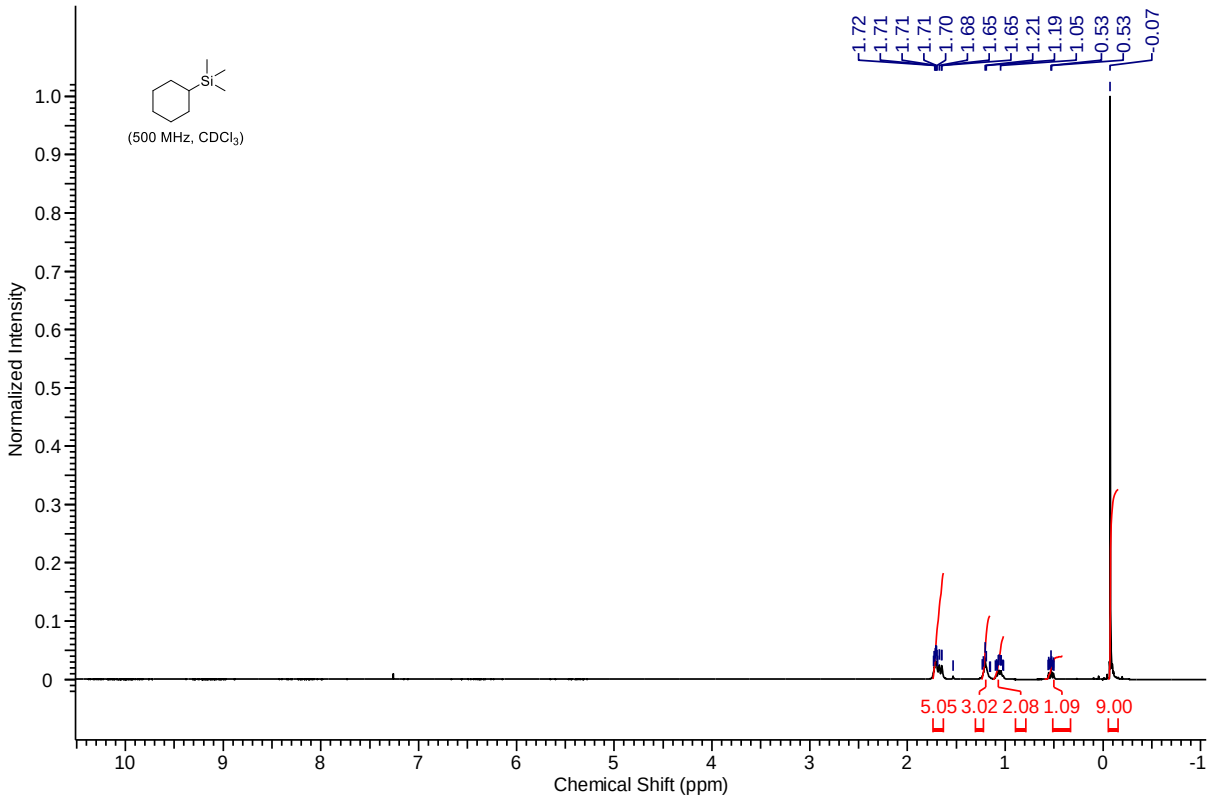
1.72
1.71
1.71
1.71
1.70
1.68
1.65
1.65
1.21
1.19
1.05
0.53
0.53
0.07
Si
(500 MHz, CDCl3)
5.05 3.02 2.08 1.09 9.00
Normalized Intensity
Chemical Shift (ppm)

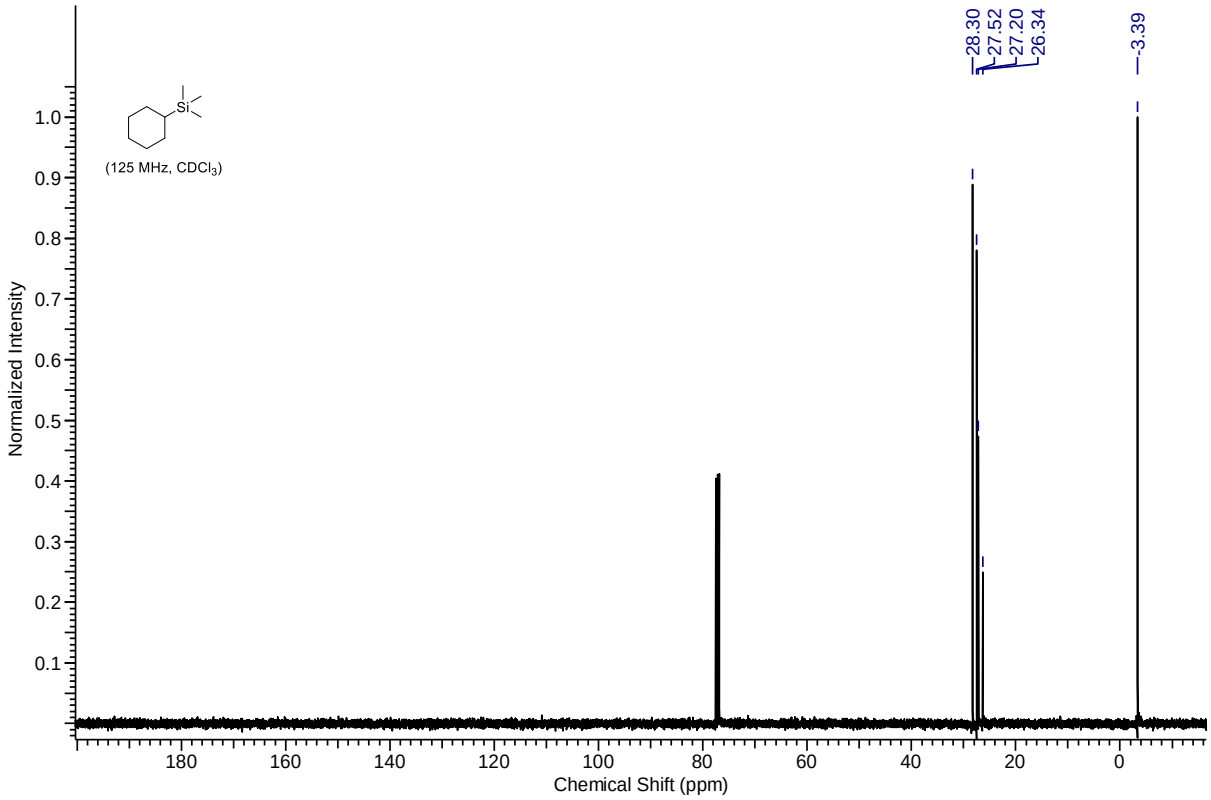
28.30
27.52
27.20
26.34
-3.39
(125 MHz, CDCl3)
Normalized Intensity
Chemical Shift (ppm)

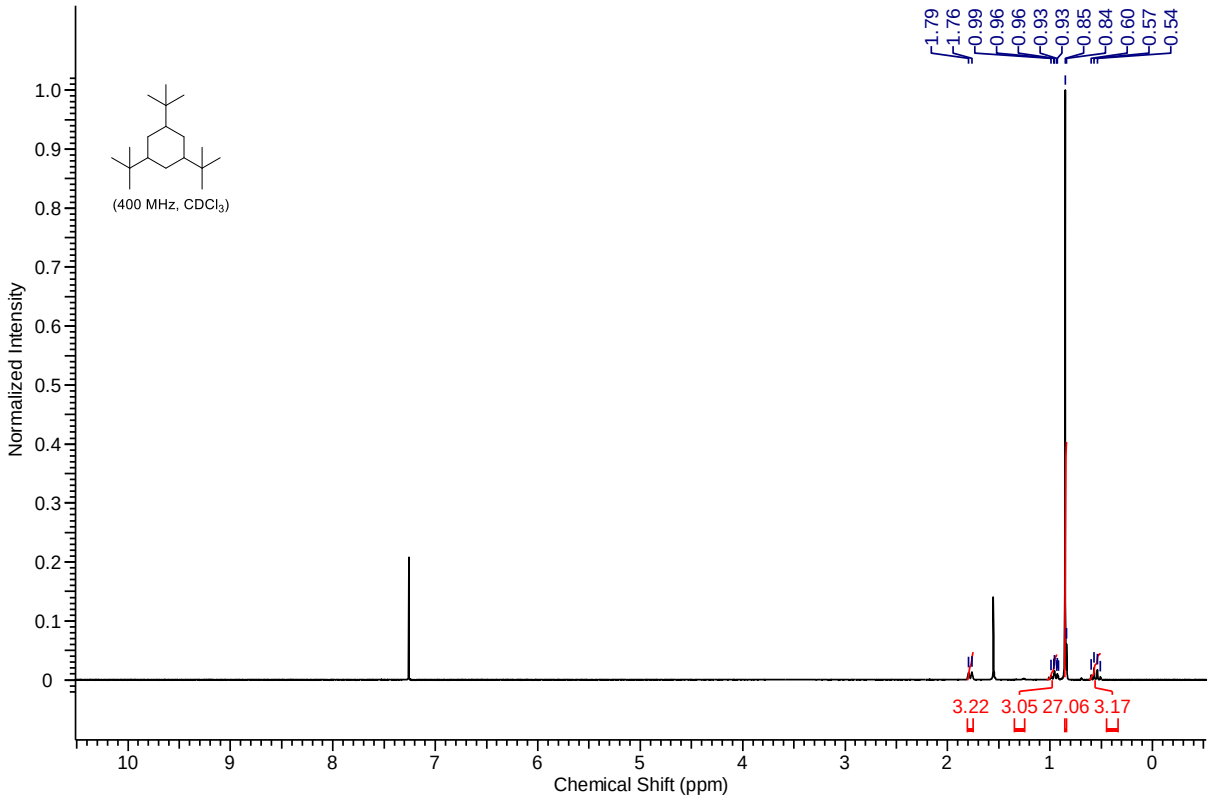
1.79
1.76
0.99
0.96
0.96
0.93
0.93
0.85
0.84
0.60
0.57
0.54
(400 MHz, CDCl3)
3.22
3.05
27.06
3.17
Normalized Intensity
Chemical Shift (ppm)

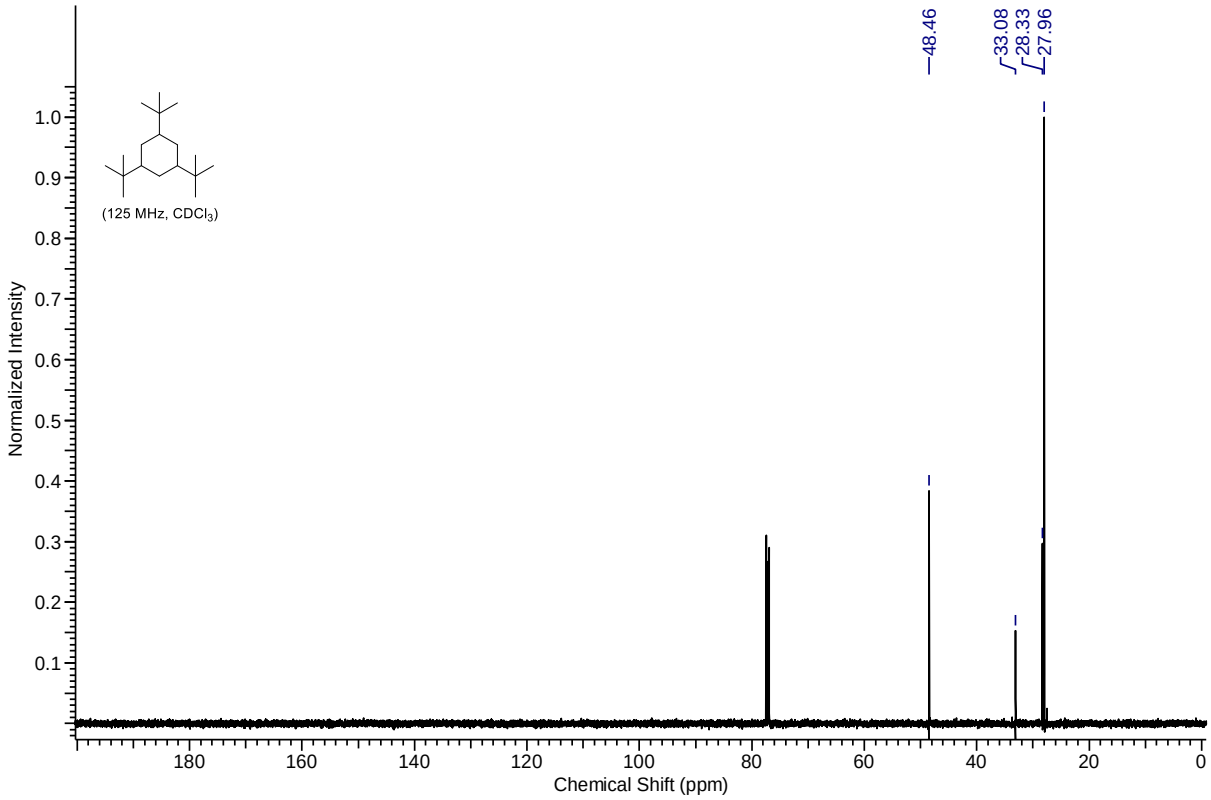
48.46
33.08
28.33
27.96
(125 MHz, $CDCl_3$)
Normalized Intensity
Chemical Shift (ppm)

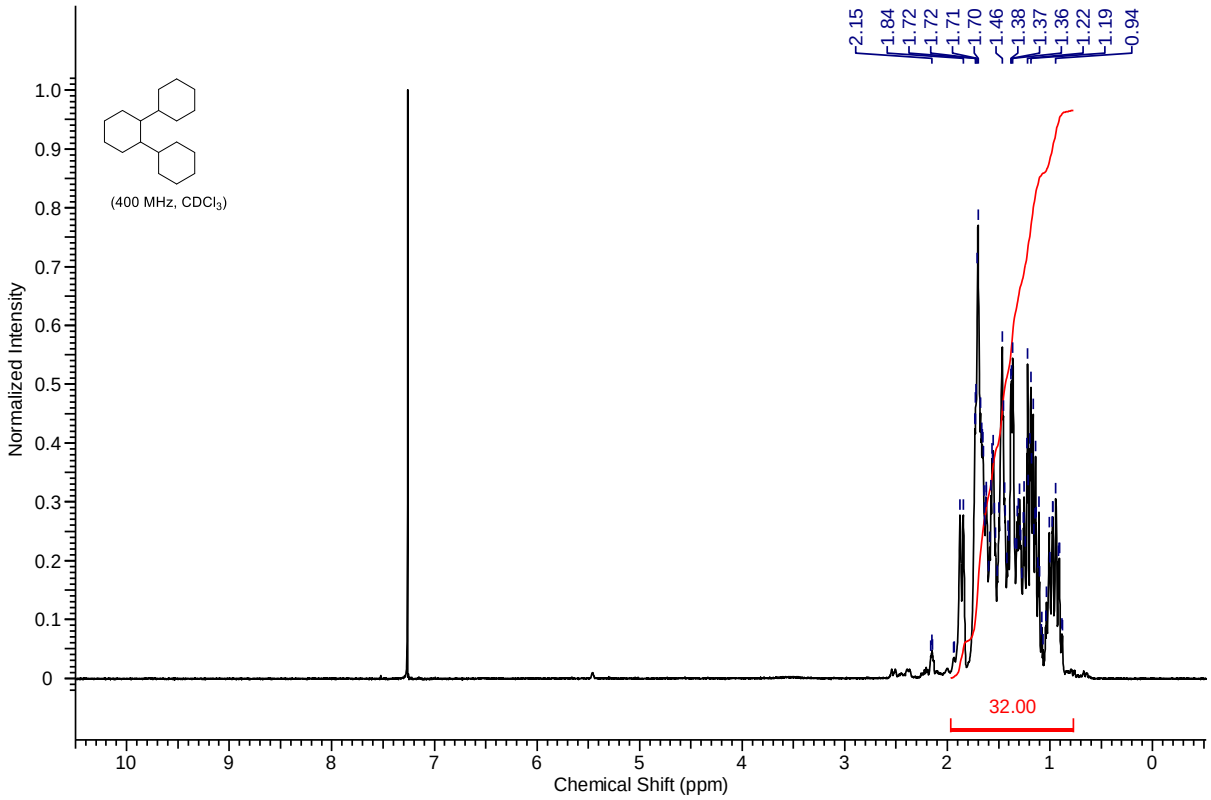
2.15
1.84
1.72
1.72
1.71
1.70
1.46
1.38
1.37
1.36
1.22
1.19
0.94
(400 MHz, $CDCl_3$)
32.00
Normalized Intensity
Chemical Shift (ppm)

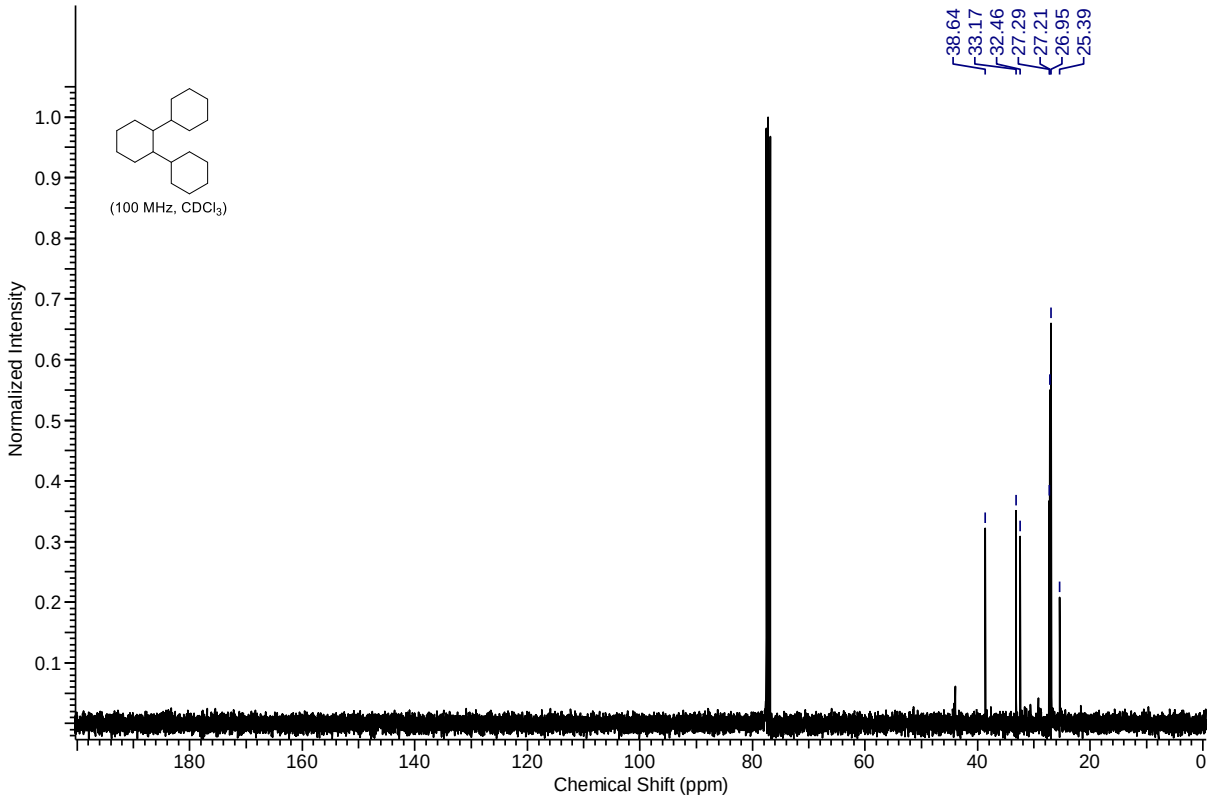
38.64
33.17
32.46
27.29
27.21
26.95
25.39
(100 MHz, CDCl3)
Normalized Intensity
Chemical Shift (ppm)

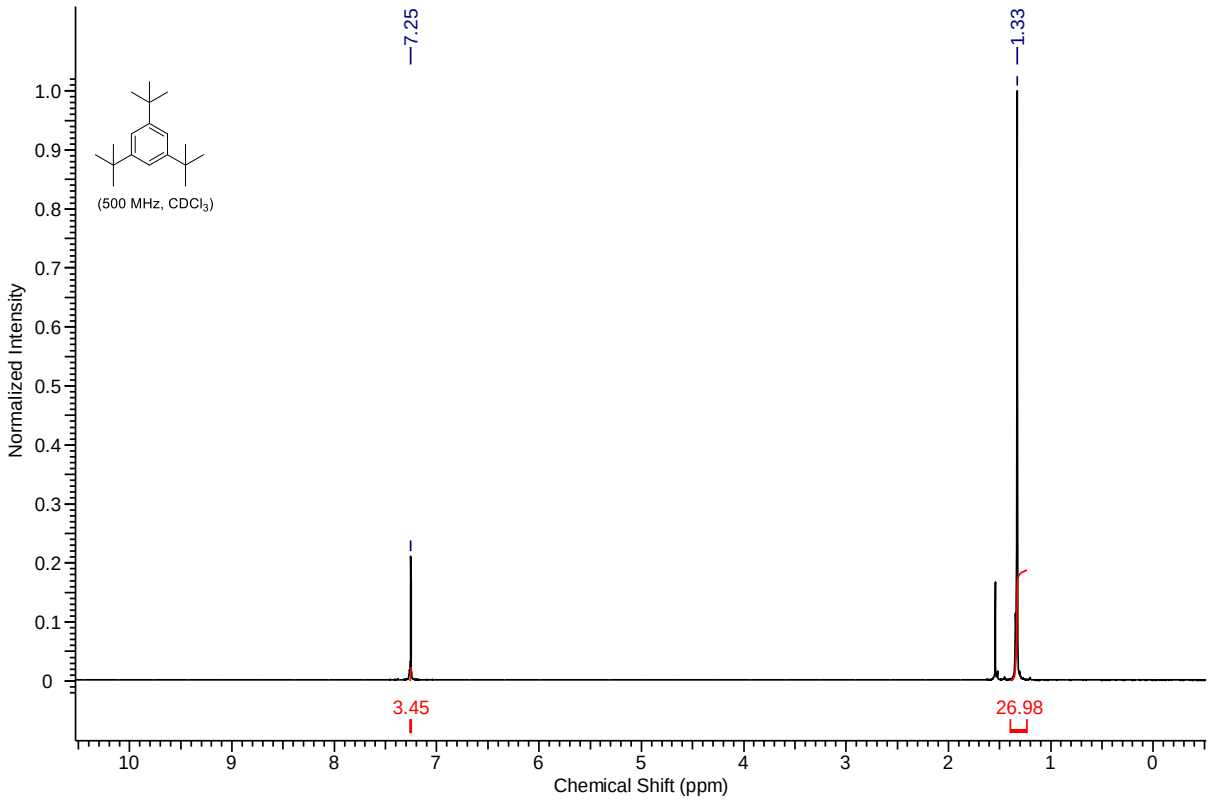
7.25
1.33
(500 MHz, CDCl3)
Normalized Intensity
3.45
26.98
Chemical Shift (ppm)

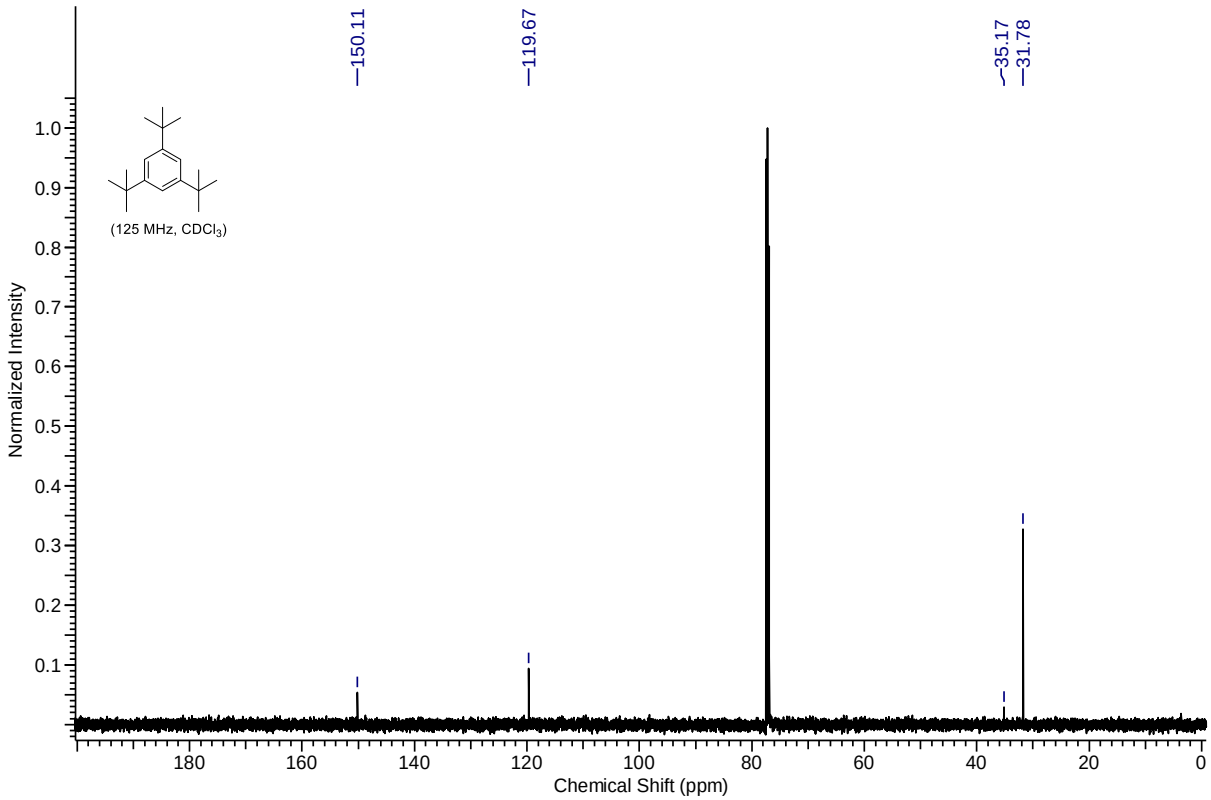
150.11
119.67
35.17
31.78
(125 MHz, CDCl3)
Normalized Intensity
Chemical Shift (ppm)

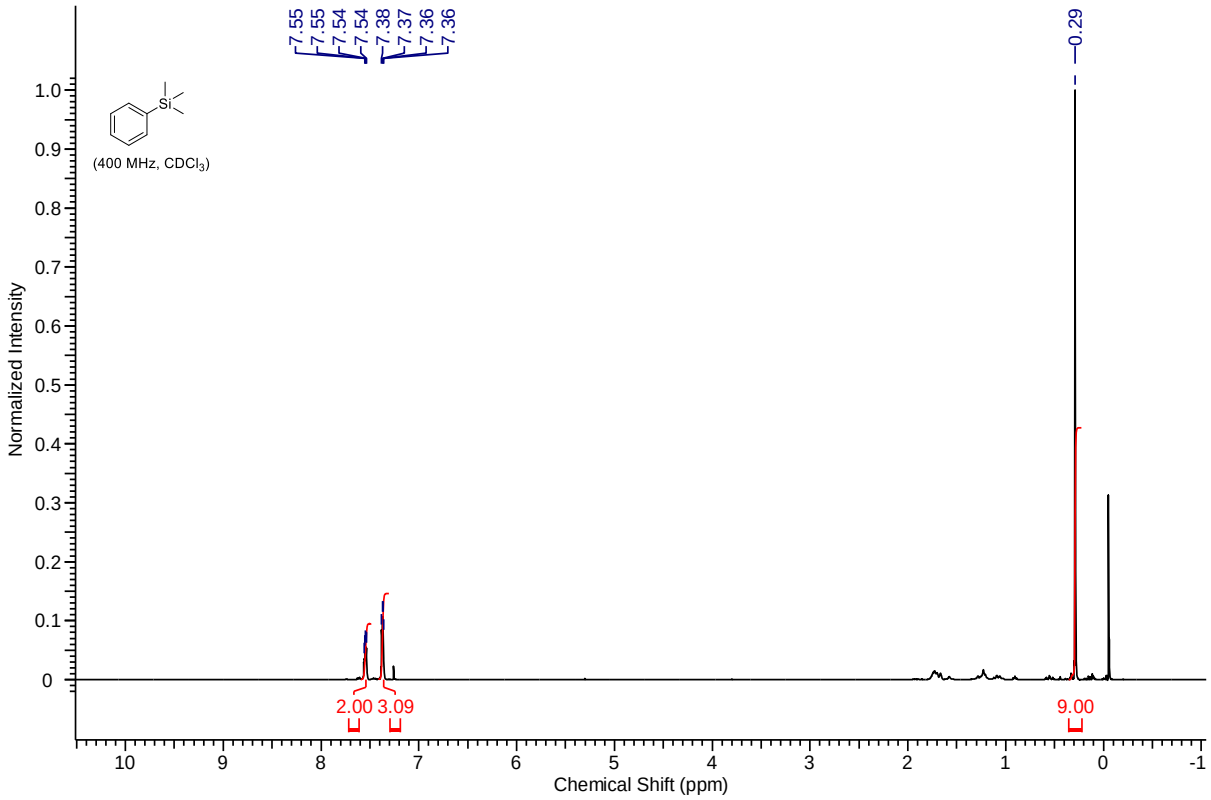
7.55
7.55
7.54
7.54
7.38
7.37
7.36
7.36
0.29
Si
(400 MHz, CDCl3)
2.00
3.09
9.00
Normalized Intensity
Chemical Shift (ppm)

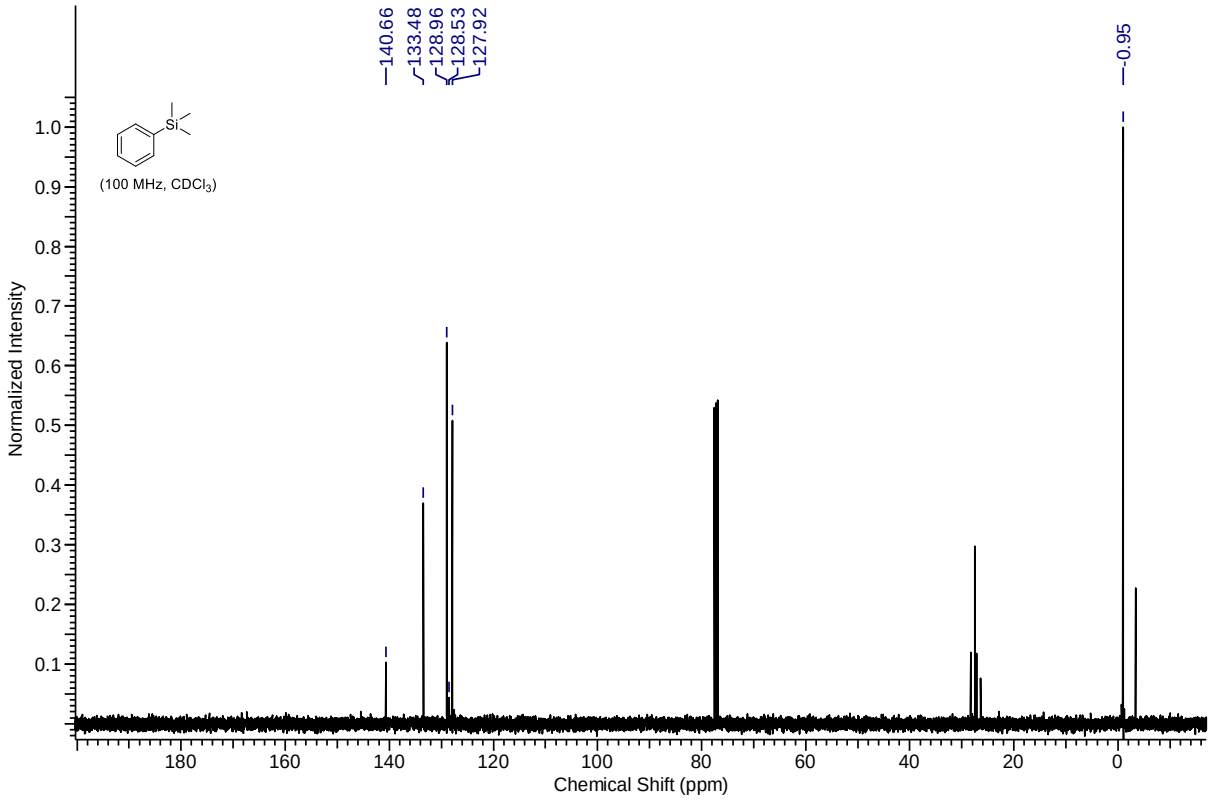
140.66
133.48
128.96
128.53
127.92
-0.95
(100 MHz, CDCl3)
Normalized Intensity
Chemical Shift (ppm)

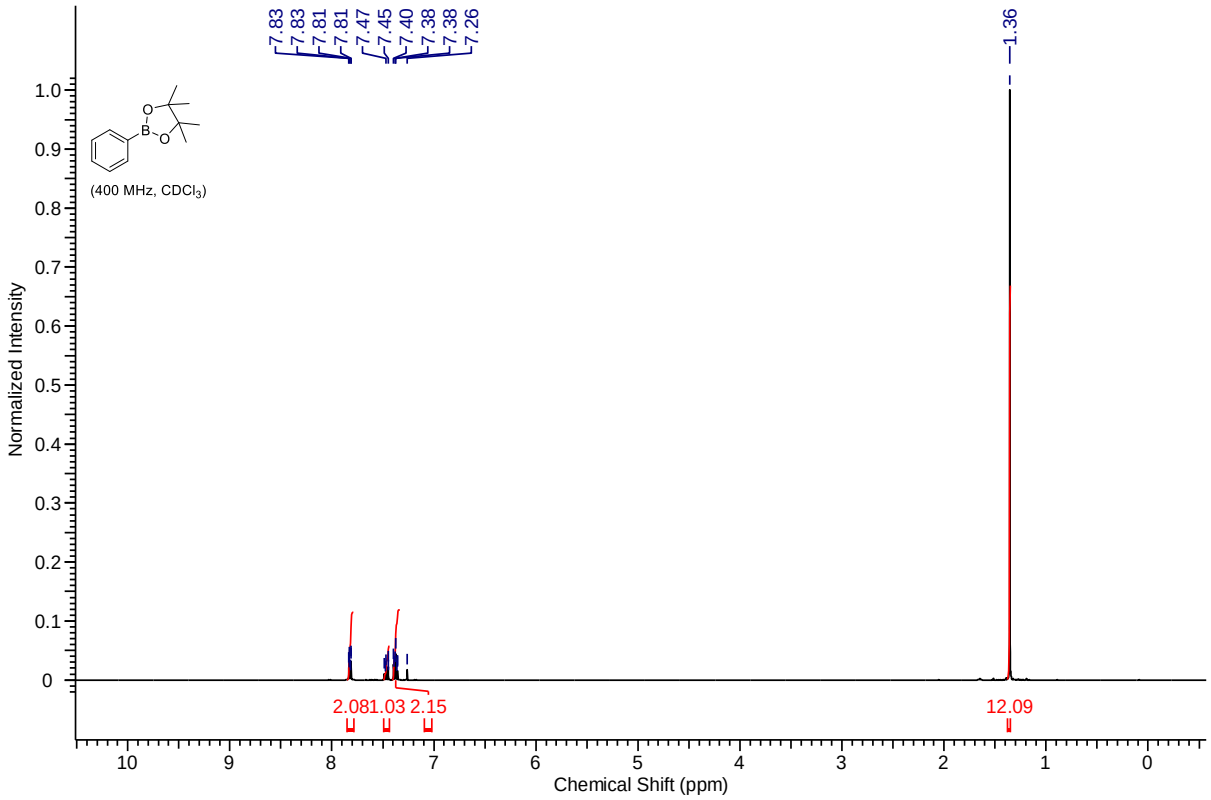
7.83
7.83
7.81
7.81
7.47
7.45
7.40
7.38
7.38
7.26
1.36
(400 MHz, CDCl3)
2.08
1.03
2.15
12.09
Normalized Intensity
Chemical Shift (ppm)

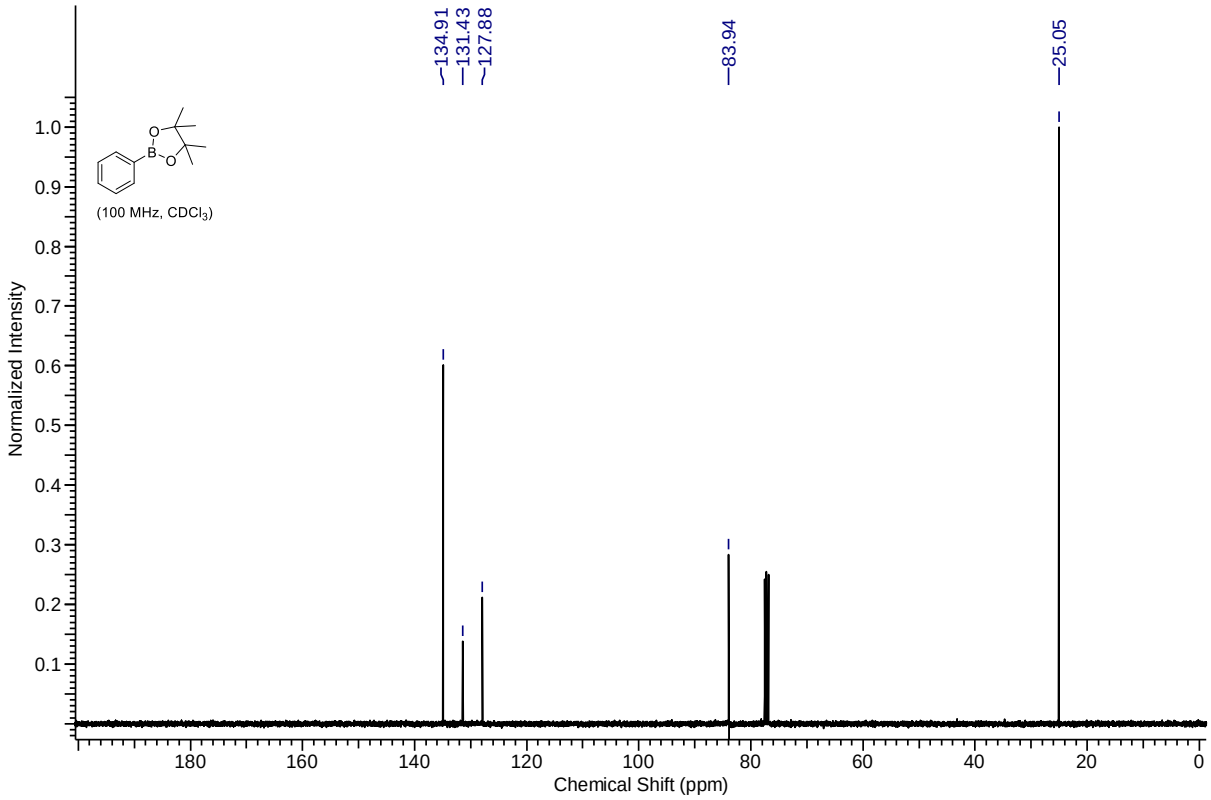
134.91
131.43
127.88
83.94
25.05
(100 MHz, CDCl3)
Normalized Intensity
Chemical Shift (ppm)

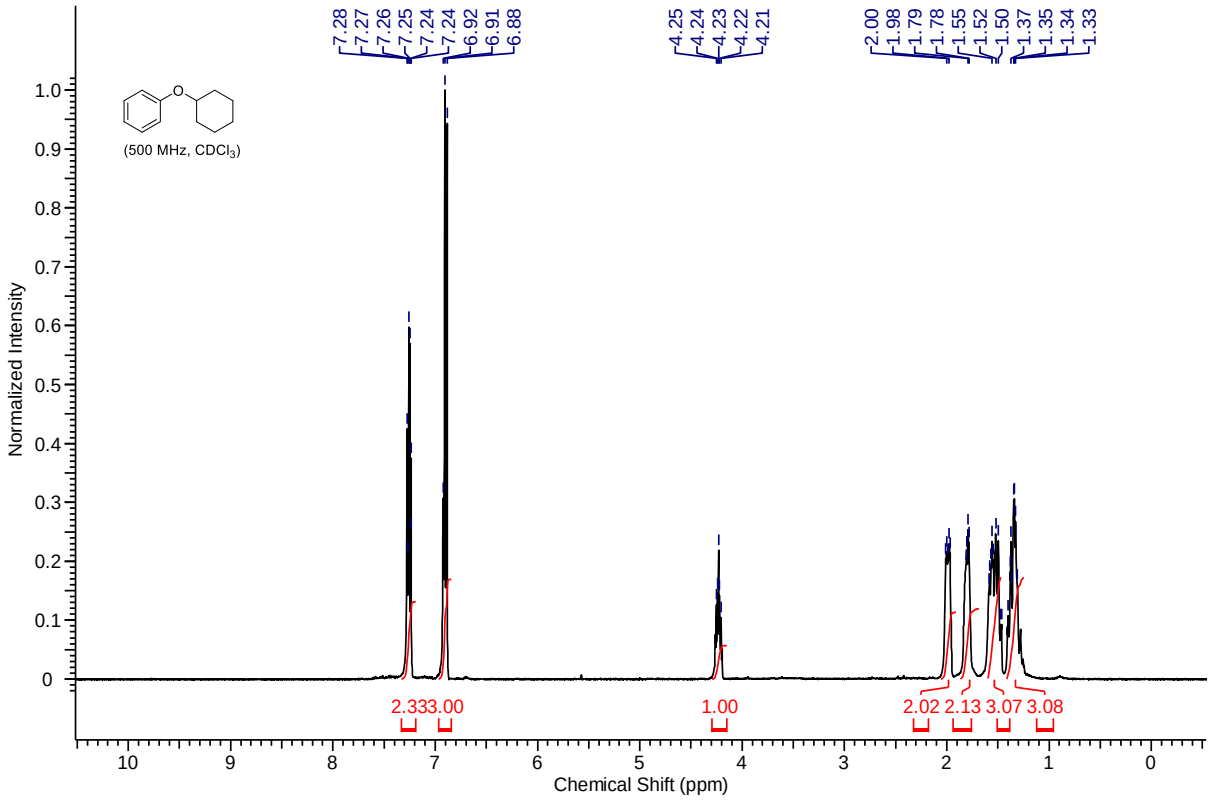
7.28
7.27
7.26
7.25
7.24
7.24
6.92
6.91
6.88
4.25
4.24
4.23
4.22
4.21
2.00
1.98
1.79
1.78
1.55
1.52
1.50
1.37
1.35
1.34
1.33
(500 MHz, CDCl3)
2.33 3.00
1.00
2.02 2.13 3.07 3.08
Normalized Intensity
Chemical Shift (ppm)

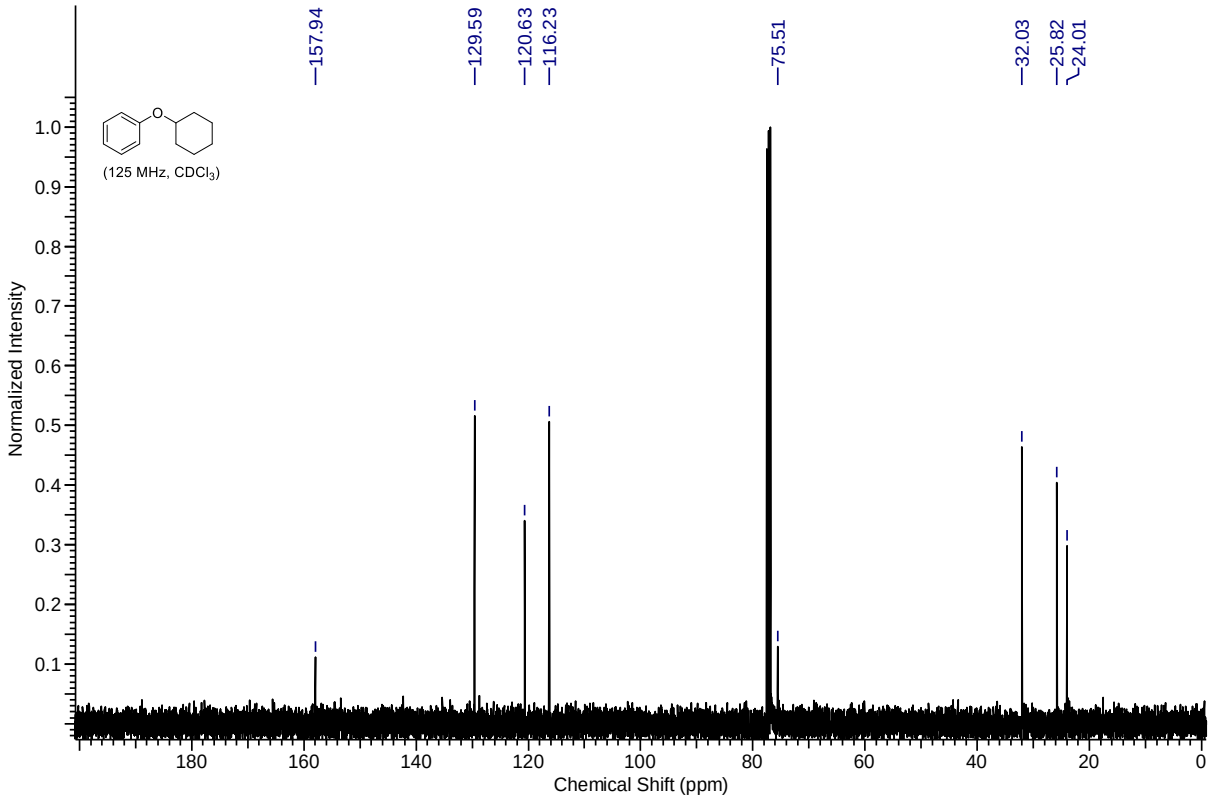
157.94
129.59
120.63
116.23
75.51
32.03
25.82
24.01
(125 MHz, CDCl3)
Normalized Intensity
Chemical Shift (ppm)

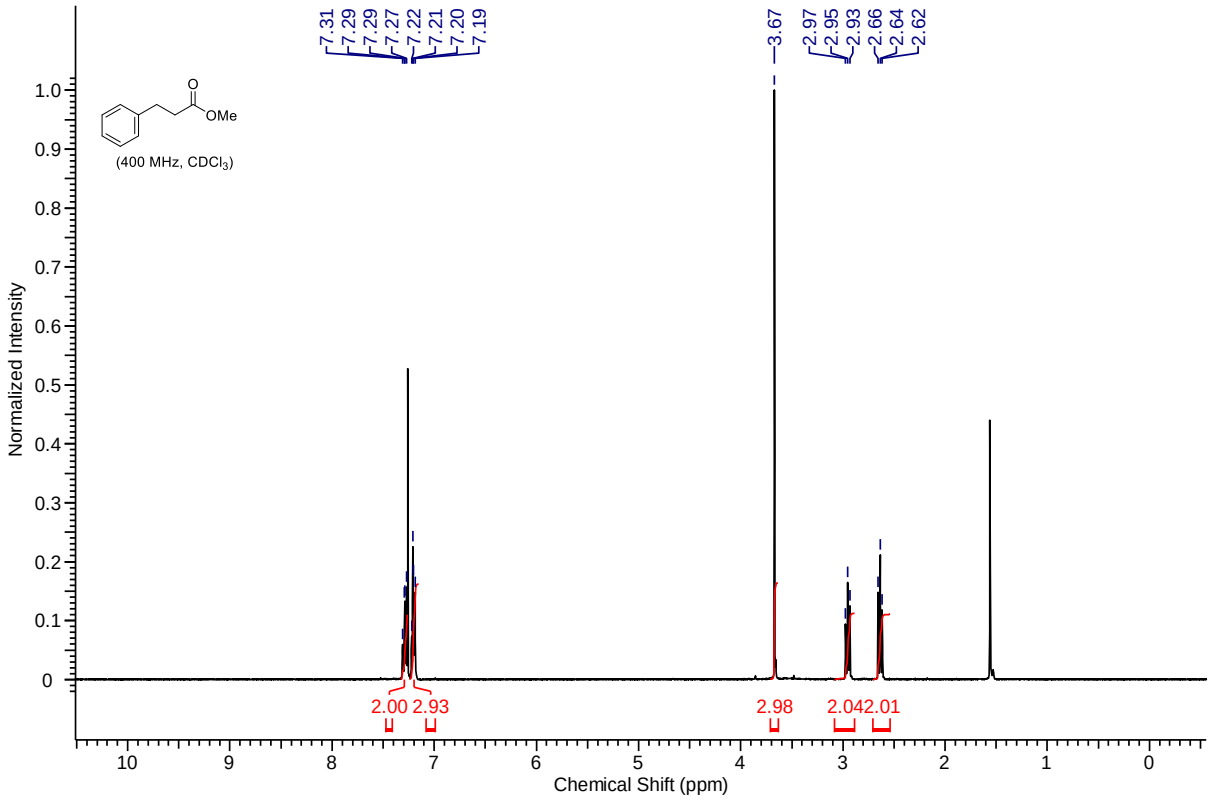
7.31
7.29
7.29
7.27
7.22
7.21
7.20
7.19
3.67
2.97
2.95
2.93
2.66
2.64
2.62
OMe
(400 MHz, CDCl3)
2.00 2.93
2.98
2.04 2.01
Normalized Intensity
Chemical Shift (ppm)

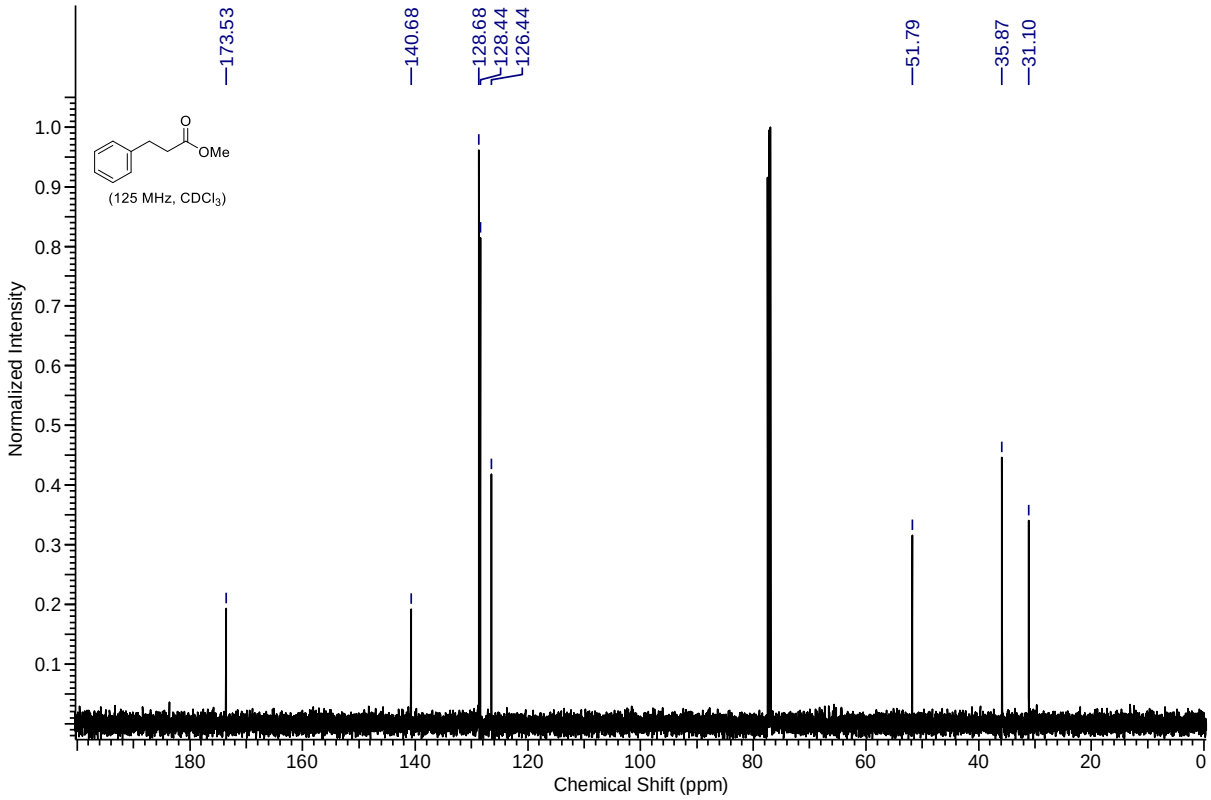
173.53
140.68
128.68
128.44
126.44
51.79
35.87
31.10
OMe
(125 MHz, CDCl3)
Normalized Intensity
Chemical Shift (ppm)

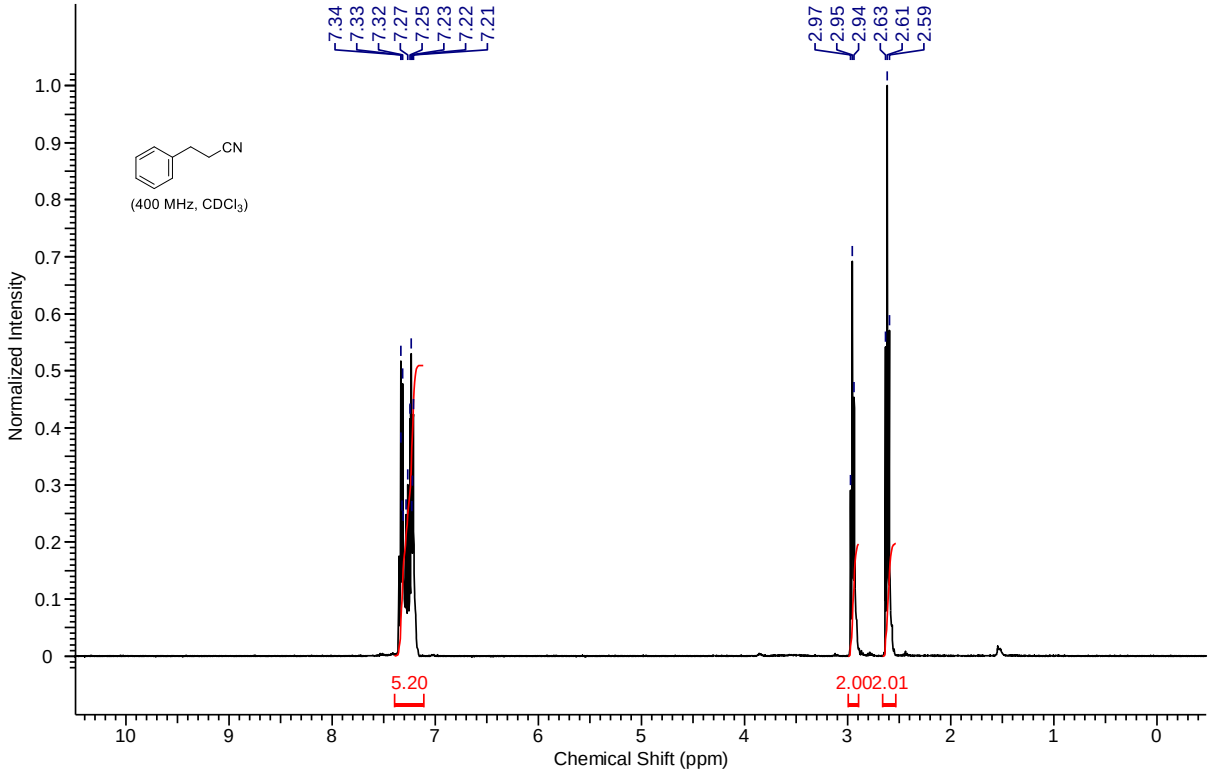
7.34
7.33
7.32
7.27
7.25
7.23
7.22
7.21
2.97
2.95
2.94
2.63
2.61
2.59
CN
(400 MHz, CDCl3)
5.20
2.002.01
Normalized Intensity
Chemical Shift (ppm)

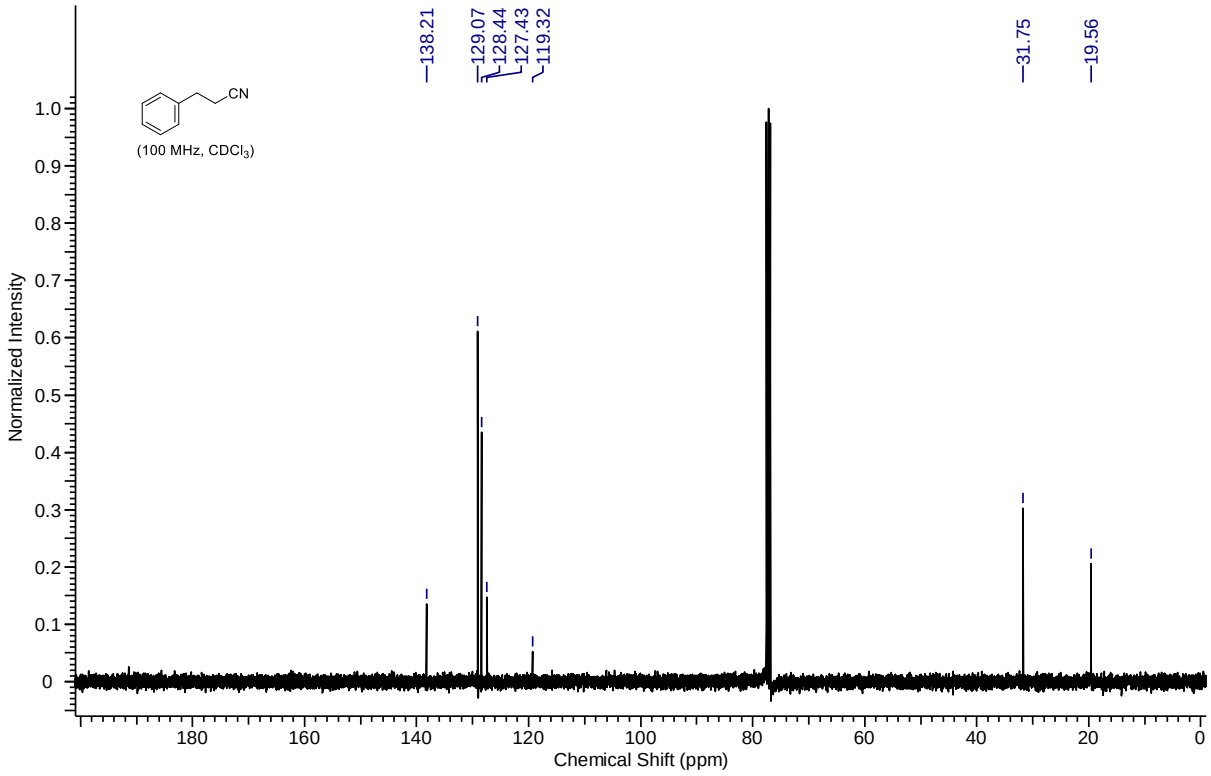
138.21
129.07
128.44
127.43
119.32
31.75
19.56
CN
(100 MHz, CDCl3)
Normalized Intensity
Chemical Shift (ppm)

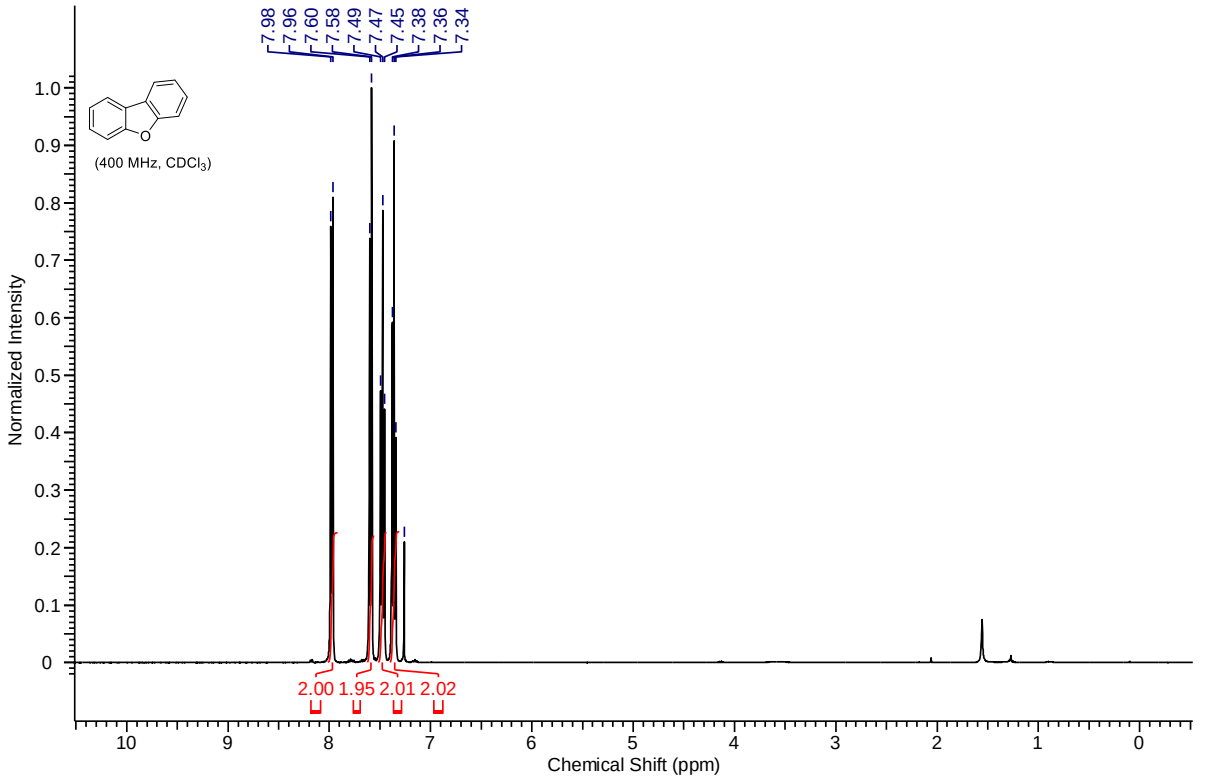
7.98
7.96
7.60
7.58
7.49
7.47
7.45
7.38
7.36
7.34
O
(400 MHz, CDCl3)
2.00 1.95 2.01 2.02
Normalized Intensity
Chemical Shift (ppm)

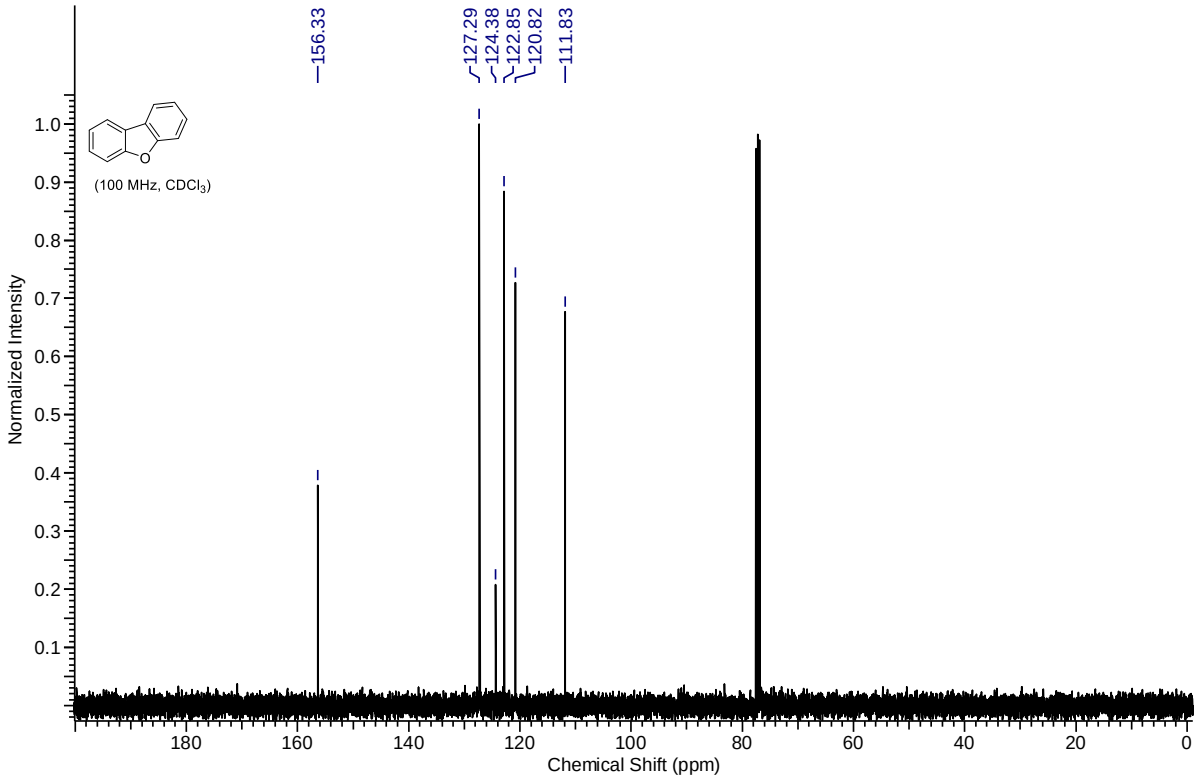
156.33
127.29
124.38
122.85
120.82
111.83
(100 MHz, CDCl3)
Normalized Intensity
Chemical Shift (ppm)

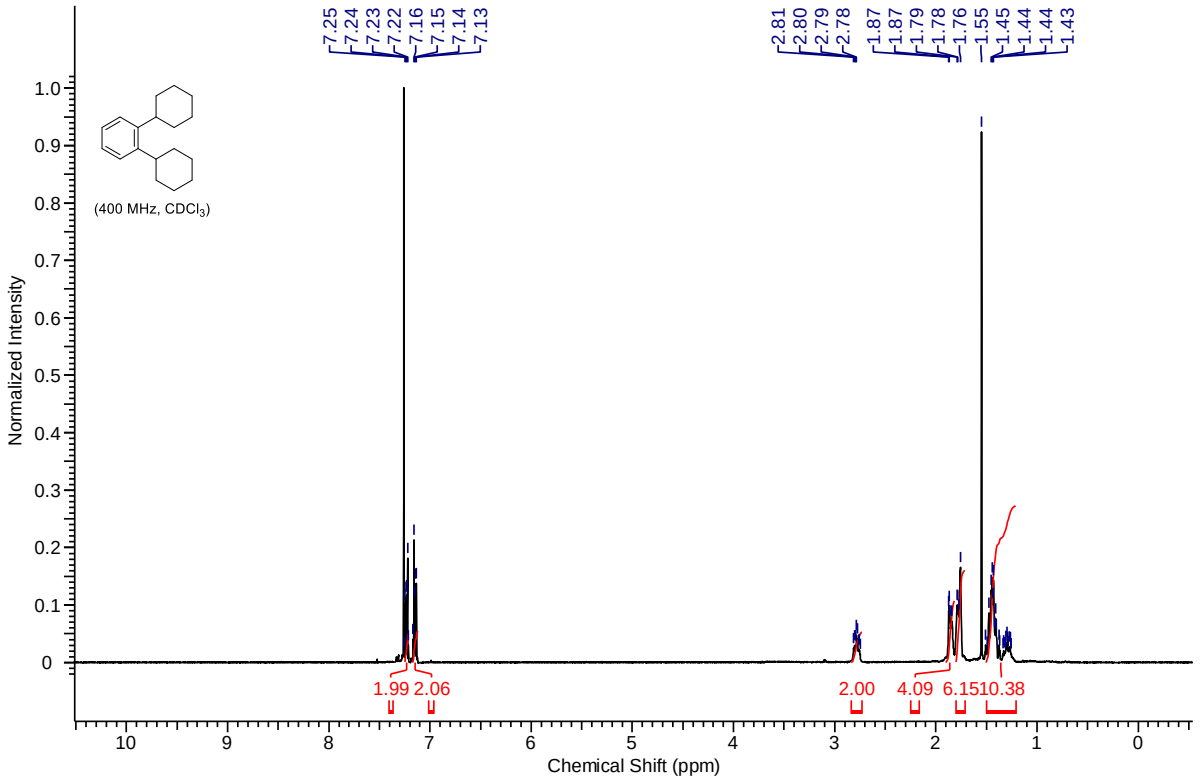
7.25
7.24
7.23
7.22
7.16
7.15
7.14
7.13
2.81
2.80
2.79
2.78
1.87
1.87
1.79
1.78
1.76
1.55
1.45
1.44
1.44
1.43
(400 MHz, CDCl3)
1.99
2.06
2.00
4.09
6.15
10.38
Normalized Intensity
Chemical Shift (ppm)

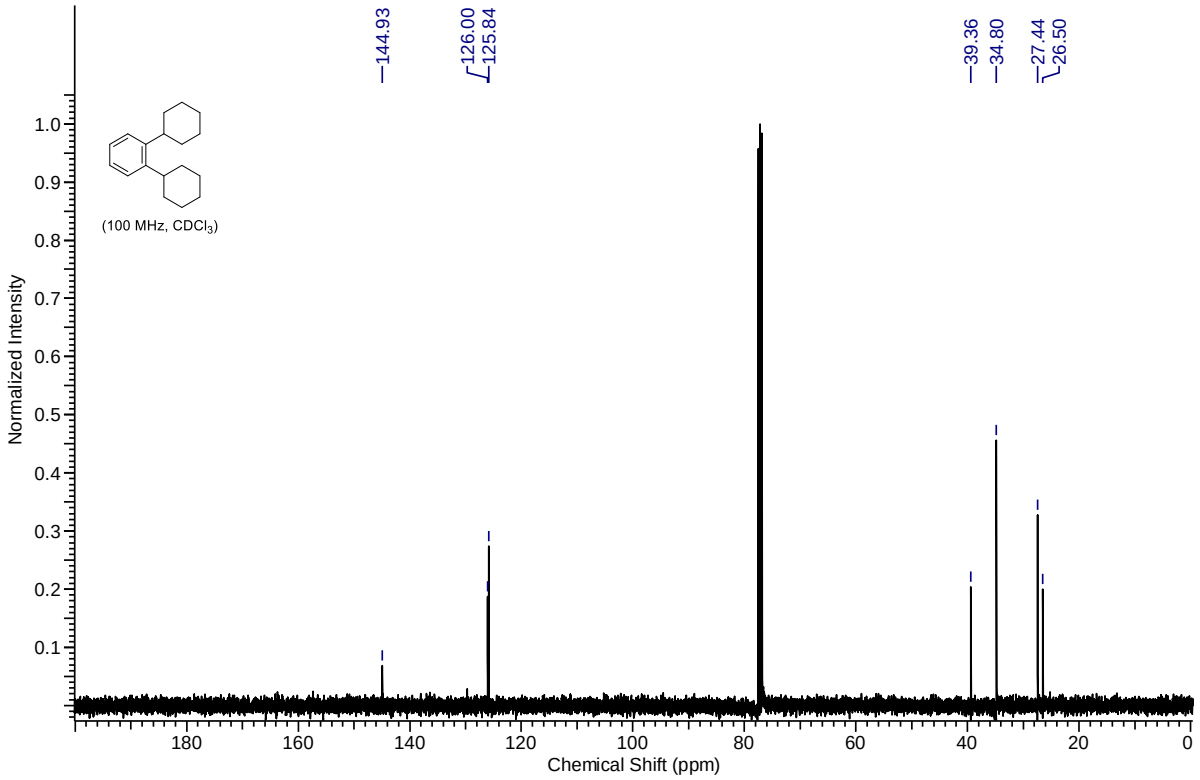
144.93
126.00
125.84
39.36
34.80
27.44
26.50
(100 MHz, CDCl3)
Normalized Intensity
Chemical Shift (ppm)

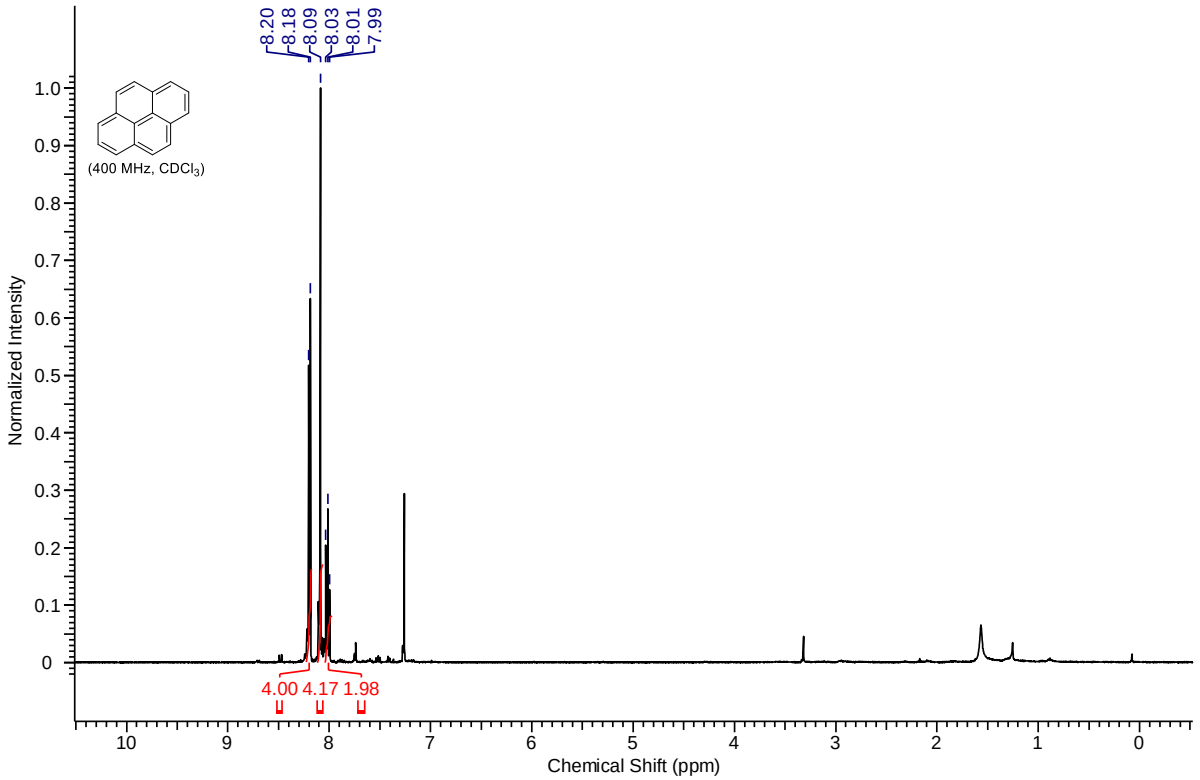
8.20
8.18
8.09
8.03
8.01
7.99
(400 MHz, CDCl3)
4.00 4.17 1.98
Normalized Intensity
Chemical Shift (ppm)

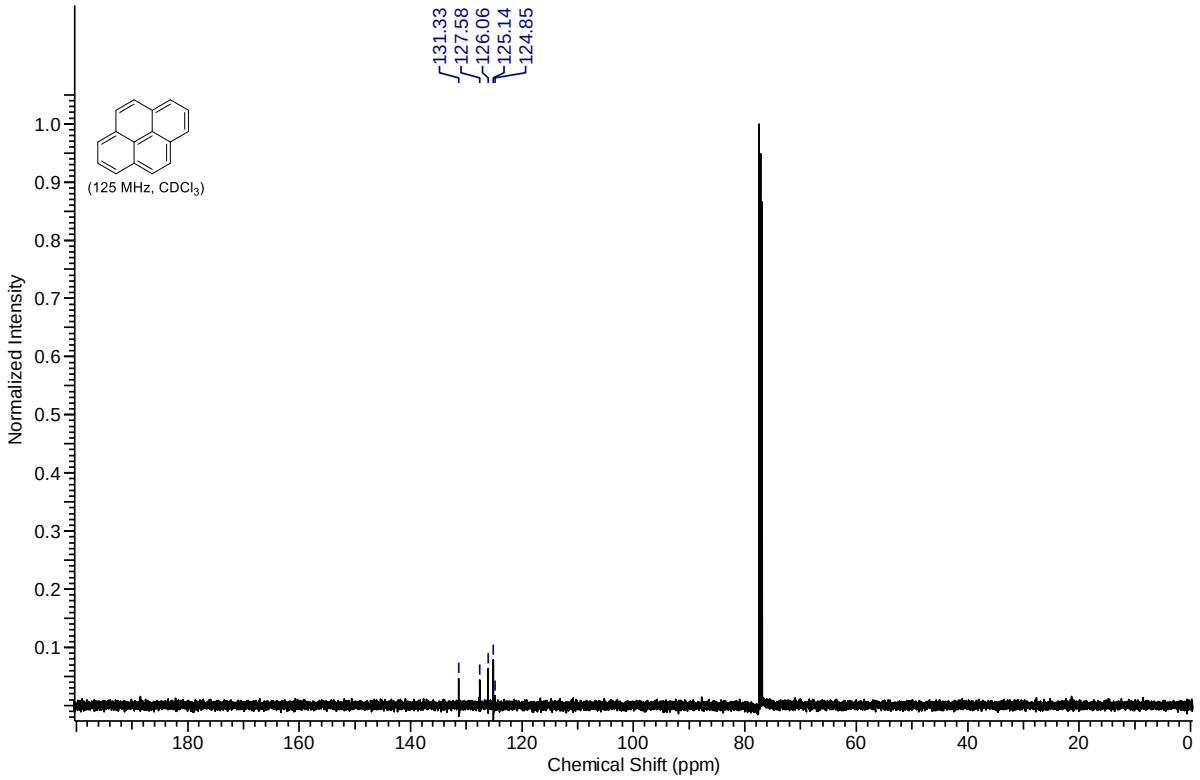

18. References

1. Zhao, H.; McMillan, A. J.; Constantin, T.; Mykura, R. C.; Juliá, F.; Leonori, D. Merging Halogen Atom Transfer (XAT) and Cobalt Catalysis to Override E2-Selectivity in the Elimination of Alkyl Halides: A Mild Route toward contra-Thermodynamic Olefins. *J. Am. Chem.Soc.* **2021**, *143*, 14806−14813.

2. Weiss, M. E.; Kreis, L. M.; Lauber, A.; Carreira, E. M. Cobalt-Catalyzed Coupling of Alkyl Iodides with Alkenes: Deprotonation of Hydridocobalt Enables Turnover. *Angew. Chem., Int. Ed.* **2011**, *50*, 11125–11128.

3. Zhou, F.; Hu, X.; Zhang, W.; Li, C.-J. Direct conjugate additions using aryl and alkyl organic halides in air and water. *Org. Chem. Front.* **2018**, *5*, 3579−3584.

4. Maegawa, T.; Akashi, A.; Yaguchi, K.; Iwasaki, Y.; Shigetsura, M.; Monguchi, Y.; Sajiki, H. Efficient and Practical Arene Hydrogenation by Heterogeneous Catalysts under Mild Conditions. *Chem. Eur. J.* **2009**, *15*, 6953−6963.

5. Torigoe, T.; Ohmura, T.; Suginome, M. Utilization of a Trimethylsilyl Group as a Synthetic Equivalent of a Hydroxyl Group via Chemoselective C(Sp3)−H Borylation at the Methyl Group on Silicon. *J. Org. Chem.* **2017**, *82*, 2943−2956.

6. W. Stroek, L. Hoareau, M. Albrecht, From the bottle: simple iron salts for the efficient synthesis of pyrrolidines *via* catalytic C–H bond amination *Catal. Sci. Technol.* **2023**, *13*, 958–962.

7. Sambiagio, C.; Noël, T. Flow Photochemistry: Shine Some Light on Those Tubes! *Trends in Chem.* **2019**, *2*, 92-106.

8. Bokarev, S. I.; Hollmann, D.; Pazidis, A.; Neubauer, A.; Radnik,J.; Kühn, O.; Lochbrunner, S.; Junge, H.; Beller, M.; Brückner, A. *Phys. Chem. Chem. Phys.* **2014**, *16*, 4789−4796.

9. Skell, P. S.; Baxter, H. N.; Tanko, J. M.; Chebolu, V. *J. Am. Chem. Soc.* **1986**, *108*, 6300−6311.

10. Fuse, H.; Irie, Y.; Fuki, M.; Kobori, Y.; Kato, K.; Yamakata, A.; Higashi, M.; Mitsunuma, H.; Kanai, M. Identification of a Self-Photosensitizing Hydrogen Atom Transfer Organocatalyst System. *J. Am. Chem. Soc.* **2022**, *144*, 6566−6574.

11. Gonzalez, M. I.; Gygi, D.; Qin, Y.; Zhu, Q.; Johnson, E. J.; Chen, Y.-S.; Nocera, D. G. Taming the Chlorine Radical: Enforcing Steric Control over Chlorine-Radical-Mediated C–H Activation. *J. Am. Chem. Soc.* **2022**, *144*, 1464−1472.

12. Russel, G. A.; Solvent Effects in the Reactions of Free Radicals and Atoms. II. Effects of Solvents on the Position of Attack of Chlorine Atoms upon 2,3-Dimethylbutane, Isobutane and 2-Deuterio-2-methylpropane. *J. Am. Chem. Soc.* **1958**, *80*, 4987-4996.

13. Snellenburg, J. J.; Laptenok, S. P.; Seger, R.; Mullen, K. M.; Stokkum, I. H. M. van. Glotaran: A Java -Based Graphical User Interface for the R Package TIMP. J. Stat. Softw. **2012**, *49*, 1–22.

14. Lowry, M. S.; Goldsmith, J. I.; Slinker, J. D.; Rohl, R.; Pascal, R. A.; Malliaras, Jr., G. G.; Bernhard, S. *Chem. Mater*. **2005**, *17*, 5712.

15. Rohe, S.; Morris, A. O.; McCallum, T.; Barriault, L. *Angew. Chem. Int. Ed.* **2018**, *57*, 15664.

16. Xu, W.; Ma, J.; Yuan, X.-A.; Dai, J.; Xie, J.; Zhu, C. *Angew. Chem. Int. Ed.* **2018**, *57*, 10357.